Assessing the climate uncertainty of the Social Cost of Carbon

IIASA - Ecole Polytechnique
Under the supervision of Thomas Gasser

Côme CHERITEL

Abstract

The Social Cost of Carbon is probably the most important metric when it comes to climate change mitigation. This term represents the economic cost caused by an additional ton of carbon dioxide emissions or its equivalent. Since its creation, the Social Cost of Carbon has become a central tool used in climate change policy-design, particularly in the case of regulatory policies that involve greenhouse gas emissions. However, the Social Cost of Carbon suffers from an absence of known uncertainties. Which means that it is not possible to ascertain a confidence interval for a given estimate of the Social Cost of Carbon whereas, on the contrary, there is great uncertainty on future global warming. In this study, we aim at estimating the uncertainty of the Social Cost of Carbon with the DICE model, probably the most often used Integrated Assessment Model to compute the Social Cost of Carbon. To this end, we develop a new compact climate model that is designed according to state-of-the-art knowledge in climate physics. Coupled with a Bayesian calibration, we perform an uncertainty analysis with a Monte Carlo setup. With this upgraded DICE framework, we estimate the Social Cost of Carbon and its uncertainty, on a various range of potential future scenarios, the Shared Socioeconomic Pathway. This finally allows us to conclude on the main factors determining the Social Cost of Carbon as well as on some of the questions raised by this study.

Contents

Introduction

Global climate change is a major challenge faced by mankind on its way to sustainable development. As the Global Mean Surface Temperature rises, it becomes clearer and clearer that global warming implies significant negative impacts on societies. Since Earth's system is a global common good, climate change can be managed effectively only through collective and coordinated policies for adaptation and mitigation.

To this end, international agreements, such as the 2016 Paris agreement, have been taken since 1997 and the Kyoto protocol. With the progresses made by complex climate models that help us understanding the physical mechanism behind climate change, there is an increasing need of guidance for action. Thus, more research is needed to create feasible mitigation policies consistent with the specified targets. These policies would aim to minimize the negative impacts of climate change on human and environmental well-being, while ensuring that other aspects of well-being, most notably economic prosperity, are not unduly compromised. "In practice, an economic analysis of climate change weighs the costs of slowing climate change against the damages of more rapid climate change" [Nordhaus, 2013]. Hence, a comprehensive analysis of the complex climate–economy system, in which these trade-offs are more realistically addressed, is still needed.

The economic mitigation challenge is measured by the Social Cost of Carbon (SCC), the economic cost caused by an additional ton of carbon dioxide emissions or its equivalent on a given greenhouse gases emission path. Since its creation in the 90's, despite some setbacks, decisions considering the SCC in the economic analysis account for benefits of one trillion of dollars. The SCC is, thus, the most significant economic concept in the economics of climate change. However, the IAMs computing the SCC only provide us one single pathway, the optimal trajectory. On the contrary, there exists huge uncertainty due to lack of data and incomplete knowledge of the systems we describe (physical as well as economic). Without confidence intervals there is no reliable estimation of any metric. Indeed, since a function's value at one point says little about the whole function, an optimal trajectory says little about the behavior of the entire climate–economy–policy system being considered. Thus, assessing the uncertainty of the SCC is essential for an efficient policy-design methodology.

The purpose of this study is to rigorously assess the uncertainty of the SCC with the framework provided by the DICE model[1]. In a first part, we describe the field of Integrated Assessment Model and therefore present the research strategy we follow in the subsequent part. Consequently, each part represents an additional step towards achieving our objective.

[1]For a complete description of the DICE model, see Annex A on page 46.

1 An introduction to Integrated Assessment Models and the Social Cost of Carbon

The comprehension and modelling of the consequences of global warming on human societies is a daunting challenge. Understanding, but also evaluating and proposing solutions are objectives that the scientific community must achieve. To this end, so-called integrated models have been developed to provide an economic as well as a physical framework for studying climate change. Evaluating and optimizing policies, these models have also developed their own metrics to assess the mitigation of climate. The Social Cost of Carbon is one of them. Present since the 1990s, it plays an essential role in political decision-making on the mitigation of global warming and the limitation of its impacts. However, these models are now, justifiably, under the spotlight of much criticism.

1.1 Different kind of Integrated Assessment Models

Following the definition of [IPCC, 2018], Integrated assessment is a "method of analysis that combines results and models from the physical, biological, economic and social sciences and the interactions among these components in a consistent framework to evaluate the status and the consequences of environmental change and the policy responses to it". Most IAMs can be divided in two categories : Policy Optimization Models (POMs)[2] and Policy Evaluation Models (PEMs). On the one hand, POMs aim at carrying out a cost-benefit analysis[3] of climate change mitigation that compares the abatement costs with the potential impacts due to climate change and thus determine an optimal policy-trajectory. On the other hand, PEMs focus on the cost-effectiveness of a particular policy to achieve a certain mitigation target. The IAMs have two core blocks. The first is an economic module that is represented by an agent who allocates its resources through an inter-temporal optimization problem. The agent chooses how much to consume, to invest, and where to invest (clean or dirty energy?). PEMs model have detailed sectoral information that allow them to compute partial or general equilibrium, whereas POMs aggregate the economic activity to a global (or regional level). From the economic component arises the greenhouse gas emissions. These emissions are handled by the second core feature, the physical module, which translates them into an increase in Global Mean Surface Temperature. What differentiate POMs from PEMs, is a third component : a damage function that links the increasing of temperature with economic damages. This aggregate function simulates the loss of worker productivity, the damages on capital, the decrease of agricultural yields as well as the risk from extreme events. This damage function and the underlying policy-optimization process is very costy in term of computationnal power, which is why POMs have simpler economic module and are more aggregate. They exchange the representation complexity for computation complexity and, thus it allows them to derive the well-known Social Cost of Carbon.

1.2 The Social Cost of Carbon

The SCC is the marginal global cost to society that results from the emission of an extra tonne of carbon at time t along a determined emission trajectory (i.e. it is the shadow price of carbon).

[2]Famous POMs are for example PAGE, FUND or WITCH. The DICE model is a POMs

[3]Climate mitigation policies, on this approach, ought to be pursued to the extent that their marginal future benefits are at least equal to or exceed their present (and future) marginal costs.

The SCC is a key indicator when it comes to global warming mitigation. Used by governments to design their mitigation policy and their regulation strategy [United States Government, 2016], the SCC can also be used to re-assess investment with a consideration of all the resulting CO_2 emissions. As Nordhaus underlines : "The most important single economic concept in the economics of climate change is the Social Cost of Carbon (SCC). At present, regulations with more than $1 trillion of benefits have been written for the United States that use the SCC in their economic analysis." [Nordhaus, 2017]. In fact Despite the significance of such a metric, only a few models are well established as estimators of the SCC. These models are FUND[4], PAGE[5] and DICE. To sum it up, POMs can estimate "policy optimal" trajectory, and therefore produce a widespread indicator, the SCC.

1.3 Criticisms raised against Integrated Assessment Models

However, IAMs are widely criticised by prominent economists [Pinduyk, 2015][6] or philosophers [Frisch, 2013] for many good reasons.

First of all, IAMs are highly sensitive to very uncertain parameters, both in the physical and economic components of the model. The criticisms relative to uncertainty focus on two key parameters, the Equilibrium Climate Sensivity and the intertemporal discount rate. [Pinduyk, 2015] states that we know very little of the Equilibrium Climate Sensivity whereas it is in fact an essential parameter of the physical response of IAMs[7]. The problem with this parameter is that some physical mechanisms that drives the strength of the warming phenomenon remain unknown. Thus, it implies a huge modelling uncertainty on this parameter when estimating it with complex model. Moreover, there is simply a wide uncertainty about the entire climate system. Indeed, there is still very little data to quantify some feedbacks and non-linear phenomena that are not, therfore, taken into account in the POMs. On the economic module side, beyond questions on the level of precision, there is a heated debate on the economic foundations of the used models [Weitzman, 2013]. What hypotheses can be made in terms of behaviour? Should we choose a discounting rate and an elasticity of consumption that correspond to current behaviours or should we have a normative approach? On what philosophical basis can such an approach be built? How then should well-being be defined and quantified [Frisch, 2013]? In the absence of anything better, the used framework is therefore that of neo-classical models by simulating different discount rates, which has a considerable influence on indicators such as the SCC.

What's more there are several issues concerning aggregation. The representative household and firms hypothesis cannot be verified. The climate change damages and risks as well as the level of development are spatially unequally distributed. PEMs can take into account cross-country economic variability but do not have a damage function, while POMs have highly aggregated economic models with damage function. Very few studies currently propose frameworks that deal with the issue of cross-country damages variability [Burke et al., 2015].

[4]FUND model website

[5]PAGE model website

[6]"In a recent article, I argued that Integrated Assessment Models (IAMs) "have crucial flaws that make them close to useless as tools for policy analysis." In fact, I would argue that calling these models "close to useless" is generous: IAM-based analyses of climate policy create a perception of knowledge and precision that is illusory, and can fool policy-makers into thinking that the forecasts the models generate have some kind of scientific legitimacy."

[7]This one of the reason why we propose a new climate module for the DICE model in part 2.

In addition, [Farmer et al., 2015] and [Ackerman et al., 2009] raise the issue of technological change. Most POMs assume exogenous technology progress through the Total Factor of Productivity, the energy efficiency, or the cost of different technologies. However, technological forecasting is highly uncertain and path dependant. To go further, it should be realized that this is the case for all scenario drivers, such as population or greenhouse gas emissions. Along POMs there is a lack of consistent global scenarios that can take into account potential futures.

Finally, the damage function is at the heart of the debate that is stirring researchers, since it is a a feature of primary importance that relies on very little reliable empirical data[8]. How is it possible to imagine or measure the damages of a sustained 3°C GMST anomaly? As most survey use weather data to estimate the impact of temperature on the economy, they are limited to short time periods and small fluctuations in temperature. Is it possible to consider this kind of data as relevant and reliable? Still, this damage function is the element that allow the research of an optimal trajectory (hence, the Social Cost of Carbon), so despite its flaws it is a necessary and useful feature.

1.4 Strategy for this research study

Despite numerous flaws, Policy Optimization Models are widely used to provide guidance for policy design. It is therefore interesting to correct these flaws with better methods and framework. In this study, we focus on the DICE model and try to improve it in order to respond to the defects mentioned in the previous paragraphs[9]. Indeed the most robust estimates possible are necessary when using IAMs as policy-design tool First, we deal with the uncertainty surrounding the future climate with an improved climate model (see part 2) that we calibrate considering observations of past climate as constraints. Then, we run this more efficient model on various consistent scenarios that are widely used in the scientific world. Therefore, it is possible to assess a more robust estimate of the Social Cost of Carbon and compute its uncertainty arising from the existing uncertainty on the depiction of the Earth system.

[8]Pinduyk considers the damage function as "the most speculative element of the analysis" [Farmer et al., 2015]

[9]For a complete description of the DICE model, see Annex A on page 46.

2 The Earth Risk Management (ERM) climate model

In this section, we perform the first step of our effort to improve the DICE model. We present the reasons why a new climate module is necessary for the DICE model, as well as a renovated physical module that represents the state-of-the-art climate science knowledge. Finally, we compare the estimates obtained with this new climate module with the one provided by the classic DICE model.

2.1 Why a new climate module?

As explained in part 1, many criticisms are raised against IAMs, in particular against the DICE model. Thus, we propose to tackle the issue of the representation of the Earth system in the DICE model. However, why should the DICE climate model be considered to be a bad one? Indeed, it is quite simple, but simplicity is no flaw in itself. So, let us understand why the climate module really needs to be changed, although Nordhaus pretends that is model has been calibrated on the latest IPCC's report estimates in [Nordhaus, 2017].

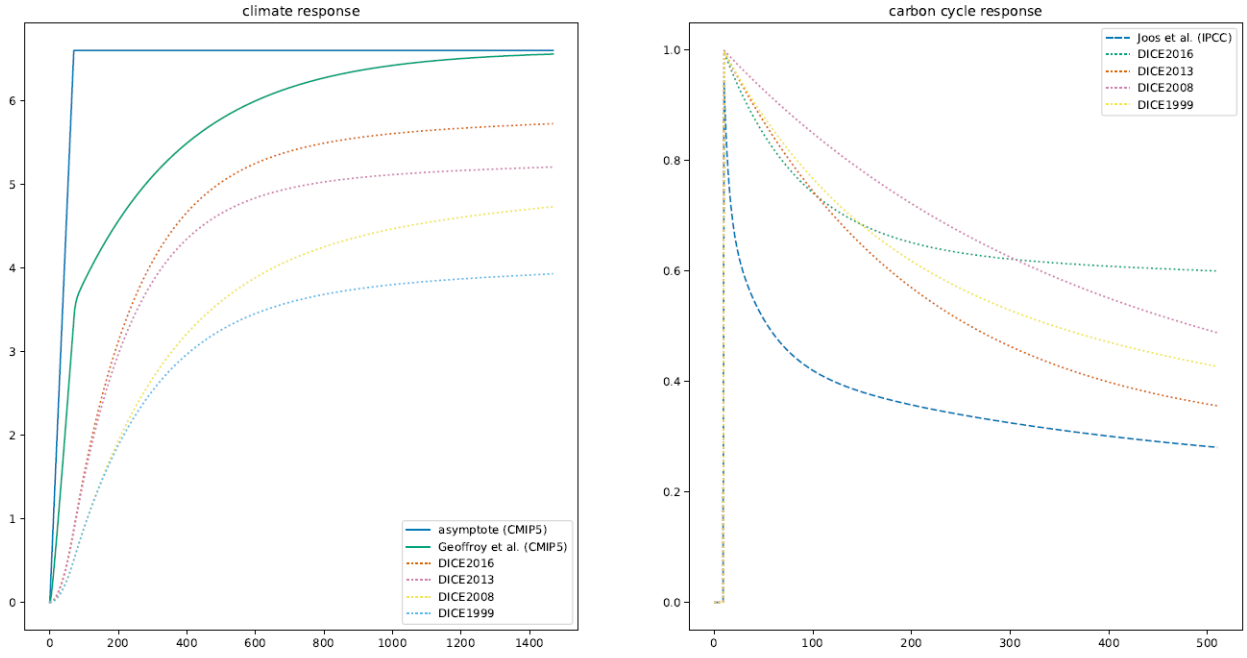

Figure 1: Climate response to a quadrupling of the CO_2 concentration at the Preindustrial equilibrium and Impulse Response Function of the carbon cycle in the current conditions (for more information about IRFs, see Annex B on page 50 or [Enting, 2007]), the horizontal scale is in year

The figure 1 on page 8 shows us the assessment of the two main features of the DICE climate model : the climate response to a variation of the CO_2 concentration and the response of the carbon cycle to CO_2 emissions (to get information on the design of the model, see Annex A.3 on page 48).

The first graph on the figure allows us to compare the climate responses of the consecutive DICE models presented in [Nordhaus, 2013] with the two-box model developed in [Geoffroy et al., 2013b] and [Geoffroy et al., 2013a] that is calibrated on the CMIP5 outputs (i.e. the best guesses of the current knowledge in the climate science field). It shows us two things. On the one hand, that the DICE model climate dynamics is too slow : looking at the beginning of the curve, it is possible to see that the short-term characteristic time is much longer than the one of the CMIP5 outputs. The dynamics of the DICE model climate module is not reliable. On the other hand, that the convergence temperature (known as the Equilibrium Climate Sensivity (ECS)) is completely different : the DICE model climate response warms less in the very long term. To sum it up, the climate response of the DICE model physical module is slower and weaker than the one provided by state-of-the-art GCMs.

The second graph presents us the IRF of the atmosphere to the emission of CO_2. It can be understood as follows : if one unit of CO_2 is emitted in the atmosphere at time 0, what percentage of this unit does remain in the atmosphere at time t (considering a constant GMST). The comparison here is made with a model developed in [Joos et al., 1996], still recognised as a precise and rigorous model, despite its not being recent. What it shows is that DICE carbon cycle retains more carbon in the atmosphere and has a characteristic time that is clearly longer than it should. In a nutshell, the DICE model carbon cycle stores more carbon and is slower than the actual Earth carbon cycle.

It is interesting to notice that both flaws in the carbon cycle and in the climate response balance themselves, so that considering emissions as the input and temperature as the output, the DICE physical module seems to be accurate and reliable whereas the internal dynamic is faulty. This is a serious problem, because it prevents the estimates of the model from being properly compared with any more complex climate model. These flaws are the reason why, developing a new climate model for the DICE model is especially interesting. More over, a new climate should also allow us to compute estimates that are used in the climate science field such as the different carbon sink fluxes or the ocean heat content and might help to bridge the gap mentioned in [Calel and Stainforth, 2017] between economists and climate scientists. Finally, with Bayesian calibration coupled with a large Monte Carlo sampling we estimate various uncertainties over the output of the DICE model as reported in Part 3 on page 31. So, now that we are convinced that a new climate is necessary and useful, let us present the model itself, the Earth Risk Management (ERM) climate model.

2.2 Representation of the ERM climate model

The ERM climate model is a very compact and simplified climate that emulates at first the carbon cycle and then the climate response. It is represented on figure 2 on page 10. On this figure, each block stands for a part of the system that is parametrized by a relevant set of variables. Arrows between blocks represent the relations between these variables that often take the form of differential equations (see Part 2.3 page 10).

Firstly, **grey blocks figure the inputs of the model** that are known as drivers. In the DICE model, the emissions from fossil-fuels are an output of the economical model (see Annex A.2 page 46). On the contrary, emissions from land-use change and the non-CO_2 Radiative Forcing are completely exogenous. Moreover, **the green blocks represent the carbon**

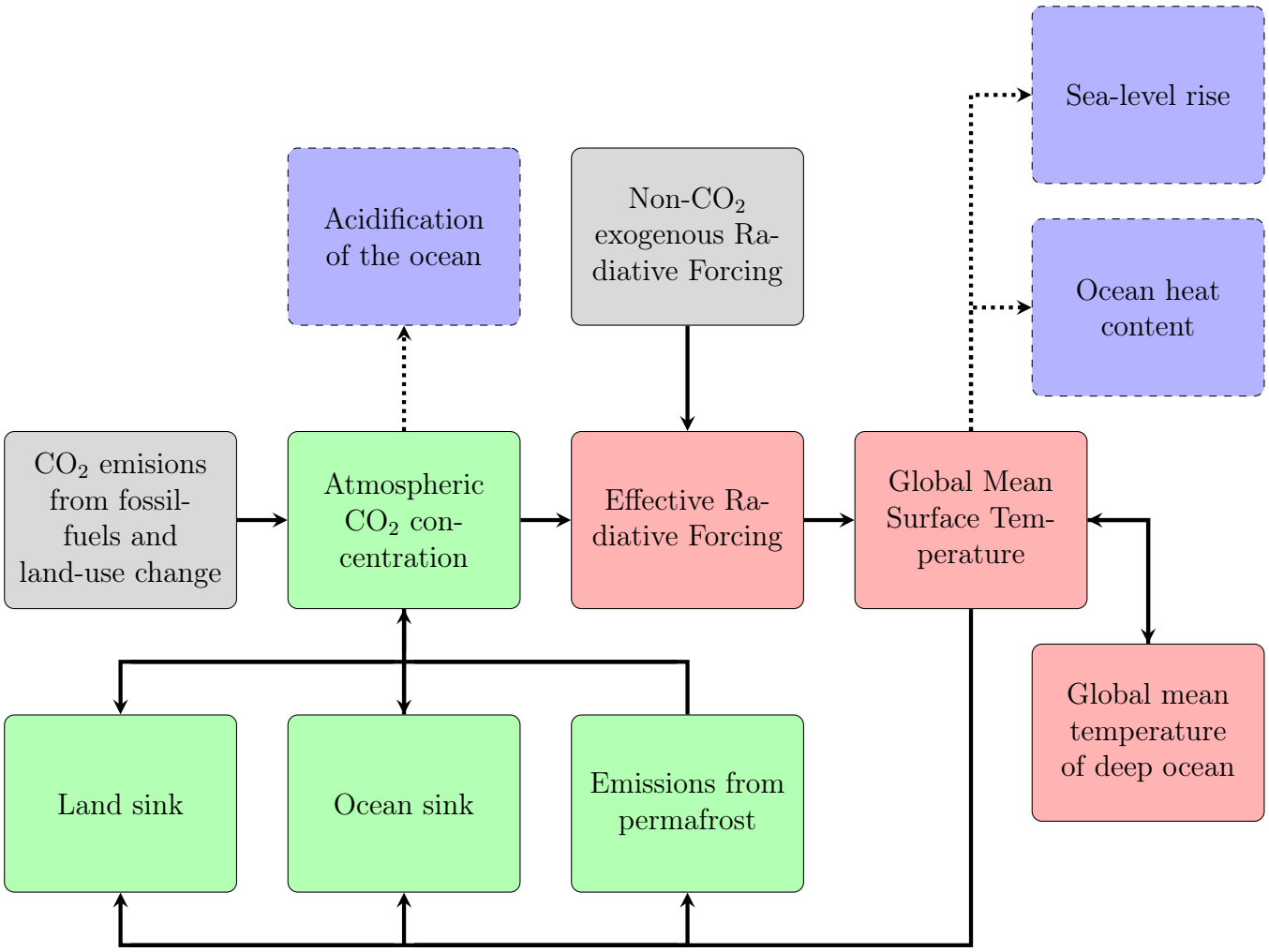

Figure 2: The ERM climate model in a nutshell

cycle. It consists of four blocks that stand for the atmosphere, the land carbon uptake, the ocean carbon uptake and the emissions from thawing permafrost. **The climate response is represented by the three red-colored blocks**. What is noteworthy is that there is a feedback of the climate response (through the GMST anomaly) on the climate cycle. Finally, **the blue blocks with the dotted arrows are impacts** that can be derived from the variables of the model.

2.3 Description of the ERM climate model

As said previously, the ERM climate model is a box-model. Using box-model is a very simple and efficient idea, that corresponds to the use of an approximation of the Laplace transformation of the system response function ([Enting, 2007] and Annex B page 50). Thus, our model does not completely show and use the physical mechanisms behind the phenomenon it describes (for instance, the ocean is not spatially divided in seven parts even if the Ocean sink model is comprised of seven boxes), but sometimes uses as division units (For instance, the division of the Land sink model relies on the structure of the biosphere and the distinction between surface and deep ocean is based on the actual structure of the ocean). We will now present the different parts of the model in the following order, first the carbon cycle, then the climate

response and finally the impacts that derive from the model.

2.3.1 Carbon Cycle

The carbon cycle is a very complex system, with still a lot to do to improve our understanding of its functioning. The Figure 3 on page 11 is a simplified schematic of the global carbon cycle that comes from [IPCC, 2013]. Numbers represent reservoir mass, also called 'carbon stocks' in PgC (1 PgC = 10^{15} gC) and annual carbon exchange fluxes (in PgC.yr^{-1}).

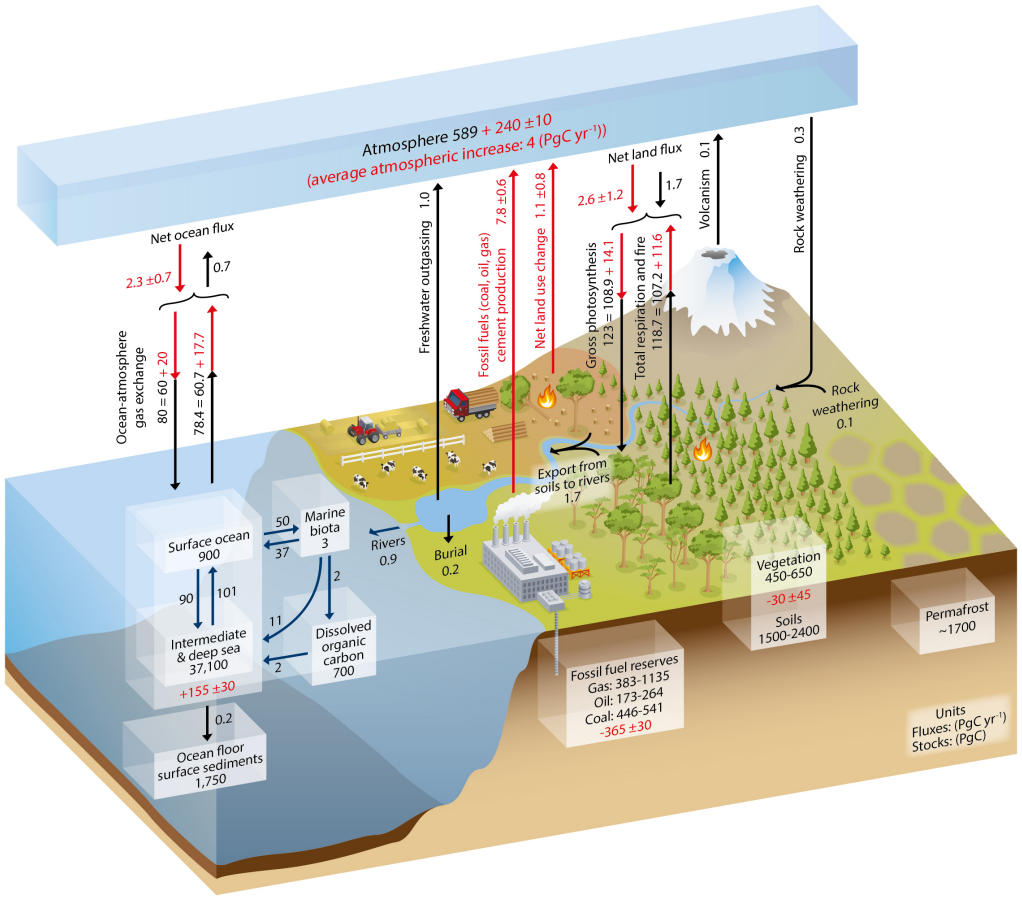

Figure 3: Schematic representation of the global carbon cycle [IPCC, 2013]

In the following paragraphs, we propose an obviously quite simple - but very efficient for our purpose - model of the carbon cycle. As it is possible to see on Figure 2 page 10, our carbon cycle model consists of four key elements (the green boxes) that finally provide us the atmospheric concentration of CO_2.

Land sink The model for the land sink is a global land module inspired from the OSCAR model described in [Gasser et al., 2017]. Its objective is to present the action of the biosphere as a carbon sink that is driven by the CO_2 concentration in the atmosphere and the GMST. Originally, the OSCAR model has nine spatially explicit regions in which there exist six biomes whose list is bare soil, forests, mix of grasslands and shrublands, croplands, and pasture. Each biome in each region has its own characteristics. For example, the Boreal forest and the Amazonian rainforest are both considered as forest but they have different characteristics that

distinguish them. However, in our model, we use a global model, which means that we limit ourselves to a single region with a single biome that represent the average biosphere of planet Earth. The model is represented in Figure 4 on page 12 and its different elements are presented in Table 1 on page 13. One strong hypothesis is that the land-use change has a negligible influence on the parameters of our land sink model, which is questionable as the deforestation has a direct impact on the ability of the forests to store carbon.

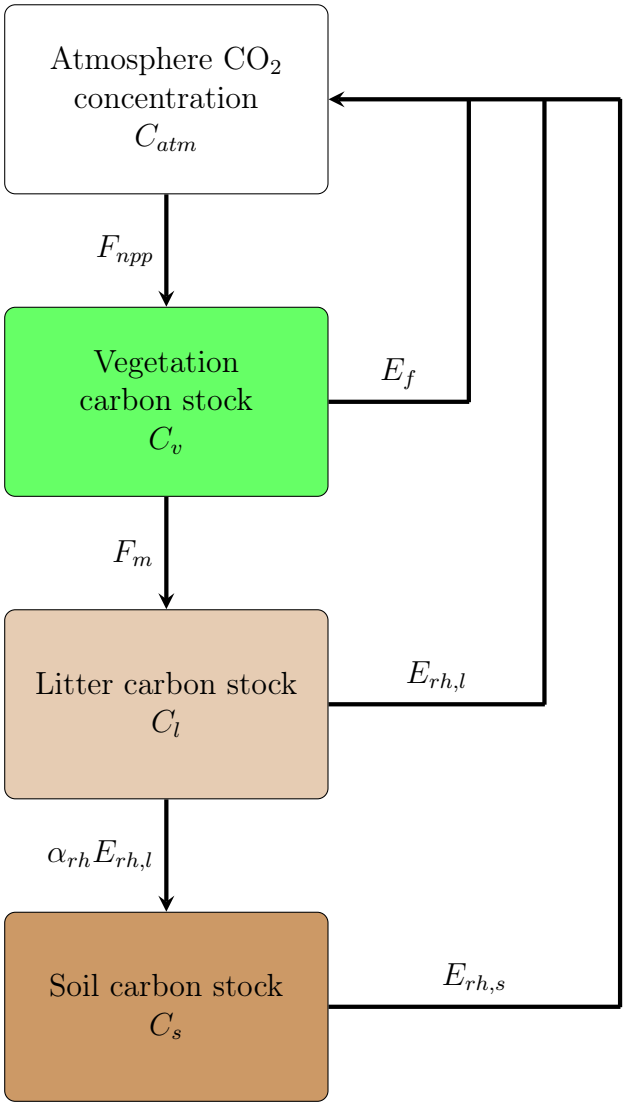

Figure 4: The land sink model of the ERM climate model

Our model presents the biosphere as a set of three carbon pools: vegetation, litter and soil. These pools exchange carbon through various fluxes that we characterise in order to find the dynamic of the carbon stocks. The equations leading these fluxes are as follows:

$$F_{npp} = F_{npp}[0] \left(1 + \beta_{npp} \log(\frac{C_{atm}}{C_{atm}[0]})\right) (1 + \gamma_{npp} T_{surface}) \tag{1}$$

The pressure dependence of the NPP corresponds to the phenomenon known as effect of fertilization. Wildfires consume a part of the biomass each year, and their intensity is an increasing

Inputs	Description	Unit
C_{atm}	Global atmospheric CO_2 concentration	ppm
$T_{surface}$	GMST anomaly	K
Variables	**Description**	**Unit**
F_{land}	Land carbon sink (positive if the land removes CO_2 from the atmosphere)	$GtC.yr^{-1}$
F_{npp}	Global net primary productivity	$GtC.yr^{-1}$
E_f	Global emissions from wildfire	$GtC.yr^{-1}$
F_m	Global mortality flux	$GtC.yr^{-1}$
E_{rh}	Global heterotrophic respiration	$GtC.yr^{-1}$
C_v	Global vegetation carbon pool	GtC
C_l	Global litter carbon pool	GtC
C_s	Global soil carbon pool	GtC
Parameters	**Description**	**Unit**
$C_{atm}[0]$	Reference preindustrial atmospheric CO_2 concentration	ppm
$F_{npp}[0]$	Preindustrial Net Primary Productivity	$GtC.yr^{-1}$
$E_f[0]$	Preindustrial emissions from wildfire	$GtC.yr^{-1}$
$E_{rh}[0]$	Preindustrial heterotrophic respiration	$GtC.yr^{-1}$
$C_v[0]$	Preindustrial vegetation carbon pool	GtC
$C_l[0]$	Preindustrial litter carbon pool	GtC
$C_s[0]$	Preindustrial soil carbon pool	GtC
β_{npp}	Logarithmic sensitivity of NPP to CO_2	
γ_{npp}	Linear sensitivity of NPP to $T_{surface}$	K^{-1}
β_{ef}	Linear sensitivity of E_f to C_{atm}	ppm^{-1}
γ_{ef}	Linear sensitivity of E_f to C_{atm}	K^{-1}
β_{rh}	Linear sensitivity of the heterotrophic respiration to C_{atm}	ppm^{-1}
γ_{rh}	Exponential sensitivity of the heterotrophic respiration to C_{atm}	K^{-1}
α_{rh}	Factor for metabolization of litter carbon to soil carbon	

Table 1: Land sink model elements

function of the GMST anomaly. The effect of CO_2 concentration variation is related to evapotranspiration.

$$E_f = \frac{E_f[0]}{C_v[0]} \left(1 + \beta_{ef} \left(C_{atm} - C_{atm}[0]\right)\right) \left(1 + \gamma_{ef} T_{surface}\right) C_v \tag{2}$$

The biomass dies at a rate that is proportional to its quantity.

$$F_m = \frac{E_{rh}[0]}{C_v[0]} C_v \tag{3}$$

$$E_{rh,l} = \frac{1}{1+\alpha_{rh}} \frac{E_{rh}[0]}{C_l[0]} \left(1 + \beta_{rh} \left(C_{atm} - C_{atm}[0]\right)\right) \exp(\gamma_{rh} T_{surface}) C_l \tag{4}$$

$$E_{rh,s} = \frac{\alpha_{rh}}{1+\alpha_{rh}} \frac{E_{rh}[0]}{C_s[0]} \left(1 + \beta_{rh} \left(C_{atm} - C_{atm}[0]\right)\right) \exp(\gamma_{rh} T_{surface}) C_s \tag{5}$$

Thus the differential equations that characterise the system are the following :

$$\frac{dC_v}{dt} = F_{npp} - E_f - F_m \tag{6}$$

$$\frac{dC_l}{dt} = F_m - (1 + \alpha_{rh})E_{rh,l} \tag{7}$$

$$\frac{dC_s}{dt} = \alpha_{rh})E_{rh,l} - E_{rh,s} \tag{8}$$

Which finally gives us the value of the land sink :

$$F_{land} = F_{npp} - E_f - E_{rh,l} - E_{rh,s} \tag{9}$$

The Preindustrial equilibrium implies :

$$0 = F_{npp}[0] - E_f[0] - E_{rh}[0] \tag{10}$$

In the OSCAR model, parameters are calibrated on nine global vegetation model, we use these parameters and their uncertainties to perform a Bayesian calibration as explained in Part 3 on page 31.

Ocean sink In order to model the ocean action as a carbon sink, we use the so-called Mix-layer pulse response function model that is firstly described in [Joos et al., 1996]. The main particularity and advantge of this model is that it allows us to take efficiently into account the carbonate chemistry and its non-linearities due to chemical balances corresponding to the CO_2 dissolution into water:

$$\mathrm{CO_{2(g)}} \rightleftharpoons \mathrm{CO_{2(aq)}} \tag{11}$$

$$\mathrm{CO_{2(aq)} + H_2O_{(l)}} \rightleftharpoons \mathrm{HCO^-_{3(aq)} + H^+_{(aq)}} \rightleftharpoons \mathrm{CO^{2-}_{3(aq)} + 2H^+_{(aq)}} \tag{12}$$

These reactions are also the ones that explain the acidification of the ocean through the formation of carbonic acid (see the Acidification of the ocean part on page 21 for more information). These effects are modelled as follows : the carbon flux from the atmosphere to the mix-layer of the ocean is proportional to the difference of CO_2 partial pressure (converted in ppm) between the atmosphere and the surface of the ocean (drivers, variables and parameters of the ocean sink model are presented in Table 2 on page 15) :

$$F_{ocean} = k_g \alpha_{CO_2} \left(C_{atm} - pCO_{2,ocean}\right) \tag{13}$$

Where the CO_2 partial pressure in the surface ocean is computed as follows [Takahashi et al., 1993] [Joos et al., 1996] :

$$pCO_{2,ocean} = \left(f_p\left(\frac{\alpha_{dic}}{\alpha_{CO_2}} C_{ocean}\right) + C_{atm}[0]\right) \exp\left(\gamma_{dic}\alpha_{sst} T_{surface}\right) \tag{14}$$

With f_p defined as follows (λ_k, μ_k and n_k are given in the Table 3 on page 16):

$$f_p(x) = \sum_{k=1}^{5} \left(\lambda_k + \mu_k T_{ocean,0}\right) x^k \times 10^{-n_k} \tag{15}$$

With this framework, the carbon stocked in the mix-layer is:

$$C_{ocean}(t) = \int_0^t F_{ocean}(t') r_{surface}(t - t') dt' \tag{16}$$

Inputs	Description	Unit
C_{atm}	Global atmospheric CO_2 concentration	ppm
$T_{surface}$	GMST anomaly	K
Variables	**Description**	**Unit**
F_{ocean}	Ocean carbon sink (positive if the ocean removes CO_2 from the atmosphere)	$GtC.yr^{-1}$
$pCO_{2,ocean}$	Partial pressure of CO2 in the surface ocean	ppm
C_{ocean}	Change in carbon pool in the surface ocean	Gtc
$C_{ocean,j}$	Change in carbon pool of one of the sub-box of the model	Gtc
Parameters	**Description**	**Unit**
$C_{atm}[0]$	Reference preindustrial atmospheric CO_2 concentration	ppm
α_{CO_2}	Conversion factor for atmospheric CO_2	$GtC.yr^{-1}$
k_g	Speed of gas exchange between the atmosphere and ocean surface	$yr^{-1}.(A_{ocean}^{-1})$
H_{ocean}	Average depth of the surface ocean (assumed well-mixed)	m
A_{ocean}	Area of the surface ocean	m^2
$T_{ocean,0}$	Preindustrial temperature of the surface ocean	K
$\alpha_{ocean,j}$	Fractions for each sub-box of the impulse response function (with $\sum \alpha_{ocean,j} = 1$)	
$\tau_{ocean,j}$	Timescales of each sub-box of the impulse response function	yr
γ_{dic}	Sensitivity of CO_2 solubility to global sea-surface temperature anomaly	K^{-1}
β_{dic}	Scaling parameter for the conversion from concentration in the surface ocean to the CO_2 partial pressure	
α_{sst}	Scaling factor between global air and sea-surface temperatures anomaly	
Ancillary parameters	**Description**	**Unit**
$c_{conversion}$	Conversion parameter between $ppm.m^{-2}.yr^{-1}$ into $\mu mol.m.kg.^{-2}$ $c_{conversion} = 1.722 * 10^{17} \mu mol.m^3.ppm^{-1}.kg^{-1}$	$\mu mol.m^3 .ppm^{-1}.kg^{-1}$
α_{dic}	Conversion factor for carbon in the surface ocean $\alpha_{dic} = \frac{c_{conversion}}{H_{ocean} A_{ocean} \beta_{dic}}$	μ $mol.kg^{-1}$ .GtC^{-1}
f_p	Function to emulate the carbonate chemistry	
$r_{surface}$	Impulse Response Function of the mix-layer	

Table 2: Ocean sink model elements

By approximately decomposing $r_{surface}$ as a sum of exponentially decreasing function (parameters α_j and τ_j are given in Table 4 on page 17 and coming from [Strassmann and Joos, 2018]):

$$r_{surface}(t) = \sum_{j=1}^{7} \alpha_j \exp\left(-\frac{t}{\tau_j}\right) \tag{17}$$

The equivalent representation of the system is given by the Figure 5 on page 16. Thus, each sub-box follows the following equation :

$$\forall j \in [1,7], \frac{dC_{ocean,j}}{dt}(t) + \frac{C_{ocean,j}}{\tau_j}(t) = \alpha_j F_{ocean}(t) \tag{18}$$

Emissions from permafrost The Earth Risk Management (ERM) climate model presents also a permafrost module, a system, whose response to the Global Mean Surface Temperature

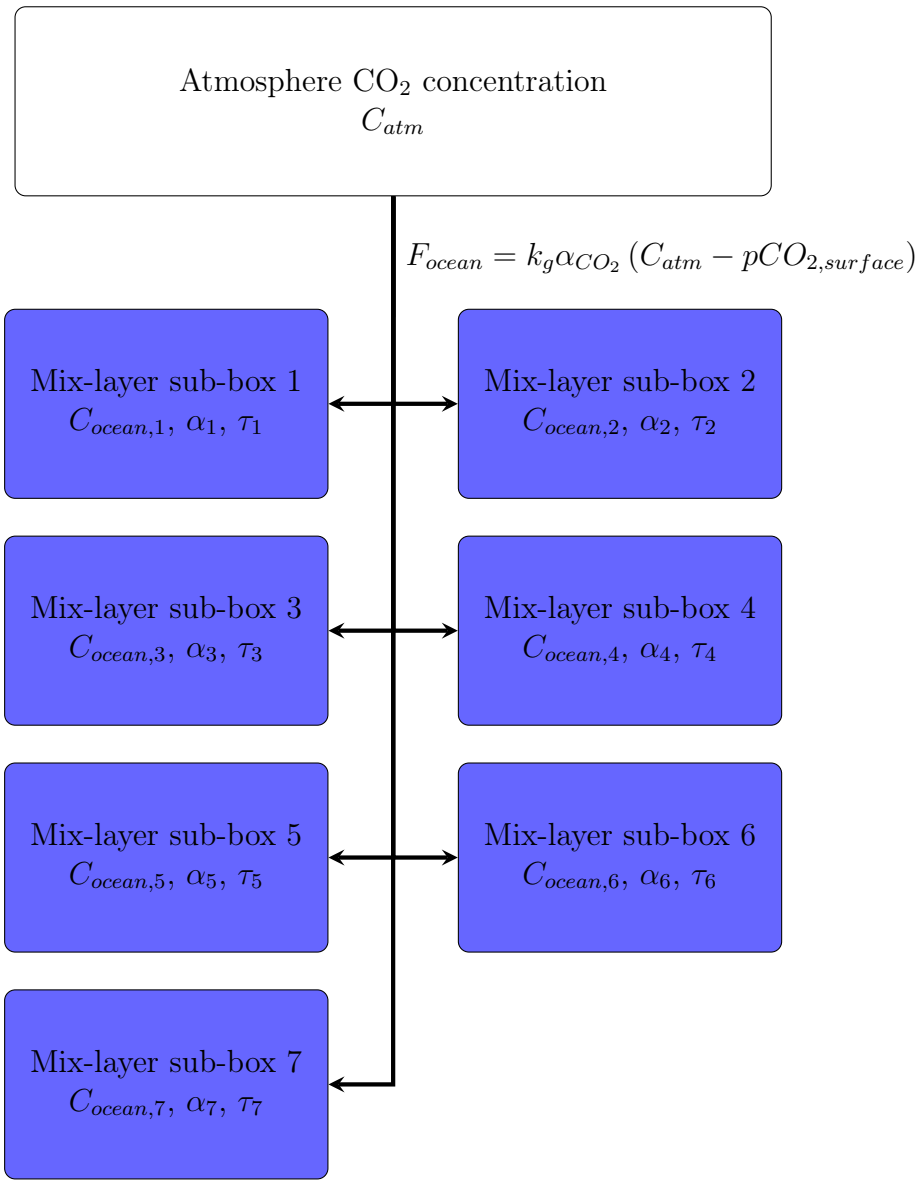

Figure 5: The ocean sink model of the ERM climate model

k	λ_k	μ_k	n_k
1	1.5568	-0.013993	0
2	7.4706	-0.20207	3
3	1.2748	-0.12015	5
4	2.4491	-0.12639	7
5	-1.5768	0.15326	10

Table 3: CO_2 partial pressure function parameters

(GMST) anomaly is highly non-linear. This is quite innovative, as very few models or studies take into account the thawing of permafrost, mainly because of the lack of data on the carbon stock frozen in the ground and the dynamics of its emission. In this study, we use a global permafrost model that includes both North-American and Eurasian carbon pools that comes from [Gasser et al., 2018]. Our permafrost is represented as an initially frozen carbon pool

j	α_j	τ_j(yr)
1	0.24014	0.03855
2	0.27830	0.45254
3	0.23337	2.1990
4	0.13733	12.038
5	0.051541	59.584
6	0.035033	237.31
7	0.022936	∞

Table 4: Ocean surface response function parameters

that thaws, driven by the increase in GMST. The carbon resulting from thawing permafrost is not immediately emitted but shared into several carbon pools each of them following a law of exponential decrease. The model is presented in Figure 6 on page 17 and its drivers, variables and parameters are on the Table 5 on page 18. First and foremost, we suppose the existence

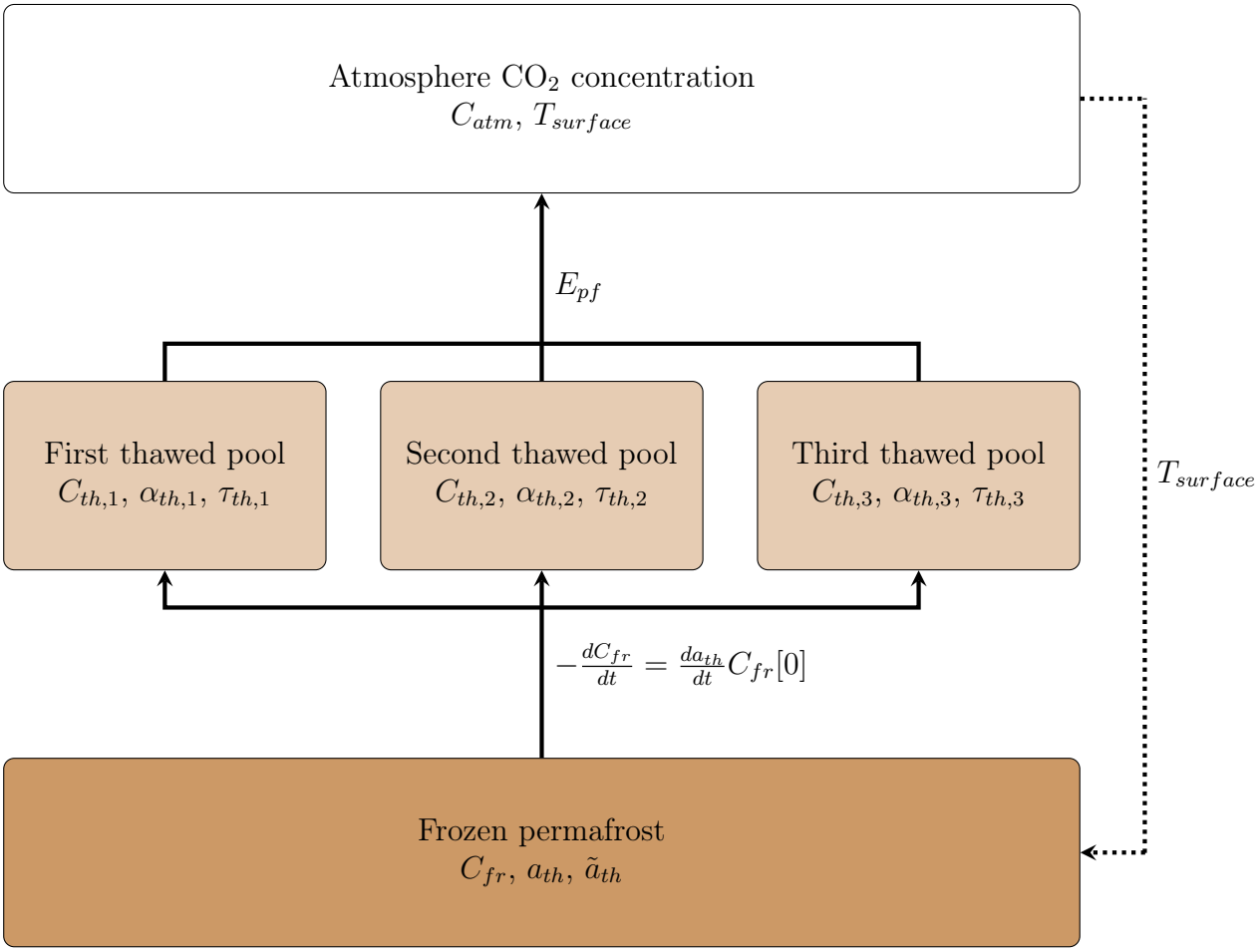

Figure 6: The ocean sink model of the ERM climate model

of a theoretical thawed fraction of permafrost $\tilde{a}_{th}$ that is 0 at the Preindustrial equilibrium and range between -p_{min} (meaning that the permafrost can freeze even more and capture carbon) and 1 (in this case the permafrost is entirely thawed). The expression of $\tilde{a}_{th}$ is given as follows

Inputs	Description	Unit
$T_{surface}$	GMST anomaly	K
Variables	Description	Unit
E_{pf}	Global emissions from permafrost	GtC.yr^{-1}
$\tilde{a}_{th}$	Theoretical thawed fraction	
a_{th}	Actual thawed fraction	
$C_{th,1}$	First thawed carbon pool	GtC
$C_{th,2}$	Second thawed carbon pool	GtC
$C_{th,3}$	Third thawed carbon pool	GtC
C_{fr}	Frozen carbon pool	GtC
Parameters	Description	Unit
$C_{fr}[0]$	Preindustrial permafrost carbon pool	GtC
α_{lst}	Scaling factor between global and local temperatures	
γ_{rt1}	Sensitivity of heterotrophic respiration to $T_{surface}$	K^{-1}
γ_{rt2}	Sensitivity of heterotrophic respiration to $T^2_{surface}$	K^{-2}
p_{min}	Minimum theoretical thawed fraction	
κ_p	Shape parameter for theoretical thawed fraction	
γ_p	Sensitivity parameter to T$_{surface}$ for theoretical thawed fraction	K^{-1}
ν_{thaw}	Thawing speed	yr^{-1}
ν_{froz}	Freezing speed	yr^{-1}
$\tau_{th,j}$	Timescale of emission for the j-th thawed pool	yr
$\alpha_{th,j}$	Fraction for the j-th thawed pool such that $\alpha_{th,1} + \alpha_{th,2} + \alpha_{th,3} = 1$	
κ_{rt}	Scaling factor for the sensitivity of heterotrophic respiration to $T_{surface}$	

Table 5: Permafrost model elements

with $\alpha_{lst}T_{surface}$ used as a proxy of the local mean temperature anomaly:

$$\tilde{a}_{th} = -p_{min} + (1 + p_{min}) \left(1 + \left(\left(\frac{1}{p_{min}} + 1\right)^{\kappa_p} - 1\right) \exp\left(-\gamma_p \kappa_p \alpha_{lst} T_{surface}\right)\right)^{-\frac{1}{\kappa_p}} \tag{19}$$

The permafrost dynamics is asymmetric because the thawing speed and the freezing speed are different.

$$\frac{da_{th}}{dt} = \nu(\tilde{a}_{th} - a_{th}) \tag{20}$$

With ν :

$$\nu = \begin{cases} \nu_{thaw}, & \text{if } a_{th} < \tilde{a}_{th}. \\ \nu_{froz}, & \text{if } a_{th} > \tilde{a}_{th}. \end{cases} \tag{21}$$

Hence the dynamics of the frozen pool :

$$\frac{dC_{fr}}{dt} = -\frac{da_{th}}{dt} C_{fr}[0] \tag{22}$$

The flux is then shared into three carbon pools with their own characteristic time. The exponential decrease that appears is due to the heterotrophic respiration (organisms in the soil and the litter reject progressively the thawed carbon into the atmosphere) :

$$\forall j \in [1,3], \frac{dC_{th,j}}{dt} = -\alpha_{th,j}\frac{dC_{fr}}{dt} - \frac{1}{\tau_{th,j}} \exp\left(\kappa_{rt}\left(\gamma_{rt1}\alpha_{lst}T_{surface} - \gamma_{rt2}\left(\alpha_{lst}T_{surface}\right)^2\right)\right) \tag{23}$$

j	$\alpha_{th,j}$	$\tau_{th,j}$(yr)
1	8.054512776004199	0.027633473810345373
2	275.5876926027671	0.1483615603989628
3	3792.542282788026	0.8240049657906918

Table 6: Thawed permafrost response function parameters

With parameters $\alpha_{th,j}$ and $\tau_{th,j}$ presented in Table 6 on page 19, we notice that the system is operating on a very long-term time-scale which explains why there are only a few observation of the emissions from thawing permafrost. Finally we obtain the carbon emissions from permafrost :

$$E_{pf} = -\sum_{j=1}^{3} \frac{dC_{th,j}}{dt} - \frac{dC_{fr}}{dt} \tag{24}$$

These emissions are considered to be 100% CO_2 whereas, in fact, CH_4 accounts for 2.3% of the carbon emissions of the permafrost [Gasser et al., 2018]. However, as there is no CH_4 cycle in this study, it is more useful and convenient to make this hypothesis.

Atmospheric CO_2 concentration The CO_2 atmospheric concentration is obtained with a simple overall matter balance (summary Table 7 is on page 19):

$$\alpha_{CO_2} \frac{dC_{atm}}{dt} = E - F_{land} - Focean + E_{pf} \tag{25}$$

Inputs	Description	Unit
E	Fossil-fuels and land-use change emissions	GtC.yr^{-1}
F_{land}	Land Carbon sink	GtC.yr^{-1}
F_{ocean}	Ocean carbon sink	GtC.yr^{-1}
E_{pf}	Global emissions from permafrost	GtC.yr^{-1}
Variables	Description	Unit
C_{atm}	Global atmospheric CO_2 concentration	ppm
Parameters	Description	Unit
α_{CO_2}	Conversion factor for atmospheric CO_2	GtC.ppm^{-1}

Table 7: Permafrost model elements

2.3.2 Climate response

On Figure 2 page 10, the climate response is composed of the three red blocks, that provide the Global Mean Surface Temperature and the global mean temperature of deep ocean.

Effective Radiative Forcing The Radiative Forcing is a key metric in terms of climate change study and assessment because it acts as an intermediate variable between gas concentration in the atmosphere and Global Mean Surface Temperature change. Hence, it allows researchers to derive impacts from individual factors, such as a particular gas (despite the immense complexity of atmospheric chemistry), which is particularly relevant concerning, for

instance, policy-design. According to [IPCC, 2014a], the Radiative Forcing is defined as : "the net change in the energy balance of the Earth system due to some imposed perturbation. It is usually expressed in watts per square meter averaged over a particular period of time and quantifies the energy imbalance that occurs when the imposed change takes place." In this study, we use a very close metric, the Effective Radiative Forcing (ERF), that includes what is called rapid adjustments and "makes ERF a better indicator of the eventual global mean temperature response" [IPCC, 2014a]. From the Table 8.SM.1 of [IPCC, 2014b], we obtain the ERM model formula whose elements appear in Table 8 on page 20 :

$$ERF = \phi \ln\left(\frac{C_{atm}}{C_{atm}[0]}\right) + ERF_{ex} \tag{26}$$

Where F_{ex} is the non-CO_2 ERF and gathers various effects such as other greenhouse gases

Inputs	Description	Unit
C_{atm}	Global atmospheric CO_2 concentration	ppm
ERF_{ex}	Exogenous non-CO_2 Effective Radiative Forcing	W.m^{-2}
Variables	Description	Unit
ERF	Effective Radiative Forcing	W.m^{-2}
Parameters	Description	Unit
ϕ	Radiative parameter for CO_2	W.m^{-2}
$C_{atm}[0]$	Preindustrial reference atmospheric CO_2 concentration	ppm

Table 8: Effective Radiative Forcing computation elements

(CH_4, N_2O ...), halogenated compounds, aerosols, volcanic activity. In the DICE model, it is set exogenously, as the model is not complex enough to take all these effects into account (and because the model focuses on the CO_2 emissions and their impact). Likewise, non-CO_2 is an exogenous driver in the ERM climate model.

Global Mean Surface Temperature In order to get the GMST climate response due to radiative forcing (i.e.energy imbalance in the Earth system we use the two-box model described in [Geoffroy et al., 2013b] and [Geoffroy et al., 2013a]. This model is broadly the same as the one used in the DICE model with different values for the parameters and an explicit physical interpretation. It is composed of two layers, one that stands for the Earth surface and the other one that features the deep ocean. The equation describing the Global Mean Surface Temperature variation is coupled with the one describing the deep ocean as the two layers exchange heat flux :

$$\Theta_{surface}\frac{dT_{surface}}{dt} = ERF - \frac{\phi \ln(4)}{T_{4\times}}T_{surface} - \theta_{exchange}\left(T_{surface} - T_{deepocean}\right) \tag{27}$$

One of the most important parameters of compact climate models appear in this equation, the equilibrium temperature under quadrupled preindustrial atmospheric CO_2, which is also known as the Equilibrium Climate Sensivity (ECS). It is a prominent parameter because it has a major effect on the dynamics (and the outputs) of a box-model such as the one we use. This prominence is reinforced because the ECS is only estimated with a huge uncertainty : in [Geoffroy et al., 2013b], the comparison between several GCMs gives a $T_{4\times}$ average of 6.975K with a standard deviation of 1.98K (considering a normal distribution, the 95% confidence interval is consequently $[3.1, 10.9]$).

Global mean temperature of deep ocean The heat exchange flux from the surface to the ocean warms the deep ocean :

$$\Theta_{deepocean}\frac{dT_{deepocean}}{dt} = \theta_{exchange}\left(T_{surface} - T_{deepocean}\right) \tag{28}$$

All elements of this model are compiled in Table 9 on page 21.

Inputs	Description	Unit
ERF	Effective Radiative Forcing	W.m^{-2}
Variables	Description	Unit
$T_{surface}$	Global Mean Surface Temperature (GMST) anomaly	K
$T_{deepocean}$	Deep ocean mean temperature anomaly	K
Parameters	Description	Unit
ϕ	Radiative parameter for CO_2	W.m^{-2}
$T_{4\times}$	Equilibrium temperature under quadrupled preindustrial atmospheric CO_2 (ECS)	K
$\Theta_{surface}$	Heat capacity of the surface : atmosphere, land and upper ocean	W.m^{-2}.yr.K^{-1}
$\Theta_{deepocean}$	Heat capacity of the deep ocean	W.m^{-2}.yr.K^{-1}
$\theta_{exchange}$	Heat exchange coefficient	W.m^{-2}.K^{-1}

Table 9: Temperature variation model elements

In [Geoffroy et al., 2013a], is made the hypothesis of an efficiency parameter in the heat exchange flux between the surface and the deep ocean. We took this into account in our study but it does not appear, because it is mathematically completely equivalent as it is underlined in the very same study.

2.3.3 Deriving impacts

With the ERM model, it is possible to derive estimates of certain impacts that are relevant to assess the physics of the model (such as the Ocean heat content), or the impacts on sectors that are not considered in the DICE model like the Acidification of the ocean or the Sea-level rise.

Acidification of the ocean It is the on-going decrease in the pH of the Earth's ocean due to the carbon uptake action of the ocean that increases the quantity of carbonic acid in the ocean (see equations (11) and (12) on page 14). Increasing acidity of the ocean could jeopardize marine ecosystems, and hence disrupt provision of goods and services related to the ocean : the consequences of this acidification could be very harmful to the human societies and their environments, which is why it is a very valuable estimate when trying to forecast the future. Thanks to the estimates provided in [Bernie et al., 2010] it is possible to compute the pH of the ocean along an estimation of the atmosphere concentration. According to this paper, it is possible to apply the rather simple formula :

$$pH = \kappa_{pH}\left(8.55 - 0.00173 \times C_{atm} + 1.3264 \times 10^{-6} \times C_{atm}^2 - 4.4943 \times 10^{-10} \times C_{atm}^3\right) \tag{29}$$

Here, the parameter κ_{ph} is only a scaling factor used for uncertainty analysis, its default value is 1.

Sea-level rise It is one of the major risk on human societies because it threatens areas like river deltas that are very densely populated or small islands by causing coastal erosion, submergence or coastal flooding. According to [IPCC, 2014d] "Without adaptation, hundreds of millions of people will be affected by coastal flooding and will be displaced due to land loss by year 2100." These are very good reasons to estimate the sea-level rise on the pathways that are computed by the DICE model. We obtain these estimates with the simple model described in [Goodwin et al., 2017]. In this model, the two main sources of the sea-level rise, the ice melt and the thermal extension are dealt with separately and summed to get the total sea-level rise. The equation of the model are the following and the elements of the model are presented on Table 10 on page 22:

Inputs	Description	Unit
$T_{surface}$	Global Mean Surface Temperature (GMST) anomaly	K
$T_{deepocean}$	Deep ocean mean temperature anomaly	K
Variables	Description	Unit
H_{sea}	Global sea level rise	mm
H_{thx}	Global sea level rise from thermal expansion	mm
H_{ice}	Global sea level rise from ice melt: glaciers and ice sheets	mm
Parameters	Description	Unit
$\Theta_{surface}$	Heat capacity of the surface : atmosphere, land and upper ocean	$W.m^{-2}.yr.K^{-1}$
$\Theta_{deepocean}$	Heat capacity of the deep ocean	$W.m^{-2}.yr.K^{-1}$
Λ_{thx}	equilibrium sea-level rise from thermal expansion	$mm.K^{-1}$
Λ_{ice}	equilibrium sea-level rise from ice melt	$mm.K^{-1}$
τ_{thx}	Timescale of sea-level rise from thermal expansion	yr
τ_{ice}	Timescale of sea-level rise from ice melt	yr

Table 10: Sea-level rise model elements

$$\frac{dH_{thx}}{dt} = -\frac{H_{thx}}{\tau_{thx}} + \frac{\Lambda_{thx}}{\tau_{thx}} \frac{\Theta_{surface} T_{surface} + \Theta_{deepocean} T_{deepocean}}{\Theta_{surface} + \Theta_{deepocean}} \tag{30}$$

$$\frac{dH_{ice}}{dt} = -\frac{H_{ice}}{\tau_{ice}} + \frac{\Lambda_{ice}}{\tau_{ice}} T_{surface} \tag{31}$$

$$H_{sea} = H_{thx} + H_{ice} \tag{32}$$

Ocean heat content It refers to the heat absorbed by the ocean which is then stored as enthalpy. This metric is very valuable as it allows to evaluate the likelihood and, thus the accuracy of the model. It is possible to compute the ocean heat content with the [Geoffroy et al., 2013b] and [Geoffroy et al., 2013a] framework (model elements are on Table 11 page 23):

$$U_{ohc} = \alpha_{ohc} \kappa_{ohc} \left(\Theta_{surface} T_{surface} + \Theta_{deepocean} T_{deepocean} \right) \tag{33}$$

The parameter α_{ohc} is nearly equal to 93% according to [Levitus et al., 2012]. In order to comply with the custom, the final ocean heat content is computed minus its average over the 1955-2006 period.

Inputs	Description	Unit
$T_{surface}$	Global Mean Surface Temperature (GMST) anomaly	K
$T_{deepocean}$	Deep ocean mean temperature anomaly	K
Variables	Description	Unit
U_{ohc}	Ocean heat content	ZJ
Parameters	Description	Unit
α_{ohc}	Fraction of total Earth energy imbalance used to heat the ocean	
κ_{ohc}	Conversion factor from W.m^{-2}.yr into ZJ (takes into acount the Earth surface)	ZJ.m^2.W^{-1}.yr^{-1}
$\Theta_{surface}$	Heat capacity of the surface : atmosphere, land and upper ocean	W.m^{-2}.yr.K^{-1}
$\Theta_{deepocean}$	Heat capacity of the deep ocean	W.m^{-2}.yr.K^{-1}

Table 11: Ocean heat content computation elements

2.4 Results comparison with the DICE model

Now that we know the differences between the DICE climate model and the ERM climate model, it is time to compare both models with the complete dice framework.

2.4.1 Set-up of the DICE-ERM model

Whereas Nordhaus DICE model is written in GAMS, our model is written in Python, using the GEKKO package ([Beal et al., 2018] [Beal et al., 2018] [Beal and Hedengren, 2019]) with the IPOPT solver [Wächter and Lorenz, 2006]. In order to have a more "physical" framework and use the full potential of the GEKKO package, we do not use anymore the DICE economic module in a discrete time-step but with a continuous time-step (for more information on the DICE model, see Annex A page 46) . Hence the state equation for capital accumulation from

$$K_{t+1} = (1 - \delta_K)^{\tau_{time-step}} K_t + \tau_{time-step} I_t \tag{34}$$

becomes

$$\frac{dK}{dt} = -\delta_K K + I \tag{35}$$

where $\tau_{time-step}$ is the computation discrete time-step (which disappears with a differential framework) and δ_K is the depreciation rate of capital. Moreover, the definition of the inter-temporal utility from :

$$W = \sum_{t=0}^{T} \frac{1}{(1+\rho)^t} u\left(\frac{C(t)}{L(t)}\right) L(t) \tag{36}$$

becomes

$$W = \int_0^T \exp(-\rho t)\, u\left(\frac{C(t)}{L(t)}\right) L(t) dt \tag{37}$$

Except for these two equations, the economic module of the DICE-ERM model is exactly the same as the one of the DICE model, and all drivers are the same[10]. However, it should be noted that the climate model initial conditions are not the same as the ones in the DICE model. These are rather very close except for the surface temperature : indeed, Nordhaus proposes a GMST

[10] i.e. the TFP, the energy efficiency, the backstop-technology cost, the population, the non-CO_2 Effective Radiative Forcing, the land-use change emissions and the maximum mitigation rate

anomaly of 0.85 °C, whereas our best-guess value is 1.05 °C (average GMST over the 2013-2017 period as the DICE model has a 5 years time-step). This might be due to two reasons. On the one hand, if the 2015 had been estimated considering the trend of the 10 previous years or so, the global warming hiatus of the period 1998-2013 would be a good explanation of such a low estimate for the 2015 GMST.

This part is not a comparison of the two climate models alone, but a comparison of both climate models with the DICE optimization framework. Consequently, as the models do not have the same climate response, the optimal allocation of production (between investment, mitigation an consumption) are not the same. So, we have to be very thoughtful when interpreting the dynamics of both models and compare things carefully.

2.4.2 Distinct climate responses

Considering the fossil-fuel emissions of the 100 first years, it is possible to state that they are quite the same (the GDPs are fairly the same, so is the control variable μ, which implies really close industrial emissions) :

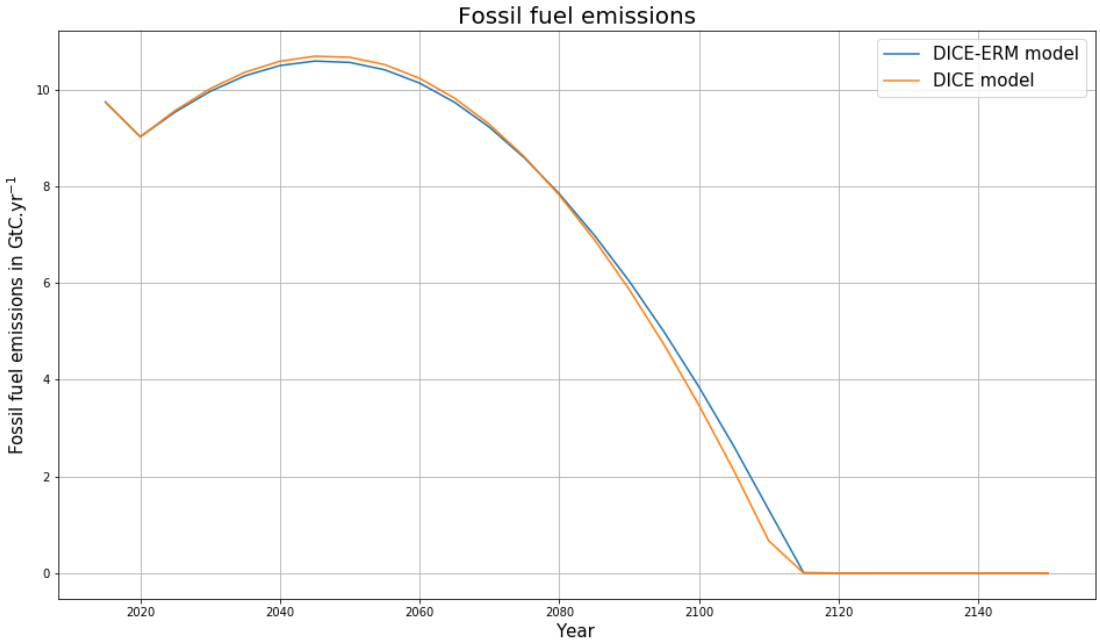

Figure 7: CO_2 fossil-fuel emissions over the period 2015-2150

On the other hand, with these fairly identical emissions, the DICE physical module stores way more CO_2 :

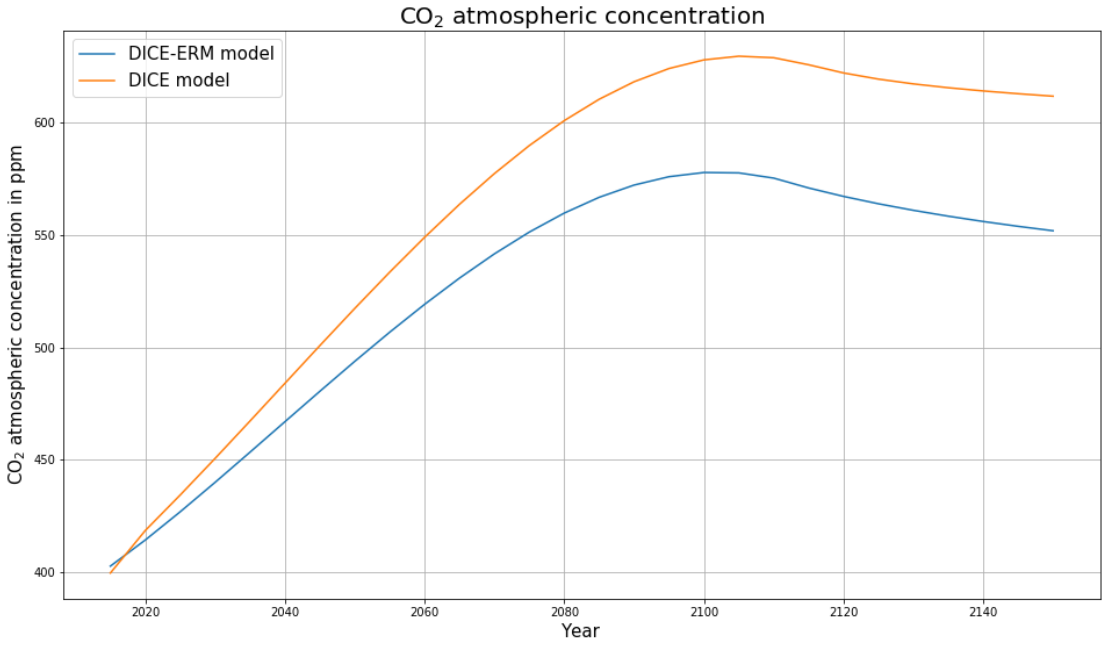

Figure 8: CO_2 atmospheric concentration over the period 2015-2150

Even if the Effective Radiative Forcing at time $t = 0$ are the same :

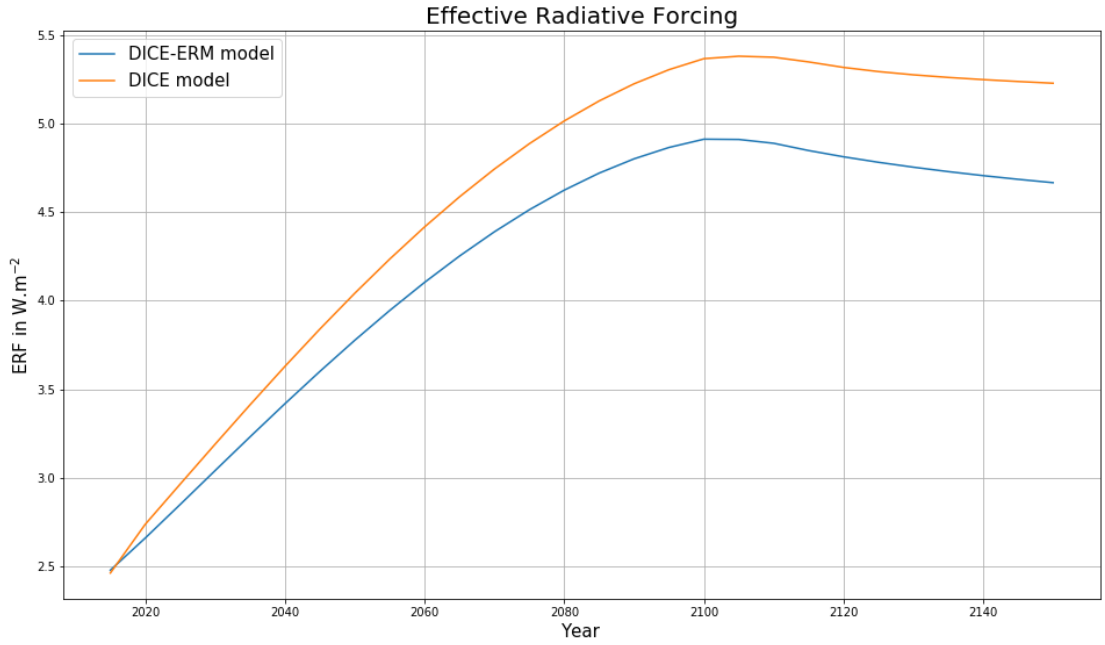

Figure 9: Effective Radiative Forcing over the period 2015-2150

The gradient of the GMST at time t=0 is less important in the case of the DICE model :

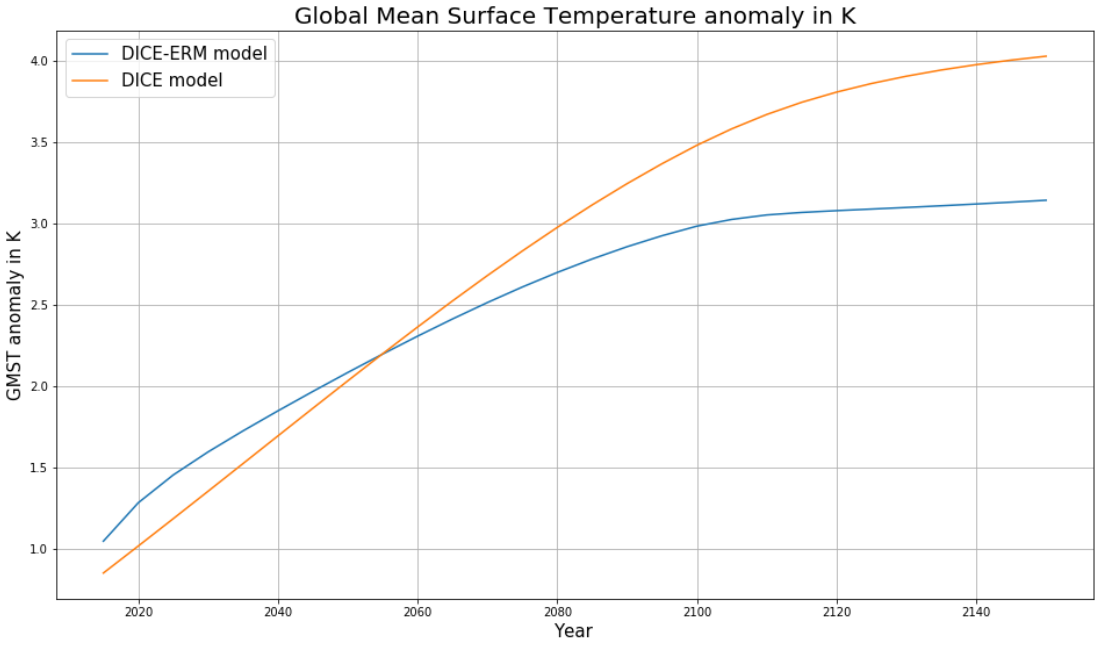

Figure 10: GMST anomaly over the period 2015-2150

That shows us that the ERM climate model corrects at least partly[11] some weaknesses of the DICE physical module, that is to say storing too much carbon in the atmosphere while responding too weakly to Effective Radiative Forcing. It is really interesting to notice that these different dynamics imply very different long-term pathways (due to the "choices" made by the social-planner). Thus the long-term GMST dynamics are strikingly different (see Figure 11 on page 27). In the DICE model outputs, after a peak around 2160 little above a 4° anomaly, the GMST decreases relatively steadily due to a mitigation rate that allows for huge negative emission[12]. On the other other hand, the GMST of the DICE-ERM model is stable and is seems that an "equilibrium" is reached. But why is a decreasing temperature a more optimal pathway? This is due to the fact that the cost of reducing the emissions outweighs the potential economic benefits that would happen. As a matter of fact, it is possible to see on Figure 29 on page 52 in the Annex C, that if the ocean still acts as sink, the land sink does not act as such as soon as the emissions from fossil fuels are negative. Aside of this, the asymmetry of the permafrost - the thawing is faster than the freezing - limits the possibilities of a negative CO_2 imbalance. To sum this up, the ERM has a quite different dynamics than the DICE climate model that, in particular, makes it more complicated to reduce the CO_2 concentration in the atmosphere for a given cost, and finally results in a very different GMST profile.

[11] To be sure of this and purely compare the climate models alone, we should have performed some comparison experiments with state-of-the-art climate models, like the ones produced for the CMIP5 phase.

[12] For the dynamics of the parameter μ see Figure 27 on page 51 in the Annex C. For the dynamics of the emissions from fossil-fuels see Figure 28 on page 51 in the Annex C.

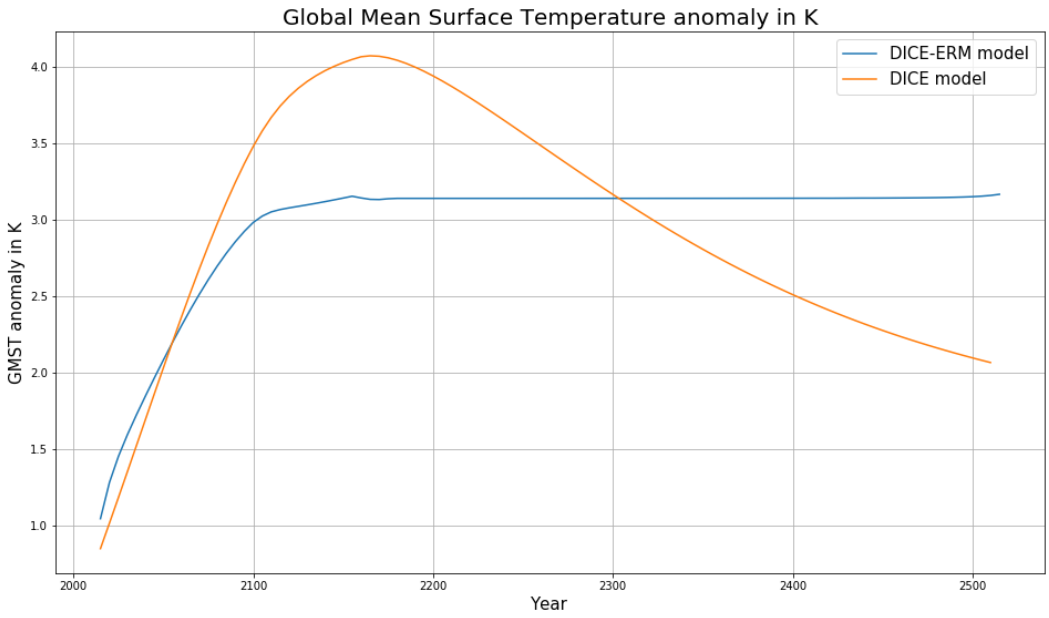

Figure 11: GMST anomaly over the period 2015-2515

2.4.3 Diverging economic indicators?

Looking at the GDP over the period 2015-2515, some features of the models output are striking.

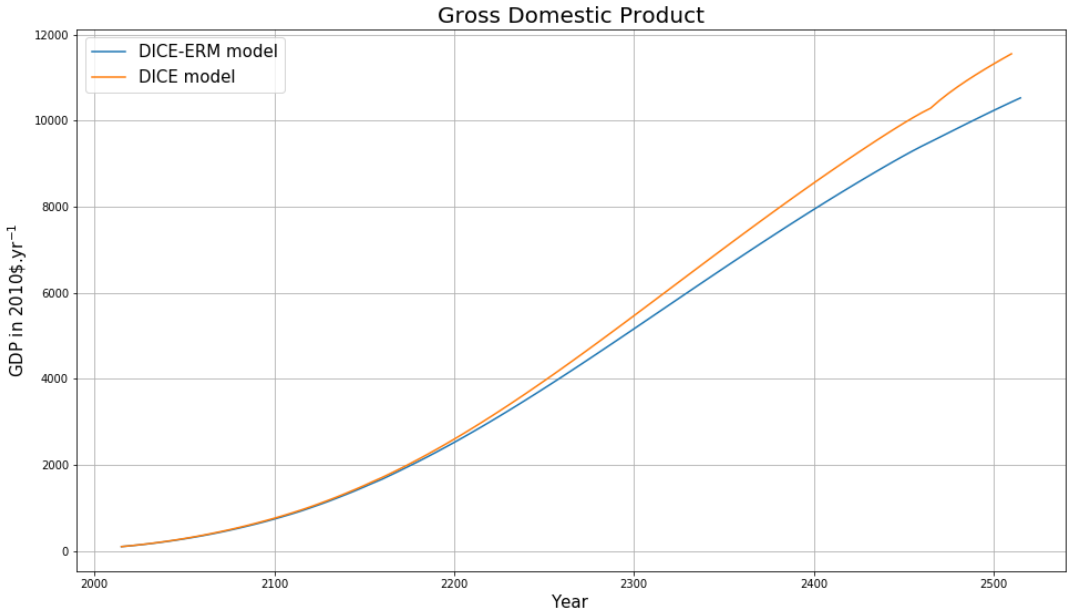

Figure 12: Gross Domestic Product over the period 2015-2515

First, their dynamics are quite the same, which is good news as they share the same economic model. However, they progressively diverge. As the population and the TFP are exogenously fixed and are the same, this difference must come from the accumulation of the capital :

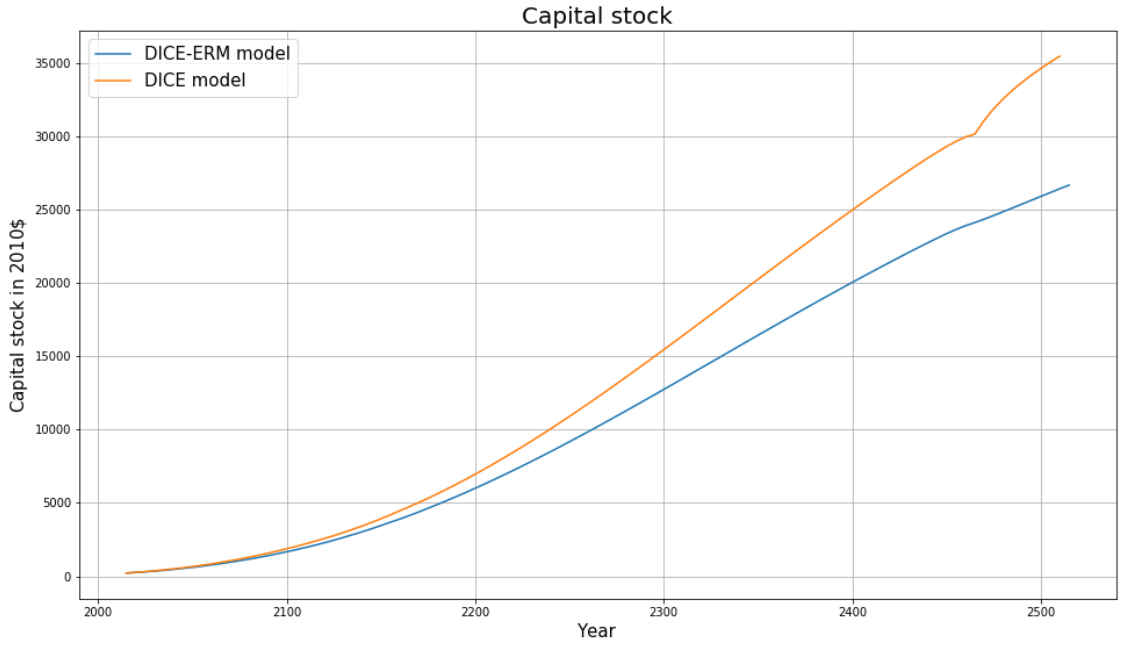

Figure 13: Capital accumulation over the period 2015-2515

This is quite strange since :

- the saving rate obtained with a simulation of the DICE-ERM model is higher compared to the one obtained with the DICE model[13]
- the mitigation rate is lower in the case of the DICE-ERM model[14], and therefore is the cost of mitigation,
- the cost due to climatic damages are globally smaller[15].

Consequently, the capital in the DICE-ERM model should be greater than with the DICE model. The explanation comes from the capital accumulation equation : the discrete equation gives a very slightly larger capital accumulation than the differential one and this small difference increases over time due to the accumulation of capital that drives the economic growth[16].

[13] See Figure 30 on page 52 in the Annex C.
[14] See Figure 27 on page 51 in the Annex C.
[15] See Figure 31 on page 53 in the Annex C.
[16] An intuition from this result might come considering these two different equations $K_{t+1} = (1-\delta_K)K_t + I$ and $\frac{dK}{dt}(t) = -\delta_K K(t) + I$ with I constant and $K_0 = K(0) < \frac{I}{\delta_k}$. The solutions are $K_t = (1-\delta_K)^t \left(K_0 - \frac{I}{\delta_k}\right) + \frac{I}{\delta_k}$ and $K(t) = \left(K(0) - \frac{I}{\delta_k}\right)\exp(-\delta_K) + \frac{I}{\delta_k}$. As $K(0) - \frac{I}{\delta_k} < 0$ and $(1-\delta_K)^t = \exp\left(\log(1-\delta_K)t\right) < \exp(-\delta_K)$ because $ln(1-\delta_K) < -\delta_K$, we obtain: $K_t > K(t)$.

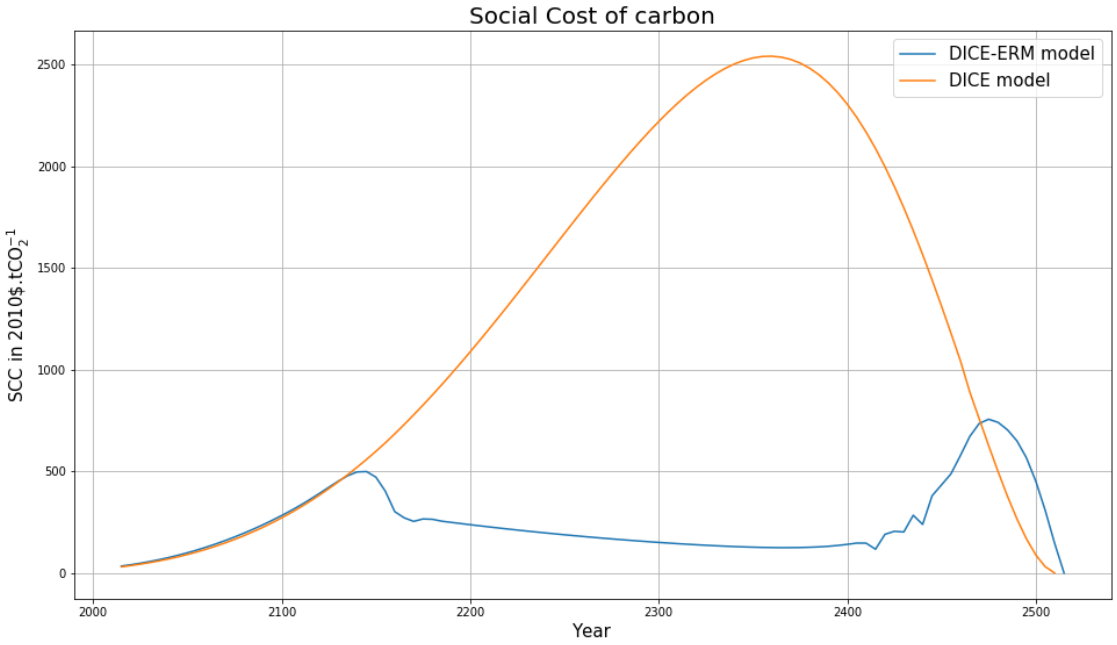

Figure 14: Social Cost of Carbon over the period 2015-2515

2.4.4 What about the Social Cost of Carbon?

Finally, let us study the final object of this study and output of both models : the Social Cost of Carbon (Figure 14 on page 29). At first sight, it is possible to state that both estimates share the same order of magnitude. If we look at it closer[17], it is possible to see that both SCCs are quite the same during the first years of the simulation. This is a logical conclusion, as the behaviours of the social-planner are very similar over the first period. The differences in terms of optimal choices begin with the possibility of negative emissions (i.e. $\mu_{max} > 1$). At this moment, the SCC in the DICE model keeps on rising, whereas it slowly decreases with the DICE-ERM model. To understand this phenomenon, we have to refer to the definition of the SCC : It is the marginal global cost to society that results from the emission of an extra tonne of carbon at time t along a determined emission trajectory. In the case of the DICE model, the mitigation and the carbon sinks are at saturation, which means that a supplementary emission of CO_2 would have a "full" impact on the system. whereas with the DICE-ERM model, as soon as there is some negative emissions, the land sink acts as a source of CO_2 rather than as a CO_2 uptake, so a supplementary marginal emission of CO_2 would only have a very small impact on the economy because it would be absorbed easier by the land sink, which explain this decreasing and lower Social Cost of Carbon. It is even possible to notice that effect is "anticipated by the social planner, as the SCC begins to decrease even before the beginning of negative emissions. In any case, even if this phenomenon is interesting to understand the source of the SCC dynamics, it is not particularly relevant to consider the value of the SCC after 2120-2150, what matters is the dynamics during the 21^{st} century.

[17]Zoom over the period 2015-2150 on the Figure 32 on page 53 in the Annex C

To put this part in a nutshell, we are now able to run simulation of the DICE model and compute the SCC with a new climate module, that is more reliable, considers more physical phenomenons, and is more physically-founded than the classic physical module. These upgrades introduce distortion in term of climate response, and in term of optimal choices, that result in a probably more suitable estimate of the SCC. However, is it possible to claim that this estimation of the SCC is really more robust? Not really, currently, this model only displays one estimate, and does not take into account the known uncertainty over physical parameters, which is why we now want to perform a particular calibration that should allow us to obtain relevant and robust uncertainty ranges over the Social Cost of Carbon. Moreover, it appears that the drivers play a very important role in the dynamics of the system and therefore their design needs to be further developed and studied.

3 Bayesian calibration and Monte Carlo estimation

None of the parameters used by the ERM climate model are known with certainty; for each, there are a certain range of permissible values, some more likely than others. Thus, the same is true for all the estimates we compute: it is not possible to produce them with certainty. How then to determine the uncertainty on these results? One possible way to do this is to use Monte Carlo analysis coupled with a very particular calibration, based on Bayesian probabilities which we propose to present in this section.

3.1 Basic principles and key ideas

Since most of our parameters are known only with a certain uncertainty, it is better to regard them not as simple point values, but as a probability distribution that represents the possible values for these parameters based on our current knowledge. By randomly sampling parameter sets from these probability densities and using them as physical parameters of the ERM model, we can obtain not only single values, but probability distributions of our outputs. This is the main idea behind Monte Carlo methods, drawing large samples of slightly different parameters to assess the uncertainties of the final estimates.

Is that fully relevant? Not completely! When we draw our parameter sets, some sets have the same probability of being drawn but are not as likely. Indeed, uncertainties about the parameters are given independently of each other (because the parameters are given independent probability laws, since they do not come from the same model, i.e. parameters are drawn independently), while some combinations of parameters are more realistic than others. For example, a set of parameters leading to a low land sink and a low ocean sink can be drawn as probably as a set leading to a low ocean sink and a very high land sink, whereas it is much less likely given the historical evolution over the past 150 years. What we would like is a joint probability density on all parameters of interest that would allow us to assess the uncertainty in the model as a whole. This is possible with a Bayesian framework. Giving the uncertainty on the parameters (coming from complex models) as prior distribution, it is possible to constrain them with observations provided by historical data and obtain a posterior joint distribution of the parameters. Finally, with samples of this joint distribution it is possible to assess the uncertainties of the ERM climate model.

Let us first briefly explain the basic principles of Bayesian inference, before going into the details of the calibration. According to Bayes' theorem :

$$\mathbb{P}(H|E) = \frac{\mathbb{P}(E|H)\mathbb{P}(H)}{\mathbb{P}(E)} = \frac{\mathbb{P}(E|H)\mathbb{P}(H)}{\sum_H \mathbb{P}(E|H)\mathbb{P}(H)} \propto \mathbb{P}(E|H)\mathbb{P}(H) \tag{38}$$

H stands for the hypothesis, i.e. what is our prior knowledge of the parameters, so $\mathbb{P}(\mathbb{H})$ is the prior belief over the parameters. E stands for the evidence that we have, i.e. the data we use to constrain the distribution of the parameters. Thus $\mathbb{P}(E|H)$ is the likelihood of the observation with some set of parameters : it allows us (or rather, the calibration algorithm) to guess whose sets of parameters are the most likely because they result in the most consistent outputs. This is what is provided by $\mathbb{P}(H|E)$, the posterior probability. In order to approximate the posterior probability distribution, there are two different methods : Markov Chain Monte Carlo (MCMC) and Variational Bayesian. Since we calibrate a lot of parameters, we prefer a Variational Bayesian method for reason of computation time.

3.2 Set-up and calibration data

Indeed, we use a variational bayesian algorithm [Kucukelbir et al., 2015] with the language Stan [Carpenter et al., 2017], [Stan Development Team, 2019], adapted to Python with the package Pystan [Riddell, 2015], the results - samples of interest parameters and historical state variables - are finally stored in xarray files, a useful format when dealing with big amounts of complex data [Hoyer and Hamman, 2017].

Our calibration idea is here to run the model over the historical since 1750, and to constrain final results with observations.The logical next step would be to run the model on the inputs, the CO_2 emissions and the non-CO_2 Effective Radiative Forcing. However, these are not very good inputs, since the latter are very little known data, with very important uncertainty. Plus the outputs - the ones that are constrained - would be the CO_2 atmospheric concentration and the GMST, that are known with a very good accuracy. Thus, we would have a real problem in terms of information flow: it is quite complicated, from an imprecise data, to obtain an estimate that we would like to constrain with precise information[18].

Therefore, we proceed the opposite way. We use the GMST and CO_2 atmospheric concentration data as inputs of the model and by reversing some equations of the model, we compute the anthropogenic CO_2 emissions and the non-CO_2 Effective Radiative Forcing. The constraints we use are detailed in Table 12 :

Variables	Description	Mean	Standard deviation	Source
F_{ocean}	Cumulated ocean sink over the period 1870-2017	150 GtC	20 GtC	[Le Quéré et al., 2018]
F_{ocean}	Mean ocean sink over the period 2007-2017	2.4 GtC.yr^{-1}	0.5 GtC.yr^{-1}	
F_{land}	Cumulated land sink over the period 1870-2017	100 GtC	50 GtC	
F_{land}	Mean land sink over the period 2007-2017	3.2 GtC^{-1}	0.7 GtC^{-1}	
E	Cumulated CO_2 emissions the period 1870-2017	615 GtC	80 GtC	
F_{land}	Mean CO_2 emissions over the period 2007-2017	10.8 GtC^{-1}	0.8 GtC^{-1}	
ERF_{ex}	Mean exogenous ERF over the period 2006-2017	0.438 W.m^{-2}	0.828W.m^{-2}	[IPCC, 2014a]
U_{ohc}	Mean ocean heat content over the period 2006-2017	164 ZJ	6ZJ	[Levitus et al., 2012]

Table 12: Observational constraints for the Bayesian calibration

[18]This is, however, what we have done at first. If this is not the best way to do it, it still doesn't work too badly. Indeed, this reduces the posterior distribution too much because we provide too much information by simulating the imprecise inputs. Nevertheless the distributions obtained are still appropriate. The only problem is that they reduce too much the uncertainty that can exist on the output parameters of the DICE-ERM model. The results provided in part 4 (A new scenario approach with the Shared Socioeconomic Pathways) come from this calibration.

Part of the model	Parameter	Unit	Mean	Standard deviation	Source
Transversal parameter	$C_{atm}[0]$	ppm	278	3	[IPCC, 2014c] [Etheridge et al., 1996]
Land sink	$F_{nnp}[0]$	$GtC.yr^{-1}$	51.84	10.4	[Gasser et al., 2017]
	$E_f[0]$	$GtC.yr^{-1}$	3.437	0.687	
	$E_{rh}[0]$	$GtC.yr^{-1}$	48.4	9.68	
	$C_v[0]$	GtC	583.2	116.6	
	$C_l[0]$	GtC	122.2	24.44	
	$C_s[0]$	GtC	1674	334.8	
	β_{npp}		0.6264	0.333	
	γ_{rh}	K^{-1}	0.02063	0.003172	
Ocean sink	k_g	yr^{-1}	0.1104	0.022	[Joos et al., 1996]
	$T_{ocean,0}$	K	17.49	0.2	
	γ_{dic}	K^{-1}	0.04721	0.00944	[Strassmann and Joos, 2018]
	β_{dic}		0.5671	0.1134	
Permafrost	γ_p	K^{-1}	0.1378	0.0276	[Gasser et al., 2018]
	$C_{fr}[0]$	GtC	557.6	11.5	
ERF	ϕ	$W.m^{-2}$	5.345	0.55	[IPCC, 2014b]
Climate response	$T_{4\times}$	K	6.975	1.91	[Geoffroy et al., 2013b]
	$Theta_{surface}$	$W.m^{-2}.yr.K^{-1}$	8.175	0.9	
	$Theta_{deepocean}$	$W.m^{-2}.yr.K^{-1}$	133.7	45.69	[Geoffroy et al., 2013a]
	$theta_{exchange}$	$W.m^{-2}.K^{-1}$	0.8679	0.2839	

Table 13: Prior distribution of the parameters

On Table 13 on page 33 it is possible to find the calibrated parameters[19], with their prior means and standard deviation. In order to model the uncertainty on the temperature and atmospheric concentration of CO_2, we add a auto-correlated random noise of zero mean around the best guess. Its standard deviation is equal to the one between the different observation datatsets (or the one estimated) by researchers. The inputs takes the following form for the i^{th} simulation:

$$T_{surface,t} = T_{surface,bestguess,t} + \sigma_{T_{surface},t} r_{T_{surface},i,t} \tag{39}$$

$$C_{atm,t} = C_{atm,bestguess,t} + \sigma_{C_{atm},t} r_{C_{atm},i,t} \tag{40}$$

With the $r_{someting,i,t}$ following an AR1 process :

$$r_{T_{surface},i,t+1} = \rho_{T_{surface}} r_{T_{surface},i,t} + \epsilon_{T_{surface},i,t} \tag{41}$$

Where $r_{T_{surface},i,0} = 0$ and $\epsilon_{T_{surface},i,t}$ has a zero mean and a standard deviation equal to $\sqrt{\frac{1}{\rho_{T_{surface}}} - 1}$, so that the standard deviation limit of $r_{T_{surface},i,t}$ is 1.

$$r_{C_{atm},i,t+1} = \rho_{C_{atm}} r_{C_{atm},i,t} + \epsilon_{C_{atm},i,t} \tag{42}$$

[19] All the prior densities are normal distribution restricted to admissible value (most values cannot be negative). Sometime, when the uncertainties are not available, we put 20% of the value of the parameter as prior uncertainty.

Where $r_{C_{atm},i,0}$ is chosen so that $C_{atm,0} = C_{atm}[0]$ and $\epsilon_{C_{atm},i,t}$ has a zero mean and a standard deviation equal to $\sqrt{\frac{1}{\rho_{C_{atm}}} - 1}$, so that the standard deviation limit of $r_{C_{atm},i,t}$ is 1.

We calibrate $\rho_{T_{surface}}$ and $\rho_{C_{atm}}$ the following way[20]. For each time-serie is is possible to compute the average slope over the years 2007-2017 with an OLG estimator. With all these slopes, we obtain a slope distribution, really close to a normal distribution, with a standard deviation that is a stricly decreasing function[21] of $\rho_{T_{surface}}$. Furthermore, we can compute the standard deviation of the average slope over the period 2007-2017 of our different GMST datasets. Finally it is possible to find the good value of $\rho_{T_{surface}}$, which is equivalent to a characteristic time, with $\rho^t_{T_{surface}} = \exp\left(\frac{-t}{\tau_{T_{surface}}}\right)$. We obtain $\tau_{T_{surface}} = 156$ years and $\tau_{C_{atm}} = 74$ years.

3.3 First results and assessment of uncertainties

After the calibration, 1000 samples of the parameters are drawn and their corresponding historical data are computed[22]. Figures 33 and 34 on page 54 of the Annex D show us the simulated historical evolution of the land sink and the ocean sink as well as the estimates provided by the Global Carbon Budget [Le Quéré et al., 2018]. What is interesting is to consider the impact of the calibration on the climate dynamics of the DICE-ERM model and on the SCC as well :

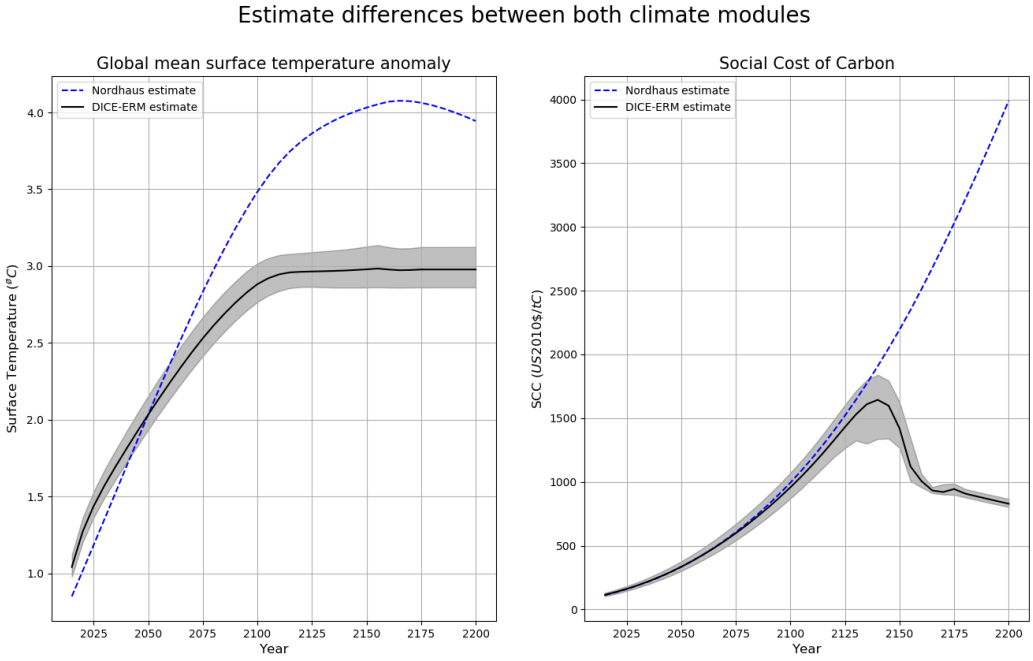

Figure 15: Comparison between the DICE-ERM model calibrated and the DICE model over the period 2015-2200

[20]The example is made with $T_{surface}$, we followed the exact same process for C_{atm}

[21]These considerations are completely empirical, since these temperature time-series come from random sampling. However, it must be possible to derive a limit distribution of slope that only depends from the parameter $\rho_{T_{surface}}$

[22]From this point on, the figures and data do not come from the calibration described in the previous paragraphs but from a calibration with the CO_2 emissions and non-CO_2 ERF as inputs.

The good news is that calibration allows us to obtain very consistent results with what we had previously obtained. We obtain an uncertainty of about 30% of the value at most, which may appear quite low. On the other hand, if we constrain the temperature by setting a maximum value (here, 2 and 2.5°), this uncertainty increases considerably and is then worth more than 150% of the SCC[23] whereas due to the constraint, the uncertainty on the temperature gets lower. Once again, we can see the extremely important influence of the maximum mitigation rate. Indeed, once negative emissions are possible, the SCC falls immensely quickly because of the phenomenon described in the previous section.

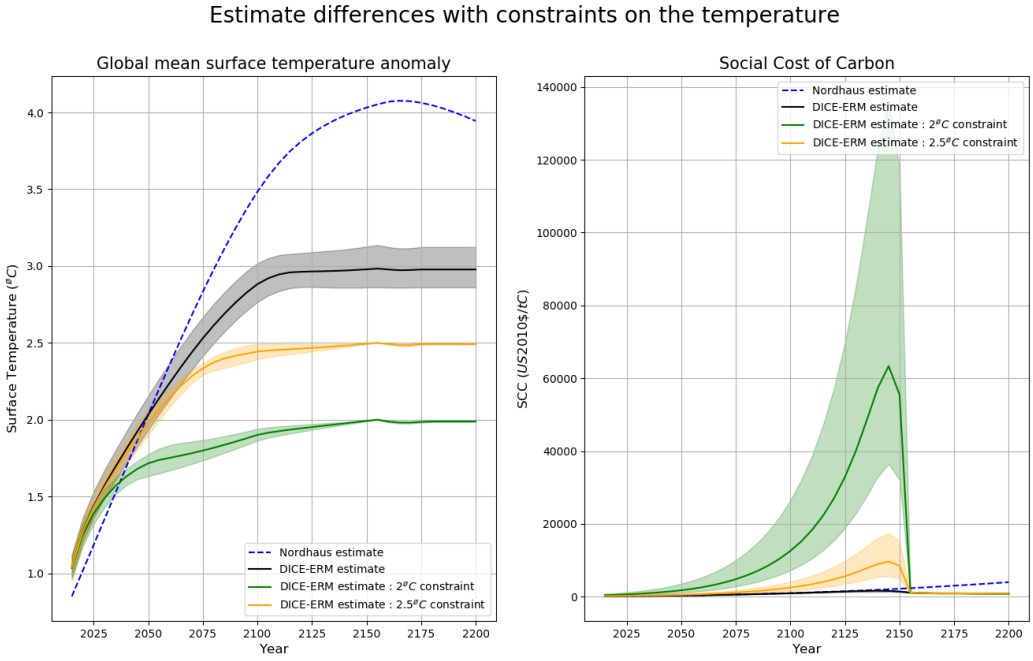

Figure 16: GMST and Social Cost of Carbon of the DICE-ERM model when the temperature is constrained

Thus, starting from modeling uncertainty constrained by observations, we were able to calibrate the erm model in a Bayesian way. This allows us to perform Monte Carlo simulations on the DICE-erm model, which allow us to assess the uncertainty about the SCC. However, we still notice that drivers have a very (too much?) important influence on the dynamics of the SCC. It is therefore of utmost importance to study these major influence factors, in order to assess how they affect the Social Cost of Carbon.

[23]For a better figure of the SCC with a 2.5°, see Figure 35 on page 55 in the Annex D

4 A new scenario approach with the Shared Socioeconomic Pathways

As noted in previous sections, the drivers of the DICE model significantly influence the entire dynamics of the model and, in particular, the Social Cost of Carbon. Thus, it is necessary to set up a study framework to estimate the latter according to different scenarios. We therefore propose to adapt the thinking framework proposed by the SSP scenarios, to estimate the social cost of carbon in different situations characterized by consistent socio-economic assumptions for each of them.

4.1 The SSP framework

The Shared Socioeconomic Pathways (SSPs) are a framework of scenarios that aims at spanning for the potential outcomes of the world economy along two socio-economic axis: the challenge for mitigation, and the challenge for adaptation. In [O'Neill et al., 2014], they are defined as "reference pathways describing plausible alternative trends in the evolution of society and ecosystems over a century timescale, in the absence of climate change or climate policies"[24]. To each SSP are associated Shared climate Policy Assumptions (SPA) that are summed up in Figure 17:

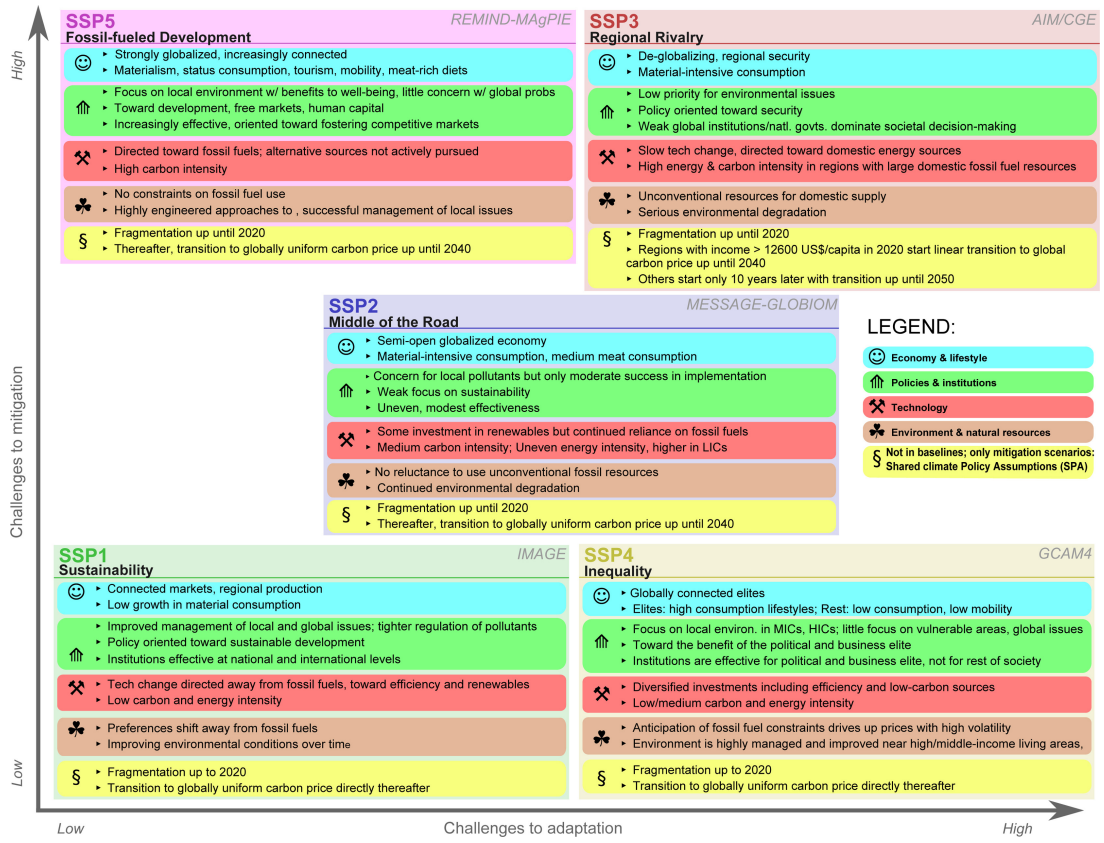

Figure 17: The Shared climate Policy Assumptions of the SSPs [Bauer et al., 2017]

[24]It is interesting to notice that SSPs do not consider the negative feedback on the economy and society due to global climate change, while our model, on the contrary, uses the potential damage to determine an "optimal pathway".

These assumptions are first then quantified as population scenarios [KC and Lutz, 2017] (IIASA) and then as GDP scenarios [Dellink et al., 2017] (OECD), [Crespo Cuaresma, 2017] (IIASA), [Leimbach et al., 2017] (PIK). After this, they are crossed with the Representative Concentration Pathway (RCP) scenarios, in order to obtain a SSP RCP matrix that couples socio-economic issues and various gas concentration trajectory as shown in Figure 18:

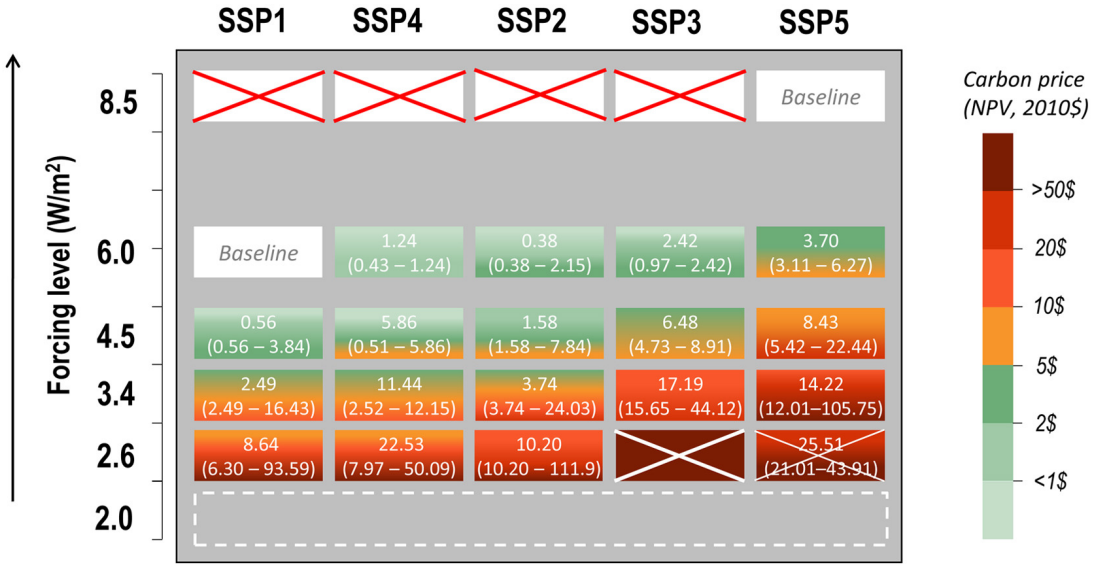

Figure 18: The SSP RCP matrix [Riahi et al., 2017]

These crossed scenarios are available online on the SSP-database[25][26] [Riahi et al., 2017]. The interest of this framework is not only that it provides quantitative scenarios data with their own coherence, but also that it offers interpretation keys relating to these scenarios. Our idea is therefore to simulate the SSP scenarios with the DICE-ERM model, in order to determine the Social Cost of Carbon (and its uncertainty) over classic scenarios for the scientific community. A difficulty that now presents itself to us is that we must extract the drivers for the model from the SSP-database and, then, extend them from the period 2015-2100 to the period 2015-2515.

4.2 How to create long-term extensions of SSP scenarios?

In order to run the DICE-ERM model on the SSP scenarios, we need to translate the information provided by the SSP-database into the drivers that are required to run the model: the population, the Total Factor of Productivity, the energy efficiency, the backstop technology price, the non-CO_2 Effective Radiative Forcing, the CO_2 emissions from land-use change and finally the maximum mitigation rate. We divide the drivers into two categories, the first four, those that depend only on the SSP and the last three, that depend on the couple SSP-RCP. After extracting the driver, there remains a second test, extend it until 2515 in a coherent way, both with the scenario and with the DICE model framework. Let us now present briefly how to obtain and extend each driver.

[25]SSP-database hyperlink

[26]Each SSP is described in the following articles: SSP1 [van Vuuren et al., 2017], SSP2 [Fricko et al., 2017], SSP3 [Fujimori et al., 2017], SSP4 [Calvin et al., 2017], SSP5 [Kriegler et al., 2017].

Population The population is a peculiar case. The DICE model framework requires a limit population, which is not possible to guess or assess from the SSP population scenario. Since, it is not possible to use a fitted logistic equation to obtain population scenario for the SSP, the best thing to do is to run the SSP population model itself, with some assumptions. From the data available online[27], we suppose that:

- Each country mortality rate remains the same as in the year 2100,
- The Total Fertility Rate (TFR) of all countries converge linearly to 1.75 toward 2200 and then remain constant over time [Basten et al., 2013] [Goujon and Fuchs, 2013].

For the three first SSPs, we obtain:

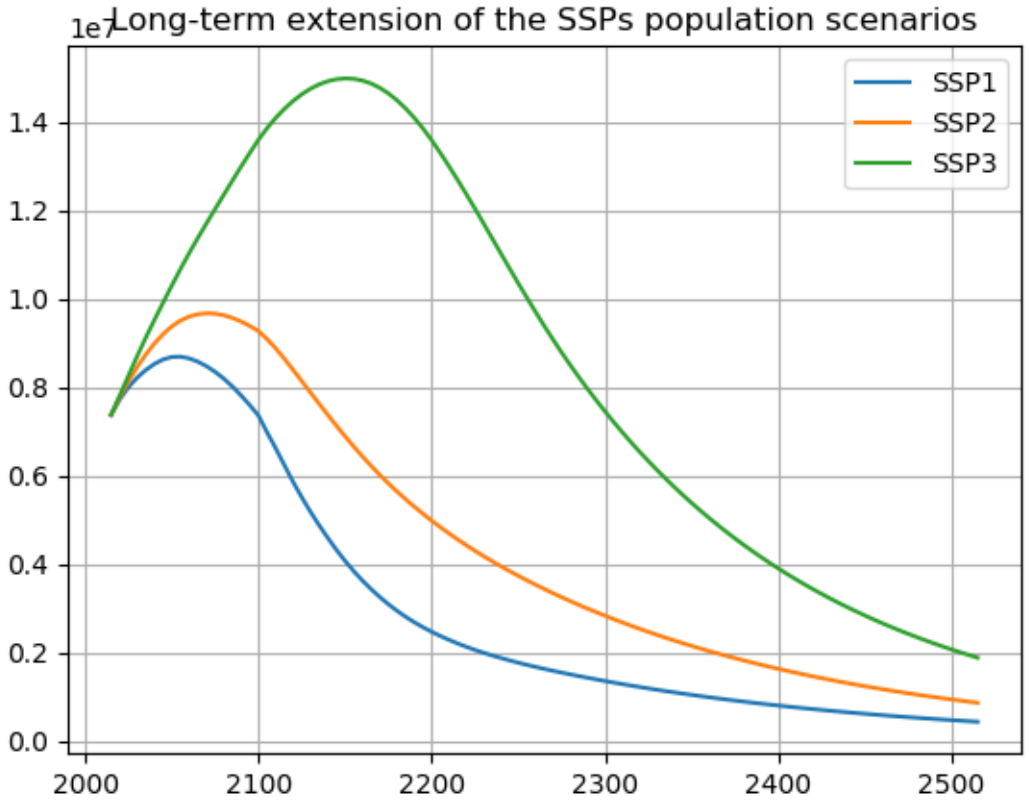

Figure 19: Population for the SSP scenarios (in tens of billions of inhabitants)

Total Factor of Productivity In the SSP-database, it is possible to get the GDP and the total consumption. By subtracting them it is possible to compute the investment, and then the accumulation of capital, which finally provides the TFP until 2095, as well as its growth rate. In the DICE model, we have:

$$\log(g_{TFP}(t)) = \log\left(1 - \delta_{TFP}\right) t + \log(g_{TFP}(0)) \tag{43}$$

[27] Wittgenstein Centre Database

So, we regress the $\log(g_{TFP}(t))$ over time to compute the future growth rate of the TFP, and then the TFP[28].

Energy effiency The energy efficiency σ can be computed by dividing the baseline CO_2 emissions from fossil-fuels by the GDP (we rescale it so that, it shares the same value as the DICE model in 2015). In the DICE model, σ is represented as follows:

$$\sigma(t) = \sigma_0 \exp\left(-\frac{0.0152}{0.001}\left(1 - exp(\delta_\sigma(t - 2015))\right)\right) \tag{44}$$

Therefore, we fit the σ time-serie over the period 2050-2095 with the above equation to derive the parameter δ_σ, and extend σ until 2515.

Backstop technology price From the SSP-database, it is possible to get the carbon price of each SSP scenario. In the DICE model, the same index is computed with the following formula:

$$P_{carbon}(t) = P_{backstop}(t)\mu(t)^{\theta_2 - 1} \tag{45}$$

With:

$$P_{backstop}(t) = P_{backstop}(0)(1 - g_{backstop})^t \tag{46}$$

Since, we can compute the mitigation rate μ (see paragraph bellow), we perform an linear OLG regression on μ and t:

$$\log\left(P_{carbon}(t)\right) = \log\left(P_{backstop}(0)\right) + \log\left(1 - g_{backstop}\right)t + (\theta_2 - 1)\log(\mu(t)) \tag{47}$$

So we obtain the backstop technology price at $t = 0$ and its growth rate.

Non-CO_2 Effective Radiative Forcing To get this driver, we subtract the CO_2 Effective Radiative Forcing to the total ERF. Then we arbitrarily keep the value of 2100 as constant.

Land-use change CO_2 emissions The land-use change emissions can be obtained directly from the SSP-database. To extend them, we add an exponential decrease of the following form so that the characteristic time is 50 years, the derivative in 2100 is zero and the emissions are continuous in 2100:

$$E_{land}(t) = E_{land}(2100)\left(\frac{t - 2100}{50} + 1\right)\exp\left(-\frac{t - 2100}{50}\right) \tag{48}$$

Maximum mitigation rate As explained in the previous paragraphs, we know how to compute the energy efficiency σ, so, for a given RCP, it is possible to compute the actual mitigation rate on the SSP-RCP couple. We suppose that this mitigation rate can be considered as the maximum mitigation rate for the driver[29].

$$\mu_{max}(t) = 1 - \frac{GDP(t)}{\sigma(t)E_{ind}(t)} \tag{49}$$

[28]For the SSP3, we first compute an increasing TFP growth rate, which is not realistic at all. So, we correct the growth rate with an exponential decrease with a characteristic time of 100 years. It is set so that it preserves the slope of the growth rate in 2100 and make the growth rate converge to 0

[29]The σ rescale increases very slightly the value of μ compared to the case there would have been no rescale. This is rather consistent with what we are looking for for the DICE-ERM model: to have a little more freedom to look for the optimal trajectory, and try to emulate the SSP scenarios

The drivers for the SSP2 have the following form, the drivers for SSP1 and SSP3 are in the Annex E[30][31]:

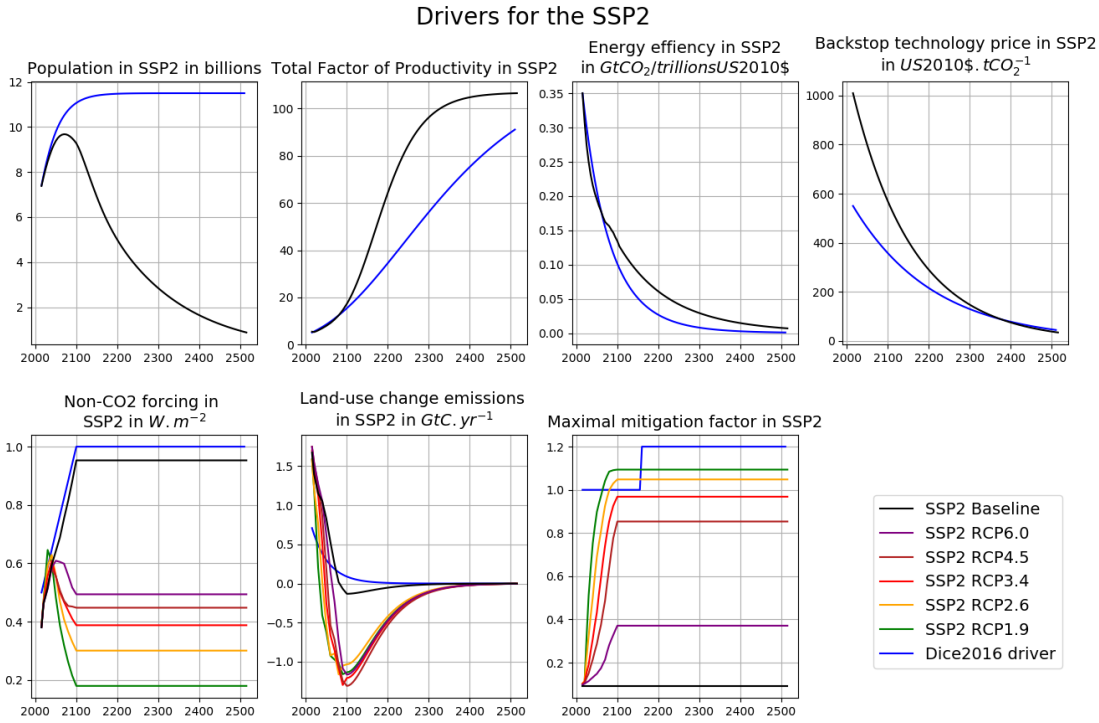

Figure 20: Drivers for the SSP2 compared to the DICE model drivers

4.3 Monte Carlo analysis with the SSP scenarios

Now that all pieces of the simulation of the SSPs with the DICE-ERM model have been presented, there is very little to add to describe the set-up. For each SSP-RCP scenario, we perform 1000 simulations with samples drawn from the Bayesian calibration[32]. As it is done in the DICE model, we constrain the saving rate at the end of the simulation to avoid edge effects due to a "burn everything" optimal behaviour. Moreover, and this is quite important, we do not constrain the Effective Radiative Forcing in 2100. Thus, a scenario on a RCP2.6 will not necessarily present an Effective Radiative Forcing equal to 2.6 W.m^{-2} in 2100: we give the social planner the means to reach a certain target, but we do not constrain it so that it reaches it[33]

So, first of all, let us consider the fossil-fuel emissions, since they are the expression of the "choices" made by the social-planner:

[30]The SSP4 and SSP5 population scenarios were not available in time, so we were not able to perform the simulations for both these SSPs

[31]From this point, we will only present the results for the SSP2, since it is considered as the middle of the road scenario. The equivalent results for SSP1 and SSP3 are in the Annex E

[32]We repeat that the results presented here are not from the previously presented calibration, but sadly from a previous calibration of lower quality.

[33]Constraining the ERF would however be very interesting because it would have a particularly strong effect on the value taken by the SCC. As a matter of fact, it would be the next step of the project.

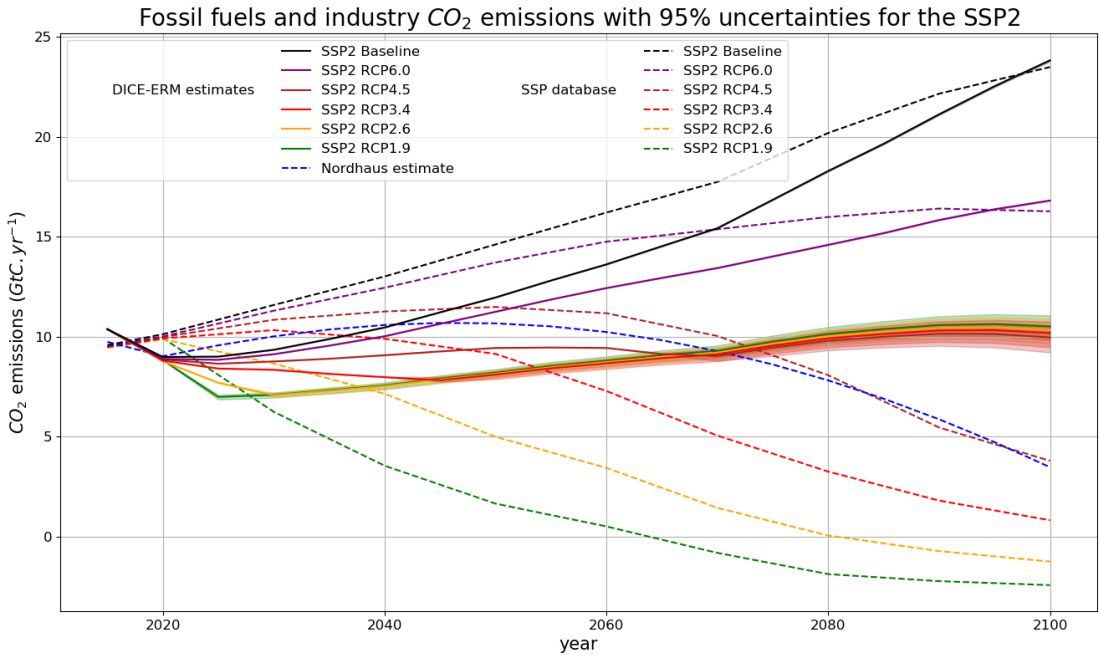

Figure 21: Fossil-fuel CO_2 emissions of the DICE-ERM model on SSP2 scenarios compared to the SSP data

It immediately shows that this way to run the SSPs scenarios is not a good way to emulates these scenarios, because the choices made by the social planner are completely different from what is expected in the SSP scenarios. However, is shows that without constraints, the maximum mitigation rate is only binding for RCP6.0 and the Baseline. Moreover, it is possible to see that, the climate uncertainty has very small influence on the "decisions" made by the social-planner, whereas it has a quite bigger impact on the Effective Radiative Forcing[34] and the Global Mean Surface Temperature on Figure 22 page 42.

[34]Figure 41 on page 58 in the Annex E

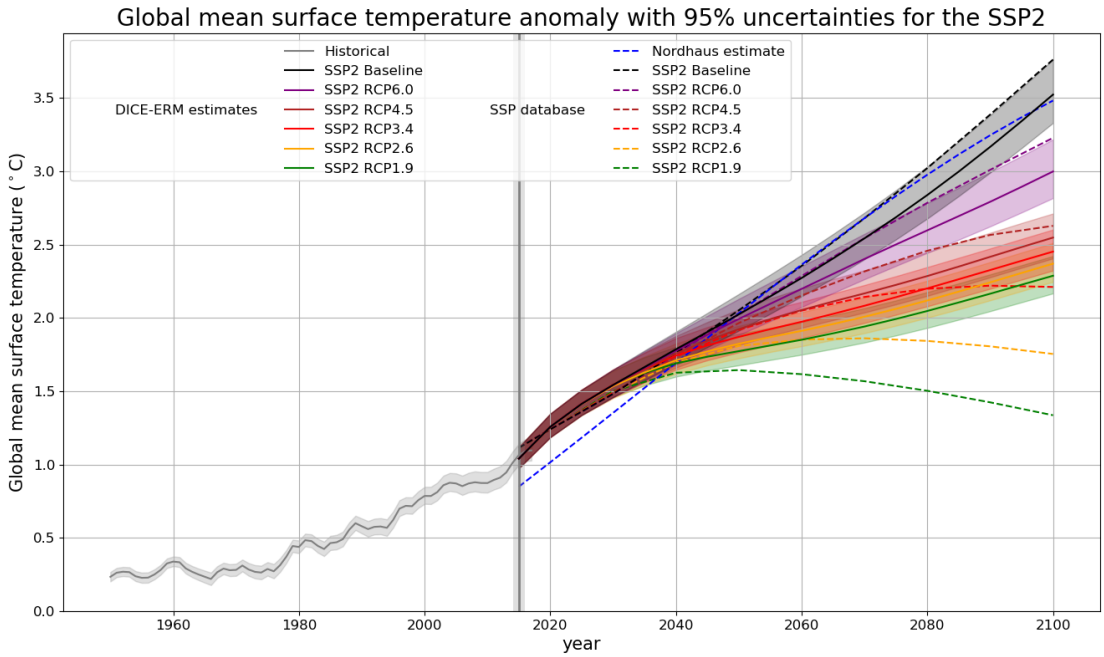

Figure 22: GMST anomaly of the DICE-ERM model on SSP2 scenarios compared to the SSP data

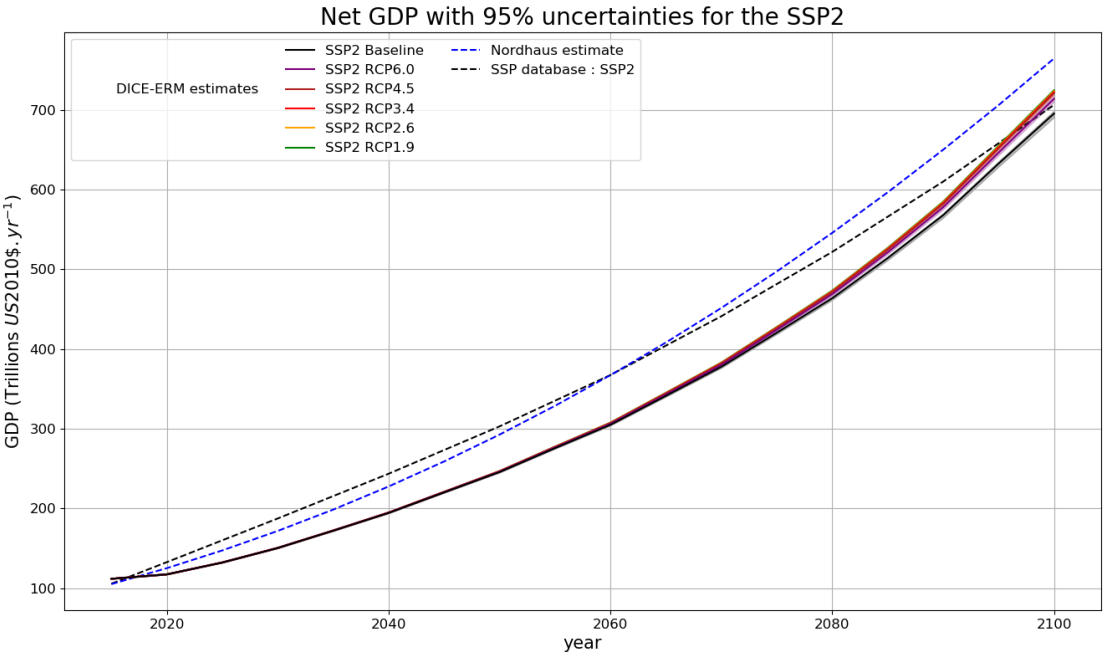

Figure 23: GDP of the DICE-ERM model on SSP2 scenarios compared to the SSP data

So, it appears that the climate uncertainty effect do not translate into the decision-making

in the model. In fact, the GDP is nearly unchanged (see Figure 23 on page 42) because the damage function do not target the growth factors, but its outcome[35]. Then, it is logical that the impact of fossil-fuel emissions is just a marginal factor for resources allocation.

4.4 An assessment of the SCC climate uncertainty?

All these considerations result in a Social Cost of Carbon that does not really depend on the RCP-dependant drivers as it is possible to see on Figure 24 on page 43 for the SSP2.

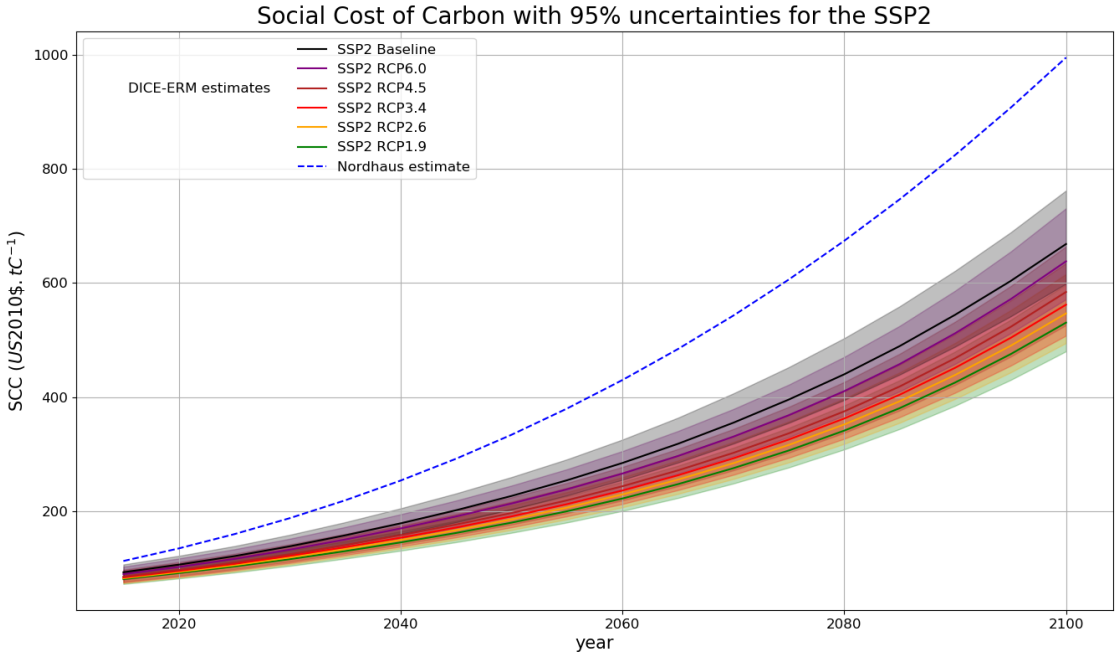

Figure 24: Social Cost of Carbon for the SSP2

Comparing the different SSP (Fifure 25 on page 44 it is possible to conclude that the main factors influencing the Social Cost of Carbon are the socio-economic assumptions that underlie behind each scenario. In fact, [Ricke et al., 2018] present the uncertainty resulting from cross-country SCC comparison, and it appears to be much more important than the one we have computed[36]. Once again, it is quite logical, the economic dynamics is highly dependant on the economic drivers and assumption, and the climate influence is not strong enough so that the existing uncertainty over the future of climate have a real influence over the loss or gain of well-fare. Thus, the climate uncertainty over the SCC mostly relies on the underlying socio-economic hypothesis.

[35] In [Moore and Diaz, 2015], the impacts of climate change are on the TFP growth rate, or to the depreciation rate of capital. In that case, climate change indeed slows growth a lot (in particular in poor countries).

[36] In this study, the uncertainty also depends on the RCP-SSP couple. It is possible to see that the SCC does not depend enormously on the RCP but more on the SSP. Moreover, with a 66% uncertainty range , the values of SCC ranges (in 2020) from -100$ to 1500$ for SSP1-6.0, from -100$ to 2000$ for SSP2-6.0, from 0$ to 4000$ for SSP3-8.5. The socio-economic disparities clearly outweigh the climate uncertainty.

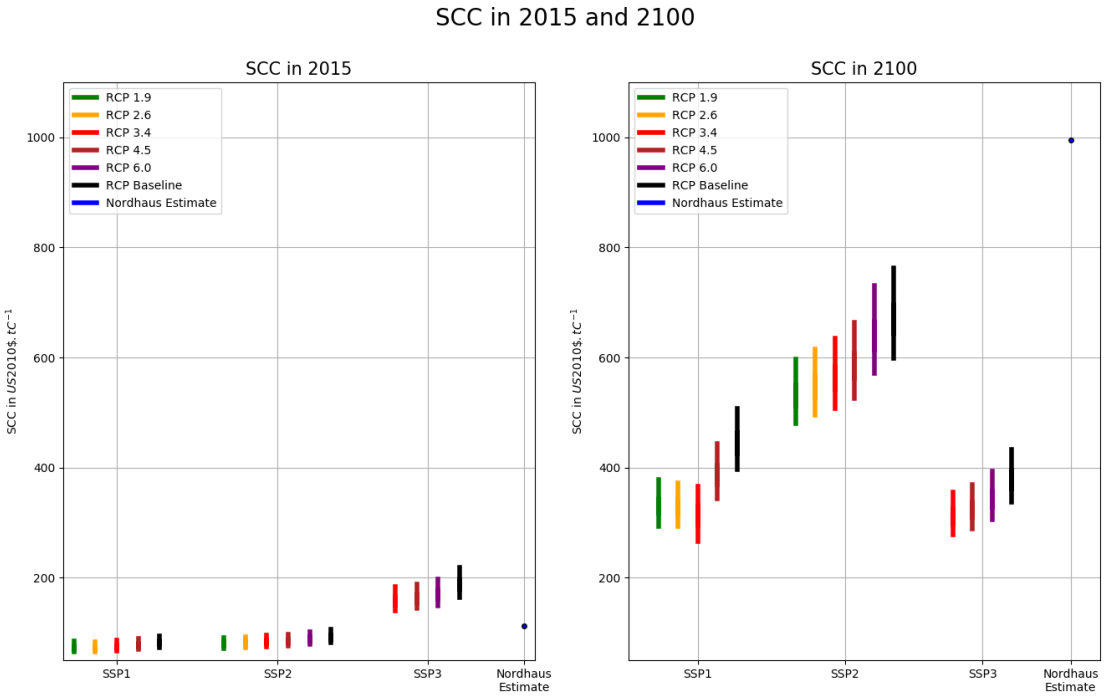

Figure 25: Comparison of the Social Cost of Carbon over different SSPs

To conclude, we use the SSP scenarios as a framework to assess the Social Cost of Carbon and its uncertainty over different and relevant scenarios. This allows us to obtain a matrix of carbon costs according to different dimensions, temporal, socio-economic, and in terms of concentration. Crossing socio-economic assumptions with (potential) concentration pathways, we obtain the following result : the Social Cost of Carbon mostly depends on the growth model assumptions that are used to simulate the economy. The distributional issues due to cross-countries inequalities of development and risk against global climate change are far more important deciding factors than the uncertainty over future climate change (at least with this model). However, despite all that, it is quite likely that constraining the Effective Radiative Forcing to follow a RCP scenario would have a enormous impact on the SCC, as it has been shown at the end of the part 3. Changing the way damage is applied also appears to be a very promising route.

Conclusion

To conclude, we have presented a compact climate model that improves the DICE model, and provides quite different estimates of the Social Cost of Carbon. The Bayesian calibration of this model allows us to evaluate the uncertainty on the Social Cost of Carbon due to the existing uncertainty over future climate knowledge. With the SSP scenarios, we can thus propose a more relevant value of the Social Cost of Carbon. These estimates are more robust because they present a range of uncertainty and are given for precise, defined and widely studied scenarios.

The estimation of the climate uncertainty is essential to have an enlightened view on the Social Cost of Carbon in order to use it as a policy-design tool. However, the conclusion arising from these simulation is not very optimistic. Indeed, we have assessed the climate uncertainty on the Social Cost of Carbon but we have also watched that the climate is not the major source of uncertainty on the Social Cost of Carbon. The estimates of the Social Cost of Carbon mostly depend on the exogenous drivers and the climate system response do not appear to be a determining factor for them, nor for the optimal pathway. It kind of means that the Social Cost of Carbon does not really depend on the carbon itself but mostly on technological scenarios, which is not really relevant when designing policies for climate mitigation. Especially since technological future is rather uncertain.

A exciting approach to counter this problem is the use of constraints that can be imposed on state variables, such as the Effective Radiative Forcing, the Global Mean Surface Temperature anomaly or even the sea level rise or the acidification of the ocean. However, it raises the question of the good use and the scope of the model : do constraints on the climate are relevant? The DICE model has been designed to endogenize the climatic risk and potential losses. So, specifying a trajectory in terms of temperature to the model because it does not take into account the real climate risk, is it not basically admitting that it is not efficient? Is it not better in this case to change the model, or to profoundly change its structure to obtain a better coupling between climate and economy? We have seen that inequalities in distributions are particularly important, much more so than the uncertainties arising from climate change. Is an aggregate model like this really relevant in this case to deal with such different economic situations? Are Policy Optimization Models really relevant, should not we rely only on Policy Evaluation Models that do not suffers the "flaws" resulting from the optimization process? Or maybe is it possible to create better behaviour-relevant optimization models that procure brighter results.

A Design and operation of the DICE model

The DICE model has been created and updated by William Nordhaus since 1992. Considered as a pioneering model, the DICE model is one of the very first IAMs that couples the climate and the economy through a damage function. Still one of the most important model in the field of climate economics, the it is a reference model for determining the SCC. For its groundbreaking breakthroughs, William Nordhaus has been awarded the NObel Price of ecnomics in 2018. The role of this part is to present the last version of the DICE model[37]. Most information can be found in [Nordhaus, 2013] and [Nordhaus, 2017].

A.1 Representation of the DICE model

Basically, the DICE model couples a neo-classical growth model with a simple climate model, with a carbon cycle. Its design is pretty simple, and quite efficient :

- Production in the economic module results in CO_2 emissions due to fossil-fuels burning,
- These emissions increase the CO_2 concentration in the atmosphere through the carbon cycle,
- This results in a higher Effective Radiative Forcing, that implies a global warming,
- This warming has an impact on the GDP through a function of damage

.

A.2 The economic module

Now let us describe the equations underlying the economic model of the DICE model.

A.2.1 A Ramsey model framework

First of all, the economic module is at first sight a Ramsey-Cass-Koopmans model [Ramsey, 1928] [Cass, 1965] [Koopmans, 1963]. The social planner aims a maximising the inter-temporal utility[38] :

$$W = \sum_{t=0}^{T} \frac{1}{(1+\rho)^t} u\left(\frac{C_t}{L_t}\right) L_t \tag{50}$$

With ρ the discount rate (pure rate of social time difference),, U_t the consumption (in trillion of 2010$ per year),L_t the population (in billion of inhabitants), and u the utility :

$$u(c) = \frac{c^{1-\alpha} - 1}{1-\alpha} \tag{51}$$

[37]The General Algebraic Modeling System (GAMS) code of this version is available online on Nordhaus Website

[38]For computation purpose, the model has a finite horizon. Thus, the saving rate is constrained over the last period to avoid "burn everything" edge effect, so that it reach an optimal saving rate: $s* = \gamma \frac{\delta_K + 0.004}{\delta_K + 0.004 * \alpha + \rho}$. This refers to the classical long term saving rate of the Ramsey model, with a TFP growth rate equal to 0.004 (at the end of the horizon, the growth rate of TFP is 0.006

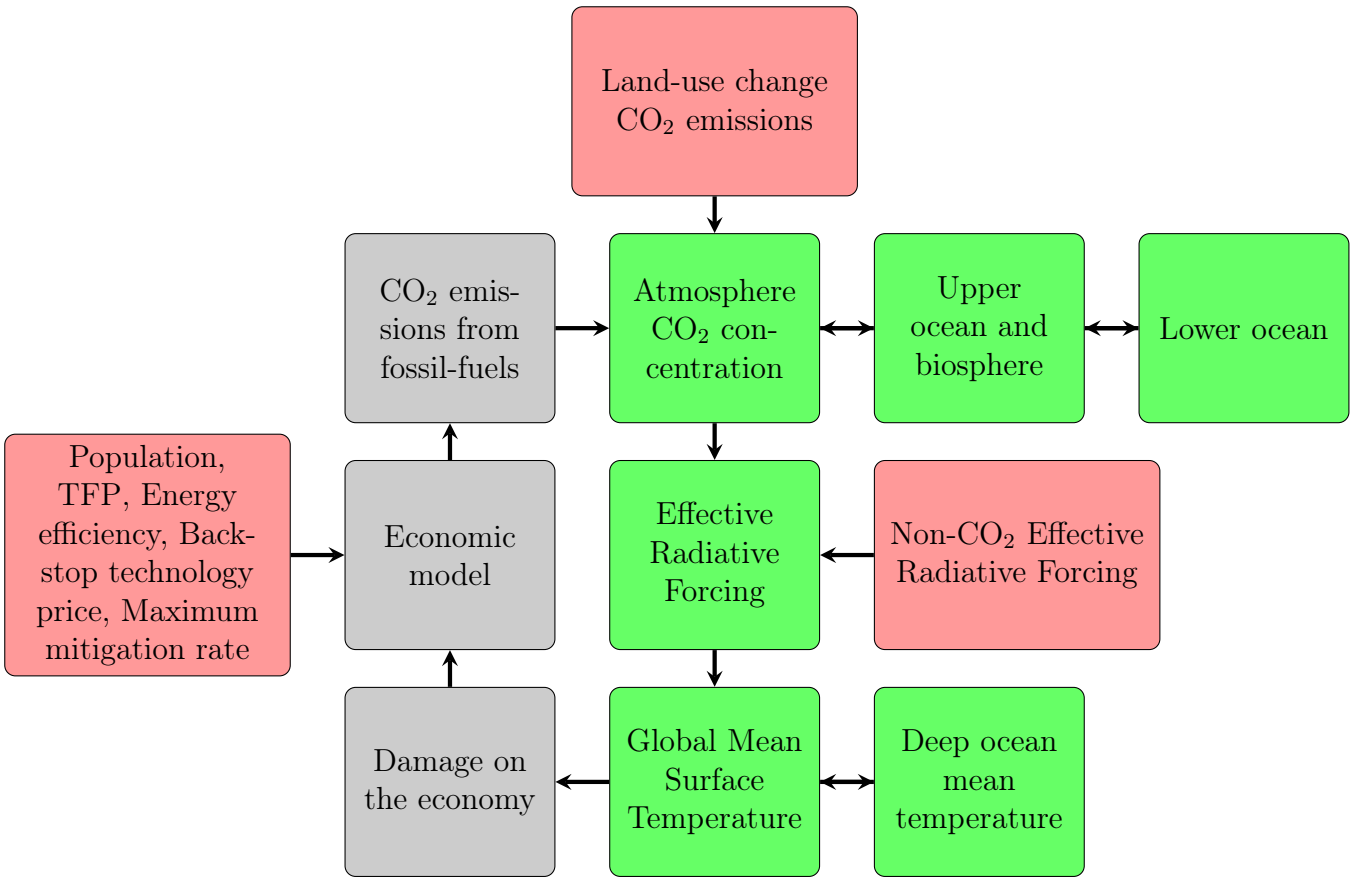

Figure 26: Schematic representation of the DICE model

where θ is the elasticity of the marginal utility of consumption. The gross output has the follows a Cobb-Douglas function :

$$Y_t = A_t K_t^{\gamma} L_t^{1-\gamma} \tag{52}$$

With A_t the Total Factor of Productivity (TFP), K_t the capital (in trillion of 2010\$) and γ the elasticity of gross output with respect to capital. The accumulation of capital is given by :

$$K_{t+1} = (1 - \delta_K)^{\tau_{time-step}} K_t + \tau_{time-step} I_t \tag{53}$$

With δ_K the annual depreciation rate of capital, $\tau_{time-step}$ the time step used (5 years in the DICE model) and I_t the investment (in trillion of 2010\$ per year).

A.2.2 Consume, invest, or mitigate ? Beware of the damage function !

The social-planner can perform three different action : to consume a part of the net output, to invest a part of the net output or to mitigate the fossil-fuel emissions. The net out put is given by :

$$Q_t = (1 - \Lambda_t - \Omega_t) Y_t \tag{54}$$

Where Λ_t is the cost of mitigation and Ω_t are the damages from global climate change. Damages are given as follows :

$$\Omega_t = \Psi_1 T_{surface} + \Psi_2 T_{surface}^2 \tag{55}$$

With $T_{surface}$ the Global Mean Surface Temperature anomalyin K. Mitigation cost are :

$$\Lambda_t = P_{backstop,t}\frac{\sigma_t}{\theta_2 \times 1000}\mu_t^{\theta_2} \tag{56}$$

With $P_{backstop}$ the price of the backstop-technology in 2010\$ per tCO_2, σ_t the energy efficiency in $kgCO_2$ per 2010\$ of output, θ_2 a convexity parameter. The 1000 parameter is there to convert the $kgCO_2$ in tCO_2. The net output might be invested :

$$I_t = s_t Q_t \tag{57}$$

Or consumed :

$$C_t = Q_t - I_t = (1 - s_t)Q_t \tag{58}$$

Therefore, the social planner has two degress of liberty : s the saving rate and μ the mitigation rate. On the one hand, mitigation has a cost, but on the other hand it avoids CO_2 emissions that would impact the economy through the global warming.

A.2.3 CO_2 emissions in the DICE model

Thus, it is really important to know the functional form of the fossil-fuels emissions :

$$E_{ind,t} = \sigma_t Y_t (1 - \mu_t) \tag{59}$$

The result is given in $GtCO_2$ per year. This functional form allows CO_2 negative emissions if $\mu_t > 1$. This is not considered as impossible, however, μ is constrained by the maximum mitigation rate so that it does not get too important : $0 \leq \mu_t \leq \mu_{max,t}$.

A.3 The physical module

The physical module model the response in term of Global Mean Surface Temperature anomaly to fossil-fuel emissions.

A.3.1 The carbon cycle

First, the model determine the CO_2 concentration in the atmosphere, through the carbon cycle :

$$\begin{bmatrix} M_{AT} \\ M_{UP} \\ M_{LM} \end{bmatrix}_{t+1} = \begin{bmatrix} 1-\phi_{12} & \phi_{21} & 0 \\ \phi_{12} & 1-\phi_{21}-\phi_{23} & \phi_{32} \\ 0 & \phi_{23} & 1-\phi_{32} \end{bmatrix} \begin{bmatrix} M_{AT} \\ M_{UP} \\ M_{LM} \end{bmatrix}_t + \begin{bmatrix} (E_{ind}+E_{land})\frac{\tau_{time-step}}{3.666} \\ 0 \\ 0 \end{bmatrix}_t \tag{60}$$

With M_{AT}, M_{UP}, and M_{LO} representing carbon in the atmosphere, carbon in a quickly mixing reservoir in the upper oceans and the biosphere, and carbon in the deep oceans (in GtC). $\frac{12}{44} = \frac{1}{3.666}$ is the conversion factor from $GtCO_2$ to GtC. Moreover $\phi_{21} = \frac{M_{AT,eq}}{M_{UP,eq}}\phi_{12}$ and $\phi_{32} = \frac{M_{UP,eq}}{M_{LO,eq}}\phi_{23}$ so that :

$$\begin{bmatrix} M_{AT,eq} \\ M_{UP,eq} \\ M_{LM,eq} \end{bmatrix} = \begin{bmatrix} 1-\phi_{12} & \phi_{21} & 0 \\ \phi_{12} & 1-\phi_{21}-\phi_{23} & \phi_{32} \\ 0 & \phi_{23} & 1-\phi_{32} \end{bmatrix} \begin{bmatrix} M_{AT} \\ M_{UP} \\ M_{LM} \end{bmatrix} \begin{bmatrix} M_{AT,eq} \\ M_{UP,eq} \\ M_{LM,eq} \end{bmatrix} \tag{61}$$

With $M_{AT,eq}$, $M_{UP,eq}$, and $M_{LO,eq}$ the equilibrium quantities of carbon in each pool.

A.3.2 The climate response

From the quantity of carbon in the atmosphere, it is possible to derive the Effective Radiative Forcing:

$$F_t = \eta \log\left(\frac{M_{AT,t}}{M_{AT,1750}}\right) + F_{ex,t} \tag{62}$$

With $F_{ex,t}$ the exogenous non-CO_2 forcing. The Global Mean Surface Temperature and the deep ocean temperature are given by :

$$T_{AT,t+1} = T_{AT,t} + \xi_1(F_{t+1} - \xi_2 T_{AT,t} - \xi_3(T_{AT,t} - T_{LO,t})) \tag{63}$$

$$T_{LO,t+1} = T_{LO,t} + \xi_4(T_{AT,t} - T_{LO,t}) \tag{64}$$

A.4 Computation of the SCC

With the DICE model, it is possible to compute the SCC the following way :

$$SCC_t = -\frac{\frac{\partial W}{\partial E_t}_{|optimum}}{\frac{\partial W}{\partial C_t}_{|optimum}} = \frac{\lambda_{E_t}}{\lambda_{C_t}} \tag{65}$$

Where λ_{E_t} and λ_{C_t} are the Lagrange multipliers relative to the total emissions and to the consumption.

A.5 The carbon tax in the DICE model

In the DICE model, Nordhaus also presents what he calls the carbon price and that present the price that should be given to the carbon, so that the firms endogenize the need of mitigation. To understand this, let us consider a decentralized equilibrium, with a representative firm and a central state. The firm produces outputs and as well as CO_2. The firm can reduce its cost, but has to pay for it. The central state collects a tax proportional to the CO_2 emitted, with a price P_{CO_2} in 2010\$ per tCO_2. The problem of the firm is thus, at time t :

$$\max_{\mu} Y - cost(\mu) - P_{CO_2} E_{ind}(\mu) \tag{66}$$

i.e.

$$\max_{\mu} Y - Y\frac{P_{backstop}\sigma}{\theta_2 \times 1000}\mu^{\theta_2} - \frac{P_{CO_2}}{1000}\sigma Y(1-\mu) \tag{67}$$

The first order condition finally gives us :

$$P_{CO_2} = P_{backstop}\mu^{theta_2 - 1} \tag{68}$$

The price of carbon depends on the mitigation rate, thus, a central state should, provided, the implementation of the tax, manage the mitigation rate of firms[39]

[39] Obviously, the model considered here is very simplistc and do not represent the reality of policy design.

B From Impulse Response Function (IRF) to box-models

The response function R of an input-output system, such as the carbon cycle, is the output of the system when the input is a dirac impulse (i.e. for the carbon cycle the proportion of carbon remaining in the atmosphere at a time t after an input at time 0). Then, for the carbon cycle the quantity of carbon C in the system is the convolution of the response function and the flux of emissions :

$$C(t) - C(0) = \int_0^t E(t - t')R(t')dt' \tag{69}$$

If it is possible to approximate R as a sum of exponential function[40] :

$$R(t) \approx \sum_i \alpha_i \exp\left(-\frac{t}{\tau_i}\right) \tag{70}$$

With $\sum_i \alpha_i = 1$, since. $R(0+) = 1$, the system is equivalent to the box-model :

$$C(t) = \sum_i C_i(t) \tag{71}$$

Where the C_i are solution of :

$$\frac{dC_i}{dt} = -\frac{C_i}{\tau_i} + \alpha_i E(t) \tag{72}$$

These equations are really easy and fast to compute, so this method provide computing-efficient approximation of a model that might be very complex.

[40]The α_i are a discrete approximation of the inverse of the Laplace transformation, since this equation is an approximation of $R(t) = \int_0^{+\infty} \alpha(p)exp(-pt)dp$

C Supplementary figures for part 2.4

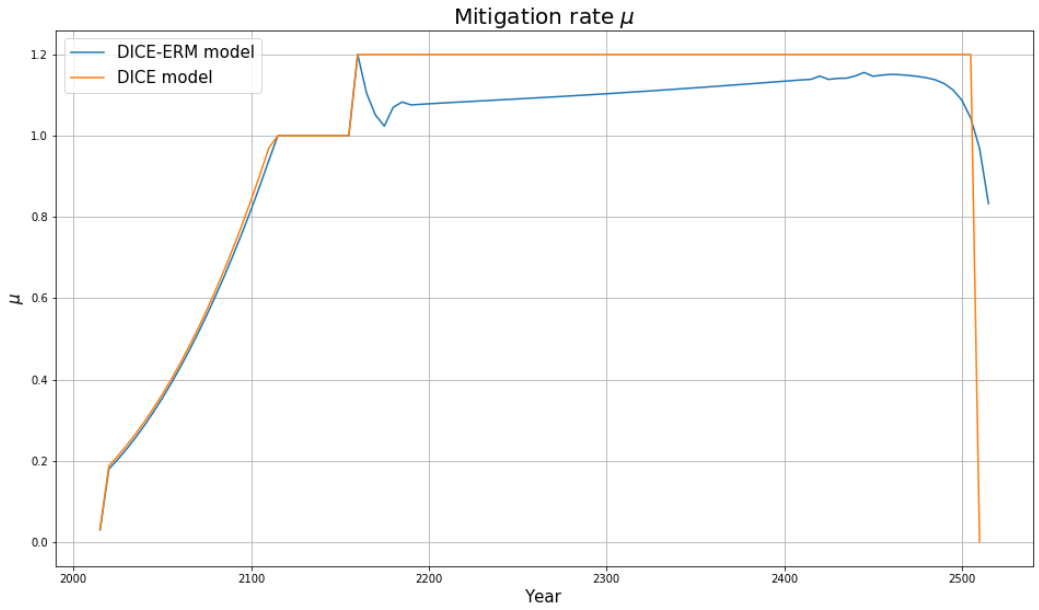

Figure 27: Mitigation rate over the period 2015-2515

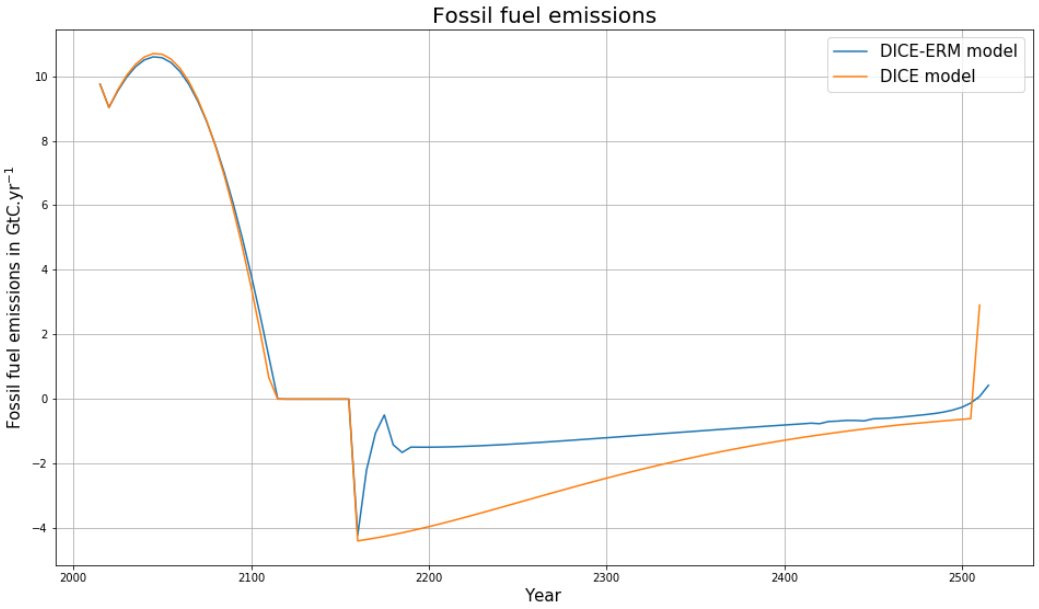

Figure 28: CO_2 fossil-fuel emissions over the period 2015-2515

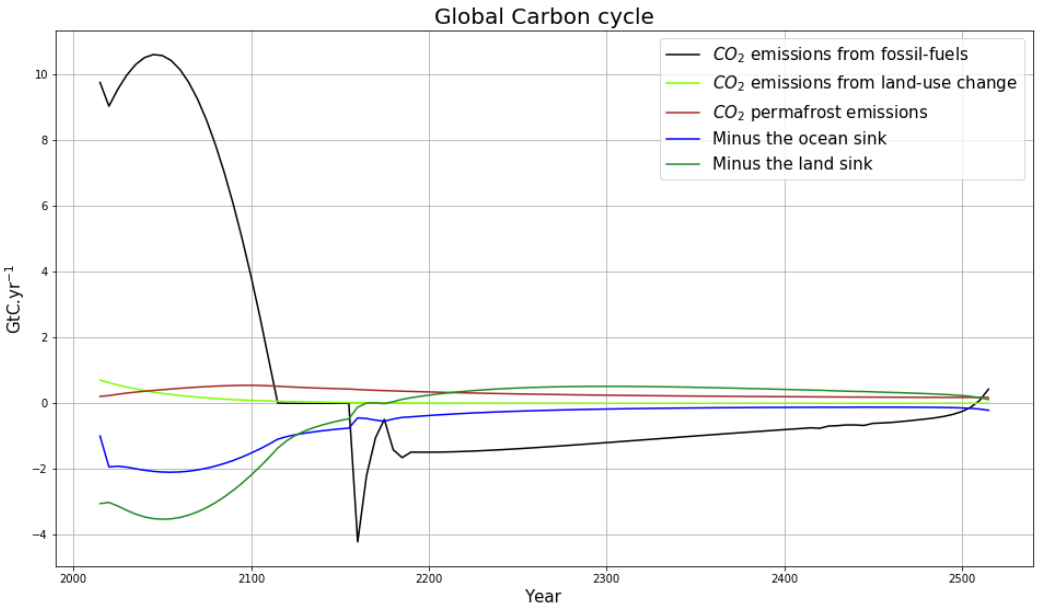

Figure 29: Carbon cycle emissions and sinks during a simulation of the DICE-ERM model

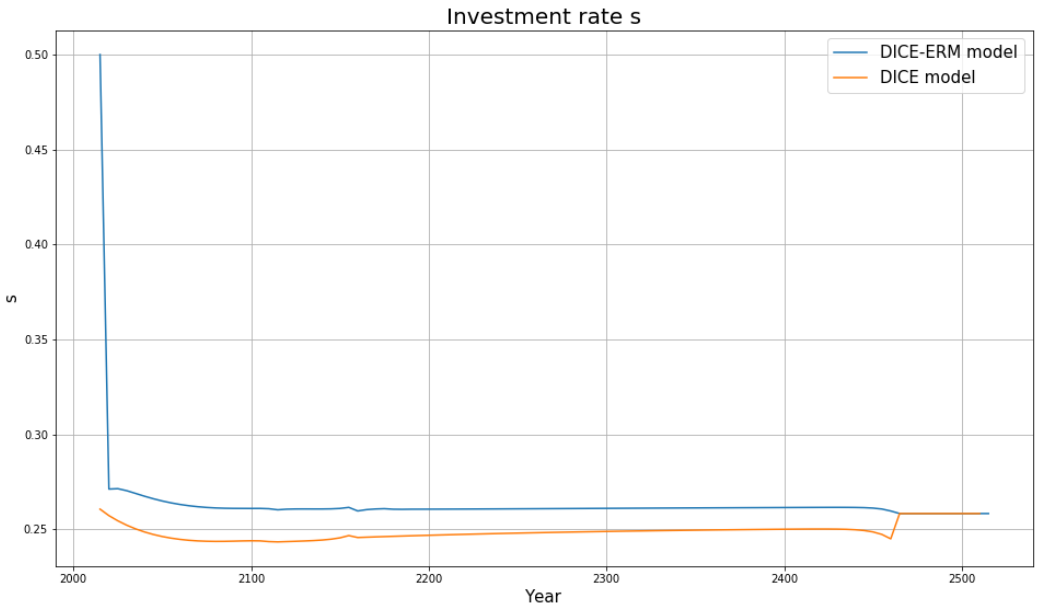

Figure 30: Saving rates over the period 2015-2515

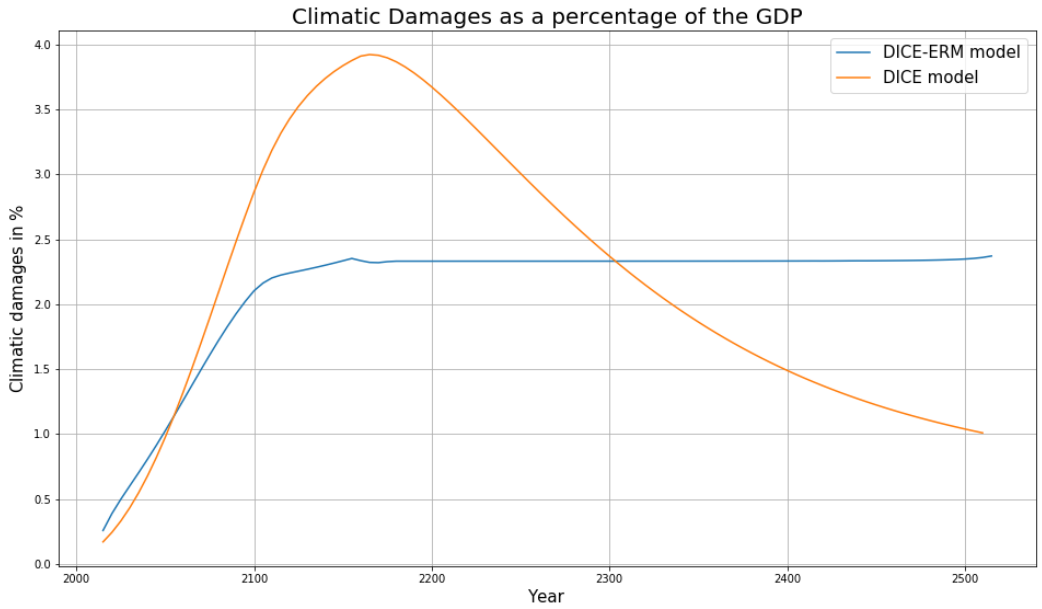

Figure 31: Damages from GMST anomaly expressed as a percentage of the GDP

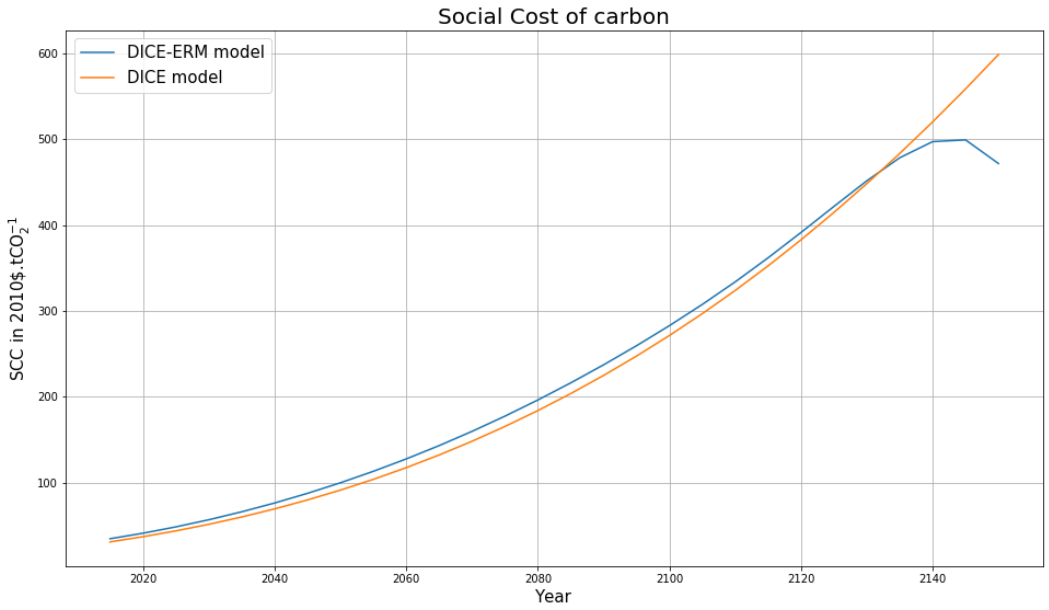

Figure 32: Social Cost of Carbon over the period 2015-2150

D Supplementary figures for part 3

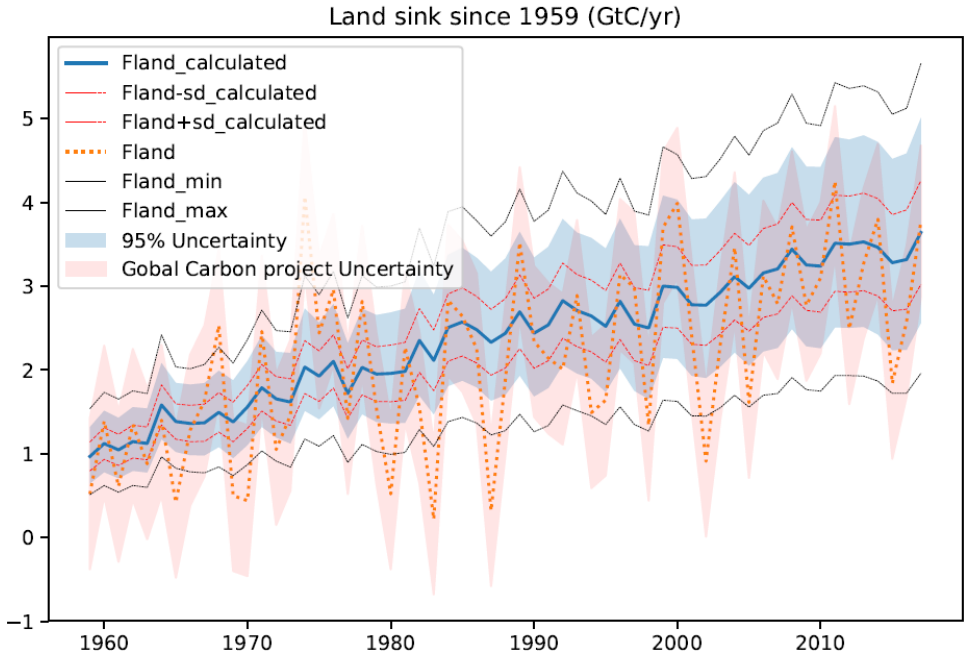

Figure 33: Land sink comparison between the samples drawn after the calibration and the Global Carbon Budget data [Le Quéré et al., 2018] since 1959

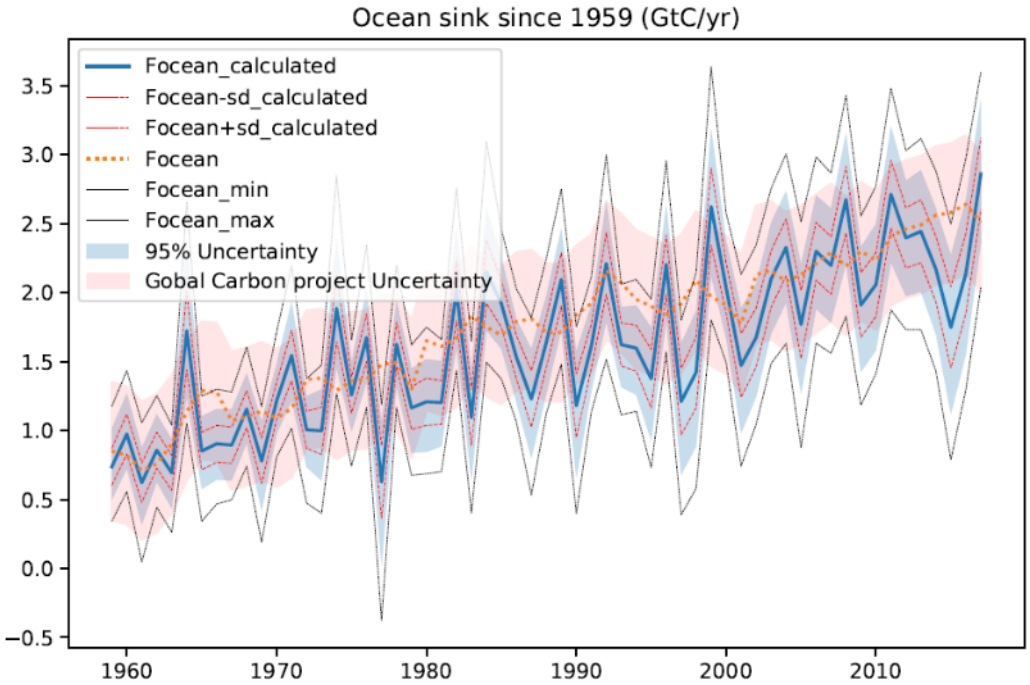

Figure 34: Ocean sink comparison between the samples drawn after the calibration and the Global Carbon Budget data [Le Quéré et al., 2018] since 1959

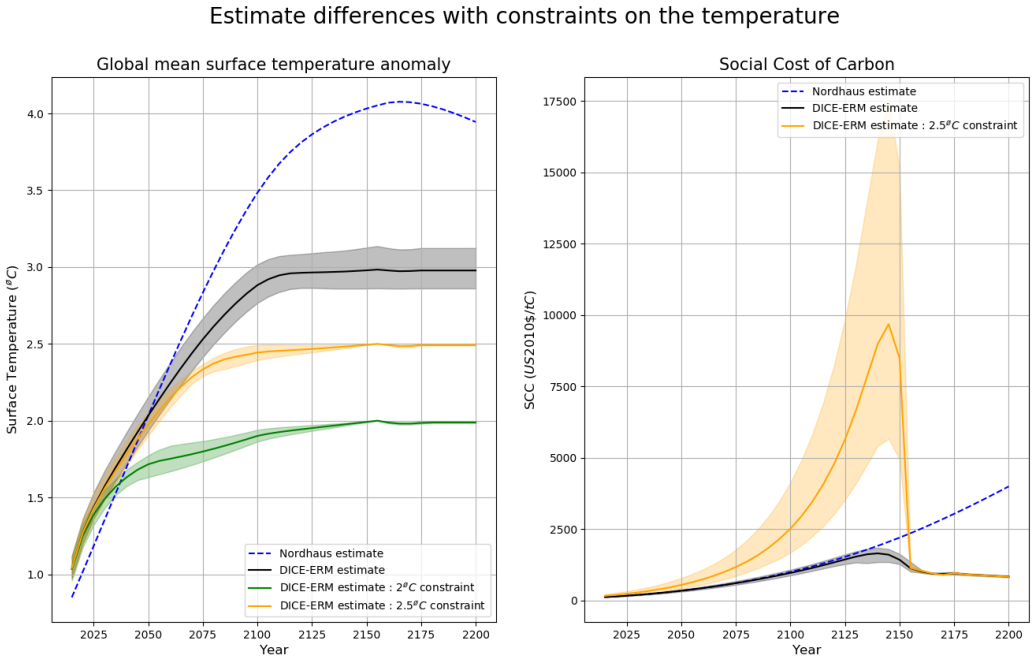

Figure 35: GMST and Social Cost of Carbon of the DICE-ERM model whith a 2.5° temperature constraint

E Supplementary figures for part 4 :SSP1 and SSP3

E.1 Drivers

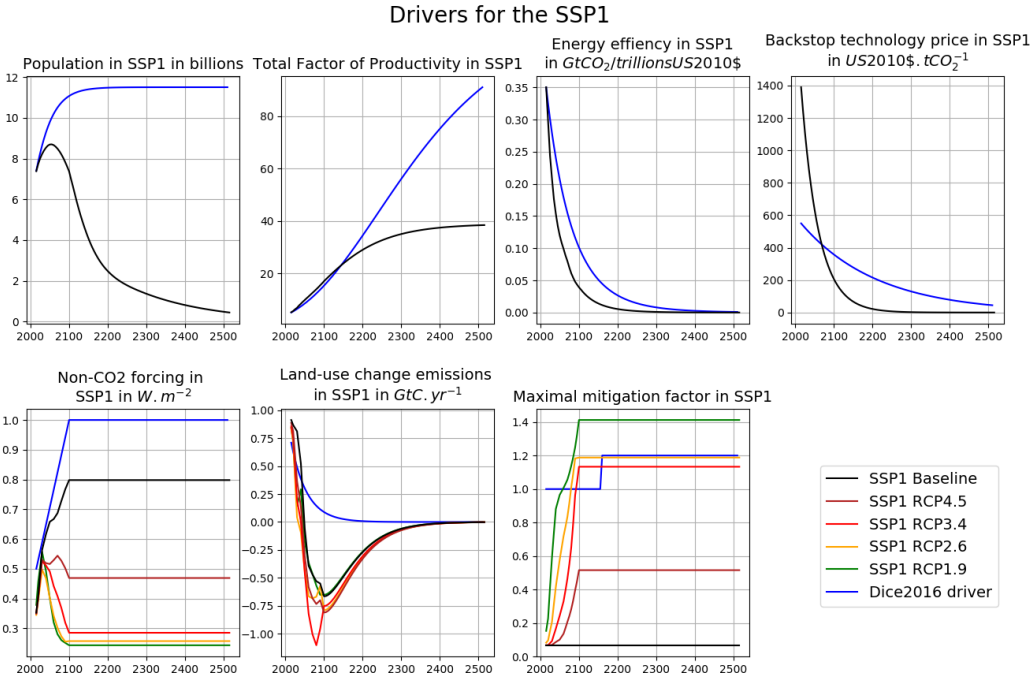

Figure 36: Drivers for the SSP1 compared to the DICE model drivers

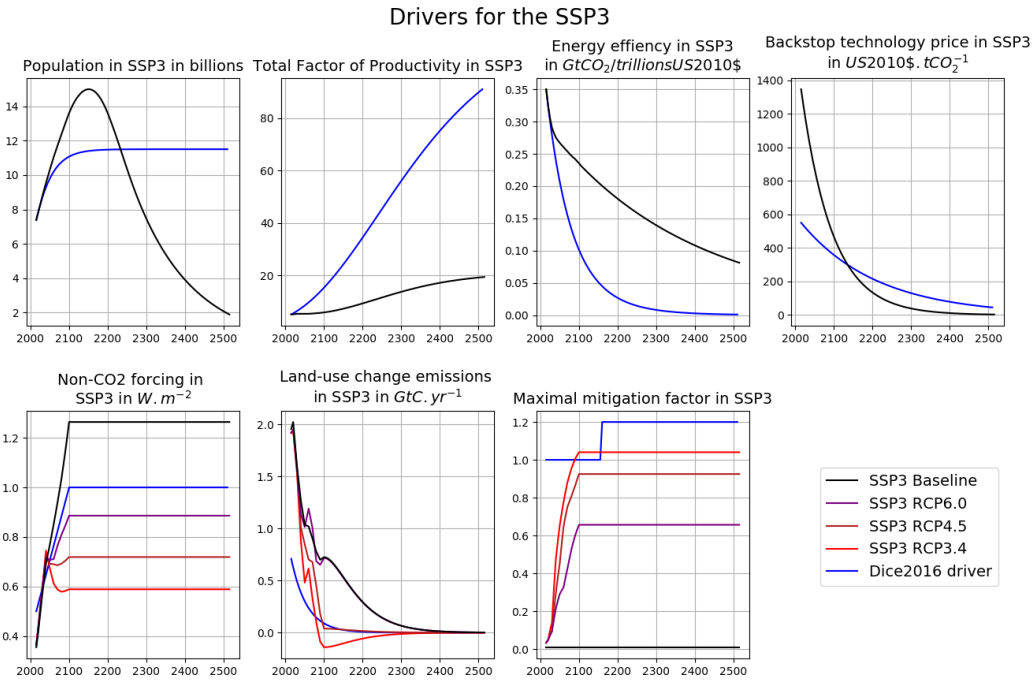

Figure 37: Drivers for the SSP3 compared to the DICE model drivers

E.2 Fossil-fuels emissions

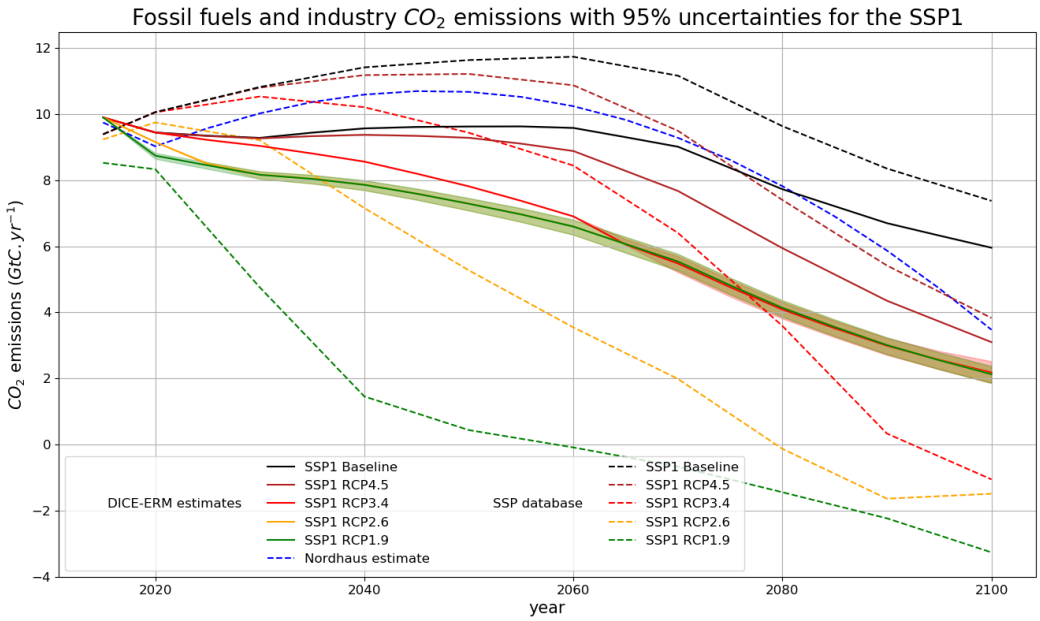

Figure 38: Fossil-fuel CO_2 emissions of the DICE-ERM model on SSP1 compared to the SSP data

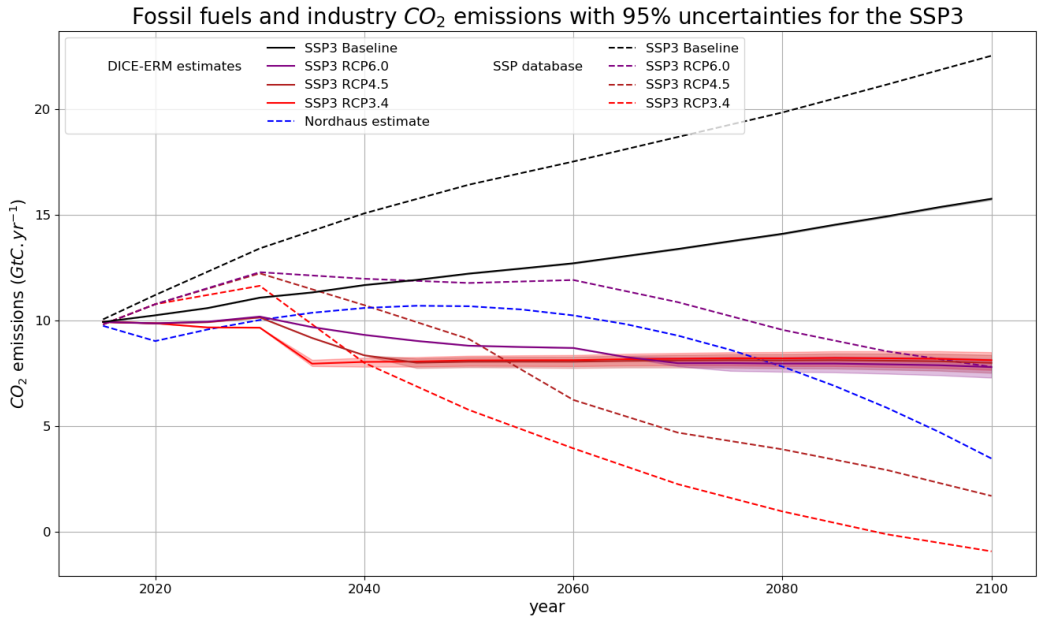

Figure 39: Fossil-fuel CO_2 emissions of the DICE-ERM model on SSP3 compared to the SSP data

E.3 Effective Radiative Forcing

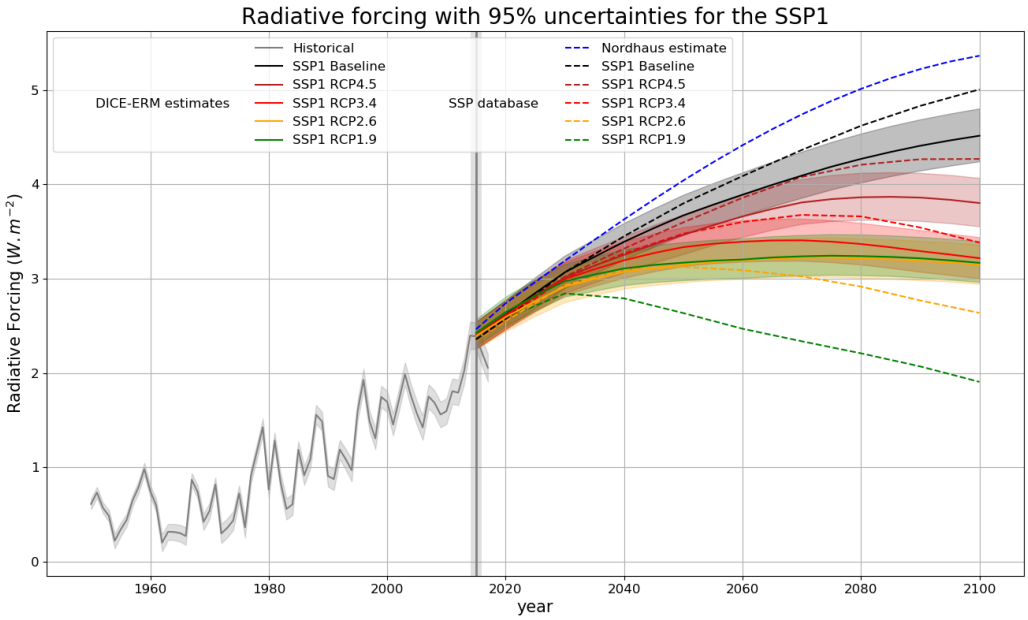

Figure 40: ERF of the DICE-ERM model on SSP1 scenarios compared to the SSP data

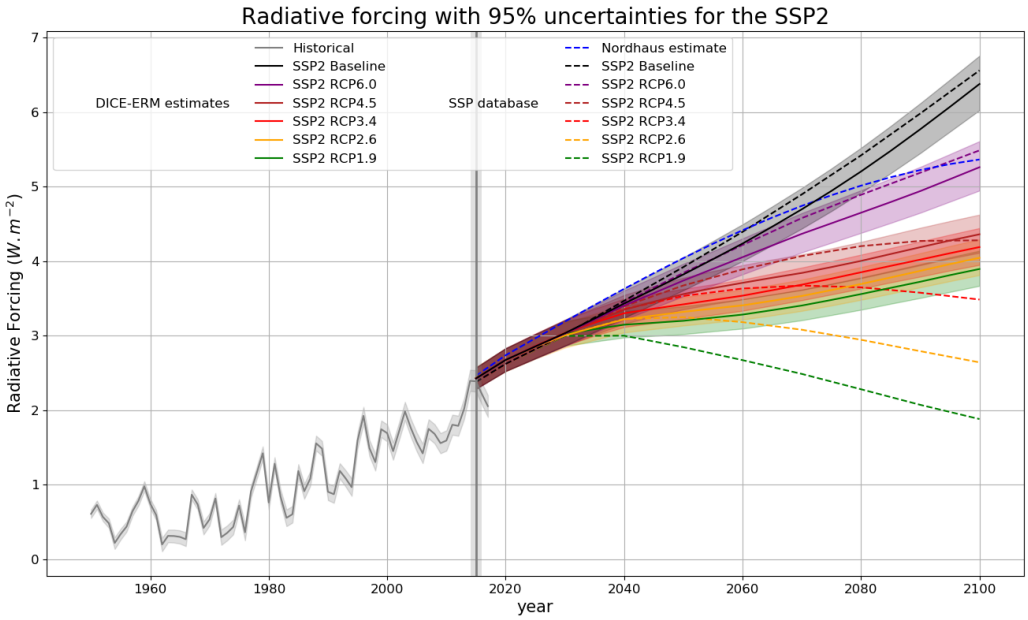

Figure 41: ERF of the DICE-ERM model on SSP2 scenarios compared to the SSP data

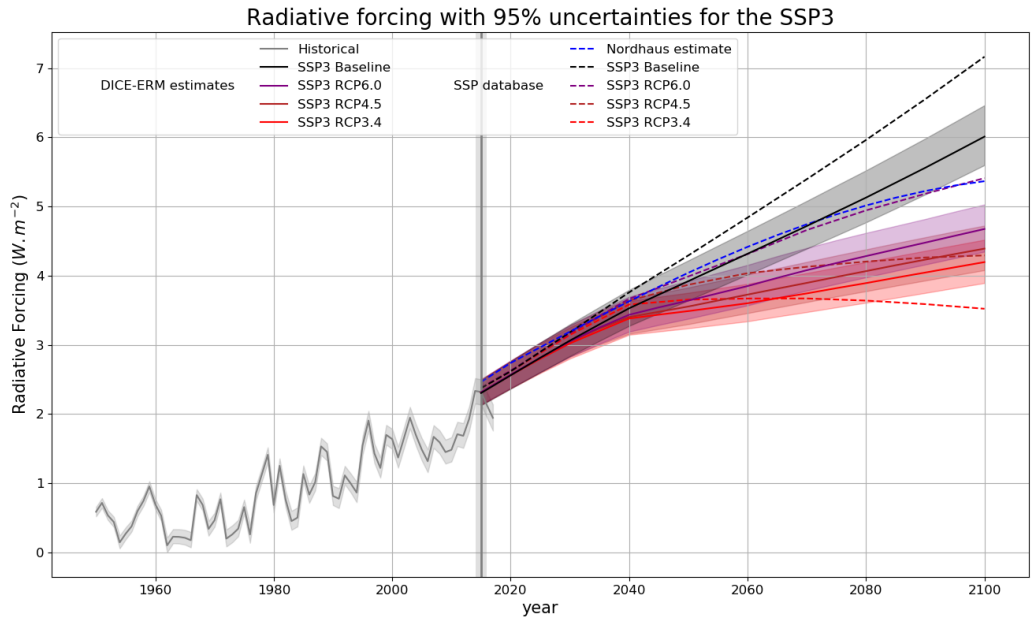

Figure 42: ERF of the DICE-ERM model on SSP3 scenarios compared to the SSP data

E.4 Global Mean Surface Temperature

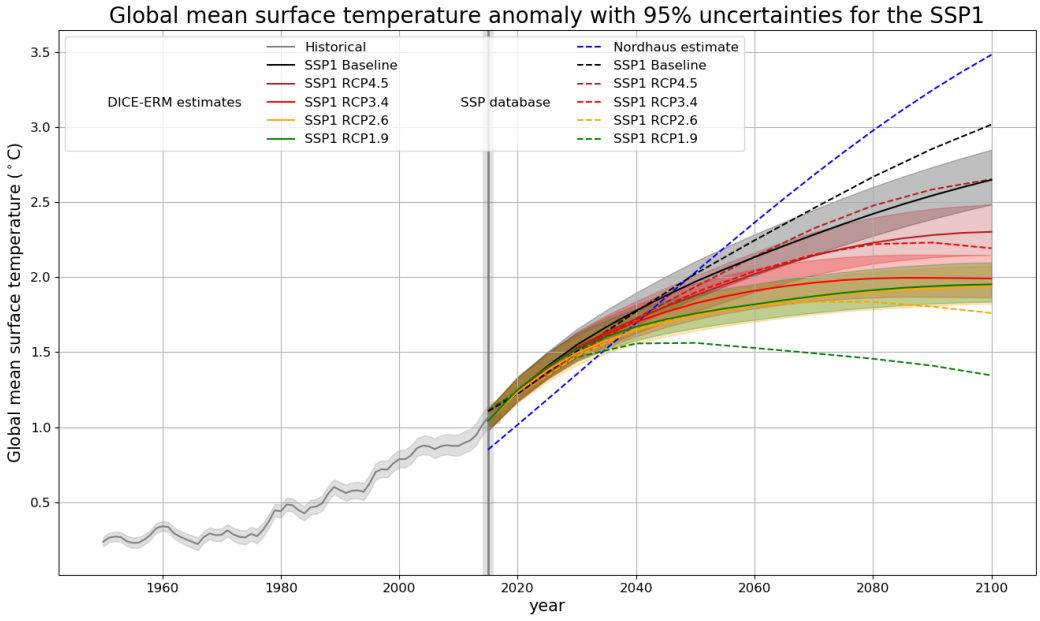

Figure 43: GMST anomaly of the DICE-ERM model on SSP1 scenarios compared to the SSP data

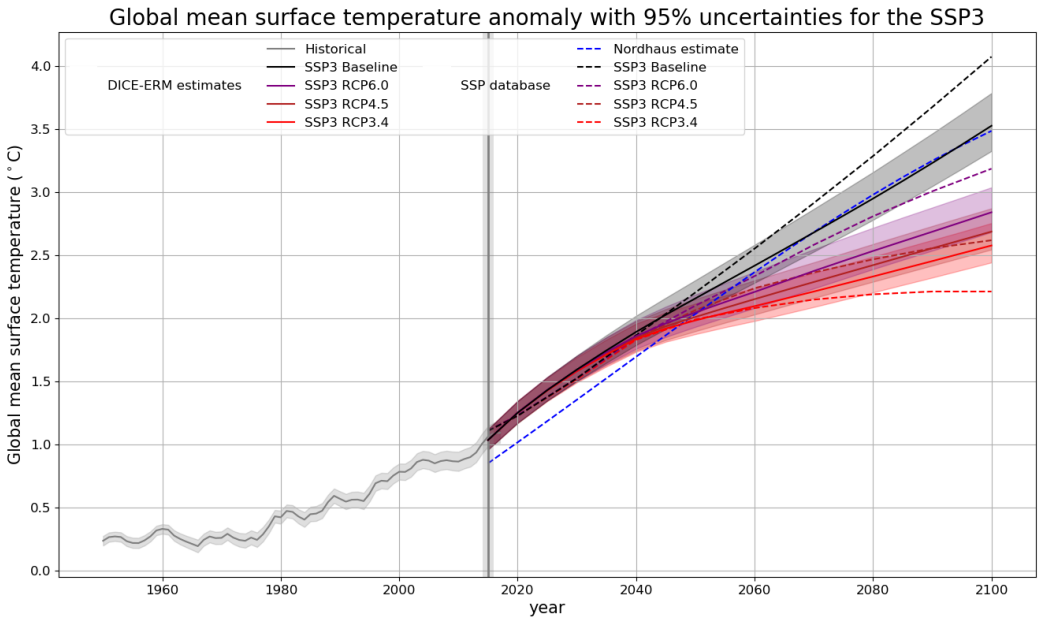

Figure 44: GMST anomaly of the DICE-ERM model on SSP3 scenarios compared to the SSP data

E.5 Gross Domestic Product

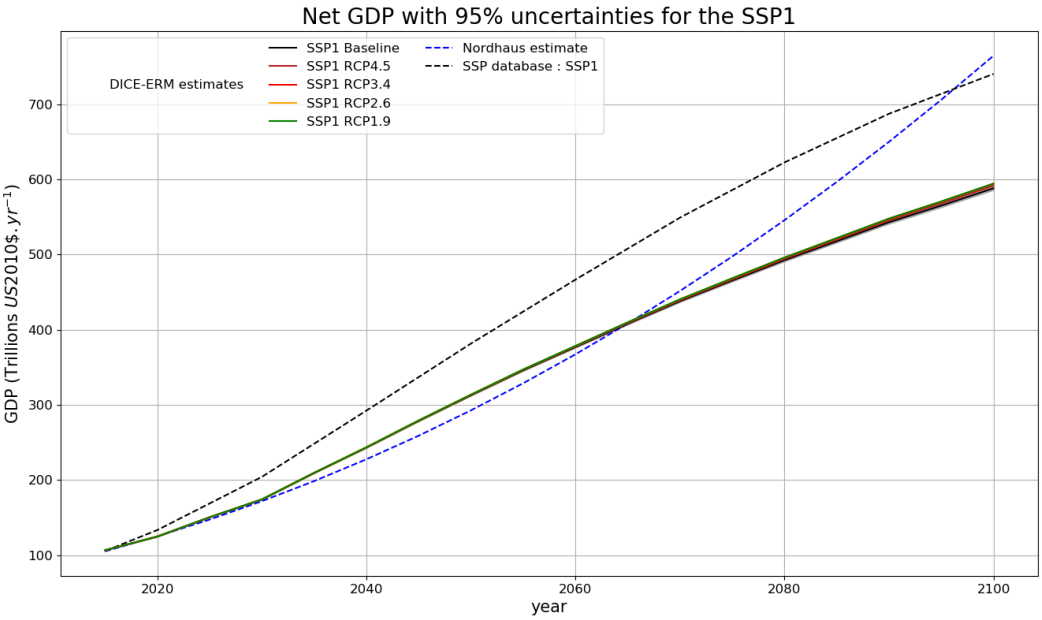

Figure 45: GDP of the DICE-ERM model on SSP1 scenarios compared to the SSP data

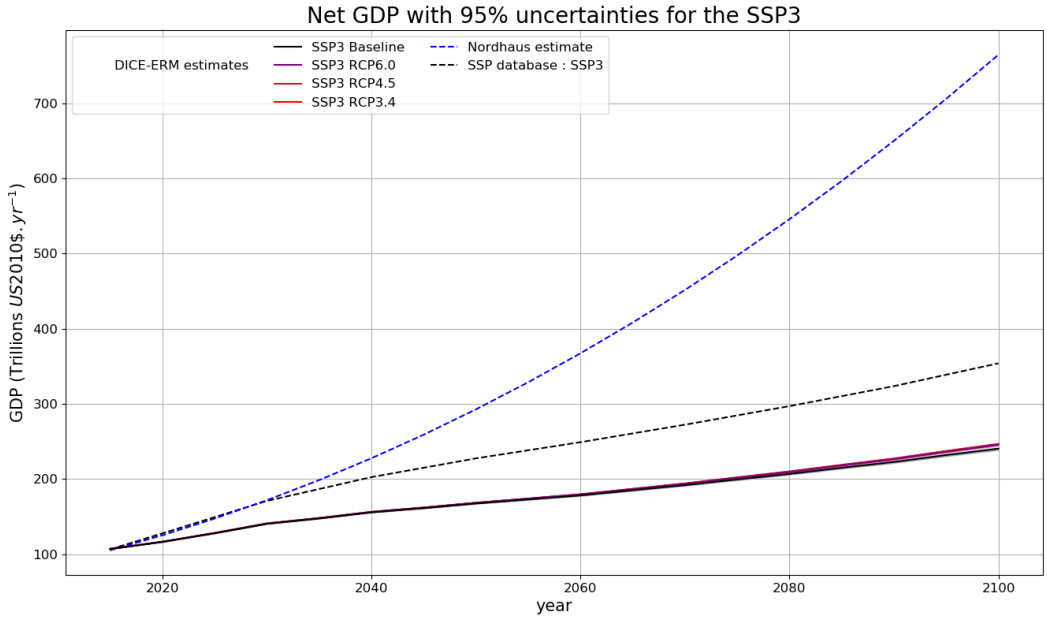

Figure 46: GDP of the DICE-ERM model on SSP3 scenarios compared to the SSP data

E.6 Social Cost of Carbon

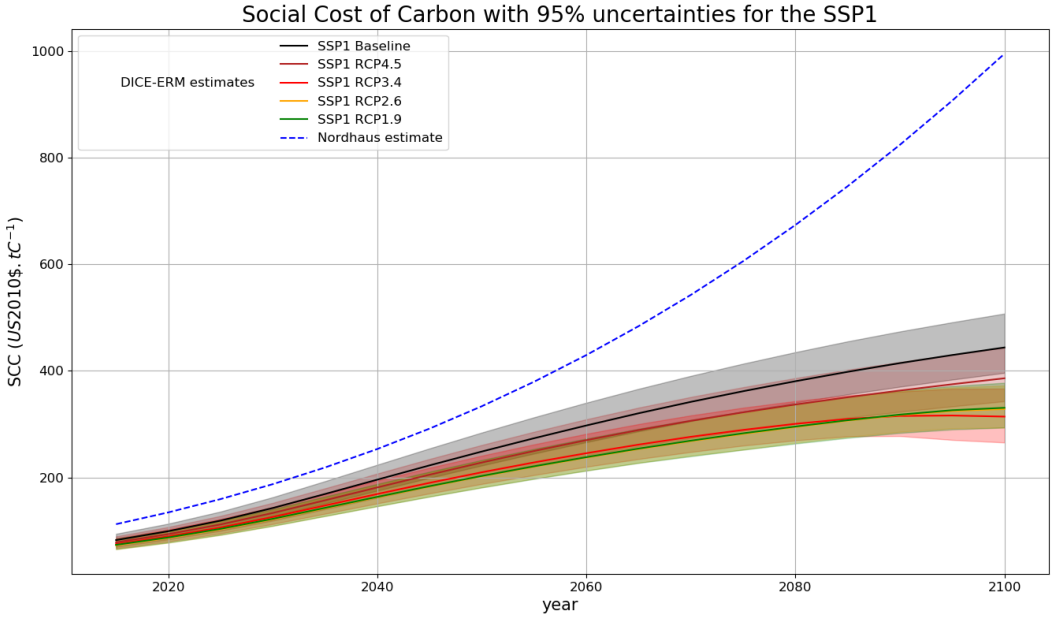

Figure 47: Social Cost of Carbon for the SSP1

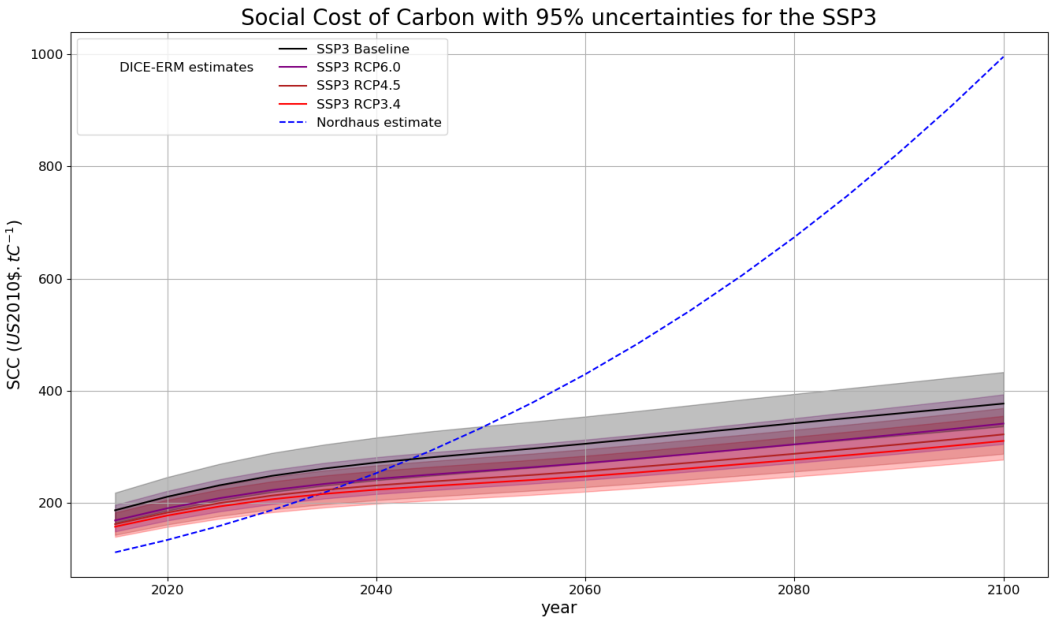

Figure 48: Social Cost of Carbon for the SSP3

E.7 Carbon price

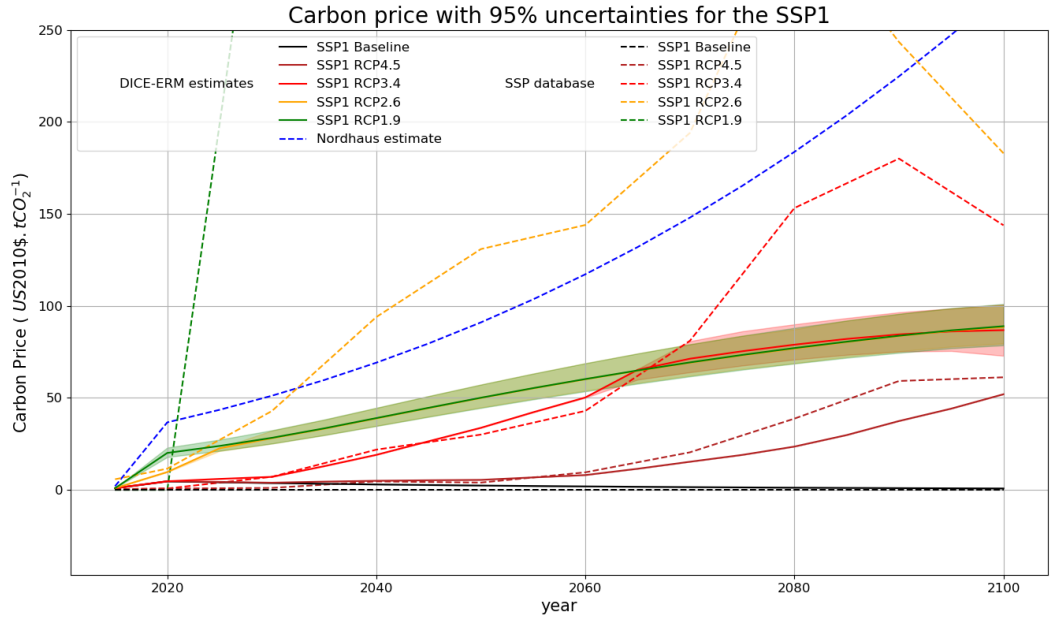

Figure 49: Carbon price for the SSP1

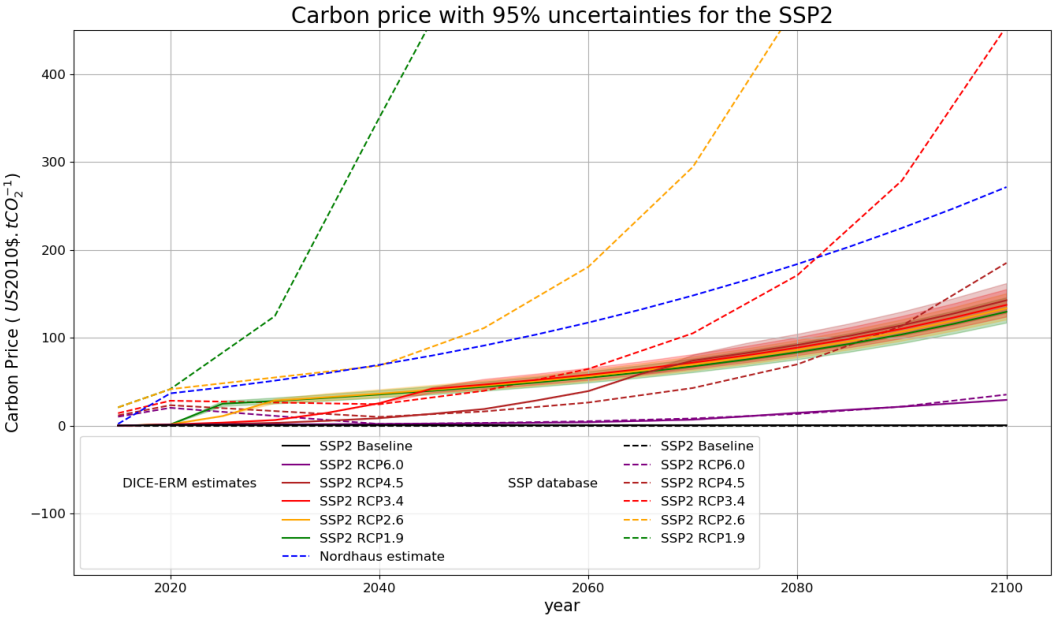

Figure 50: Carbon price for the SSP2

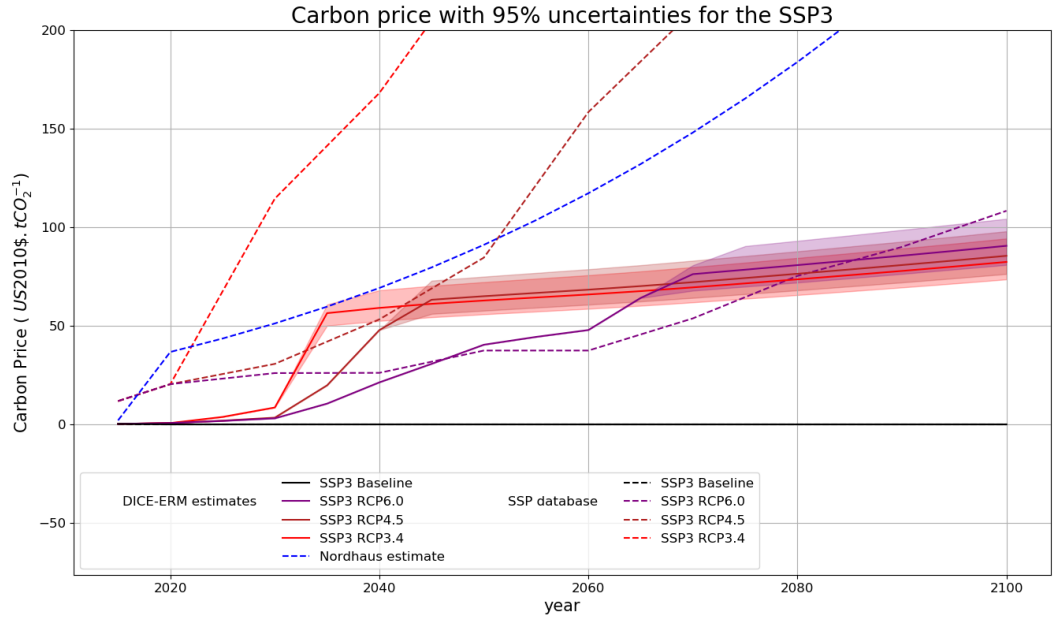

Figure 51: Carbon price for the SSP3

Glossary

anomaly The Global Mean Surface Temperature anomaly is the difference between the current GMST and the GMST of the preindustrial area, which is usually - in particular in this study - defined as the average GMST over the period 1850 - 1900. 7, 10, 13, 15, 16, 18, 21–24, 26, 27, 42, 45, 48, 53, 59, 60, 65, 66

carbon sink A carbon sink is a natural reservoir that stores carbon in certain chemical states (within carbon-containing compounds, such as, for instance organic compounds for the biosphere, or carbonates for the ocean). Carbon sinks are key elements of the carbon cycle, their description in the ERM climate model is made in Part 2.3.1 on page 11. 9, 14

Computational Infrastructure for Operations Research COIN-OR is a project that aims at "building an open-source community for operations research software in order to speed development and deployment of models, algorithms, and cutting-edge computational research, as well as provide a forum for peer review of software similar to that provided by archival journals for theoretical research". The IPOPT solver is a COIN-OR solver, available in the GEKKO Python package. 68

Coupled Model Intercomparison Project It is a collaborative scheme designed to improve knowledge of climate change, by comparing several GCMs outputs on common simulations (historical control runs, 1% per year increasing-CO_2, doubling and quadrupling of the Preindustrial equilibrium CO_2 concentration...). There has been several CMIP phases since 1995, CMIP5 is currently the latest phase of the project and serves as reference data in the field of climate science. Moreover, the CMIP6 outputs should be soonly released. 68

Dynamic Coupled Climate Economy Developed since 1992 by William Nordhaus, the DICE model is one of the first IAMs that couples economy and climate. Still one of the most important model in the field of climate economics, it famous for deriving the Social Cost of Carbon (SCC). A full description of the DICE model is available in the Annex A page 46 or in [Nordhaus, 2013]. 68

Effective Radiative Forcing It correspond to the Radiative Forcing in addition to which we have taken into account the rapid adjustments. 3, 10, 19–21, 23, 25, 26, 32, 37, 39–41, 44–47, 49, 58, 68

Equilibrium Climate Sensivity It refers to the variation of the GMST due to a variation of the CO_2 concentration in the Preindustrial equilibrium. It is often defined as the variation of GMST due to a doubling of the Preindustrial equilibrium CO_2 concentration. However, in this study, we will consider the quadrupling of the Preindustrial equilibrium CO_2 concentration, as it is done in [Geoffroy et al., 2013a] and [**?**]. An important thing to notice is that in most IAMs, the ECS is a specified parameter, whereas in GCMs, it is an emergent property that arises from the simulation. 6, 9, 20, 68

GEKKO It is a Python package for machine learning and optimization of mixed-integer and differential algebraic equations. It is coupled with large-scale solvers for linear, quadratic,

nonlinear, and mixed integer programming. [Beal et al., 2018] [Beal and Hedengren, 2018] [Beal and Hedengren, 2019]. 23, 64

General Algebraic Modeling System The General Algebraic Modeling System (GAMS) is a high-level modeling system for mathematical optimization. GAMS is designed for modeling and solving linear, nonlinear, and mixed-integer optimization problems. GAMS is connected to a group of third-party optimization solvers, which includes the COIN-OR solvers.. 46, 68

General Circulation Model or Global Climate Model GCMs are complex climate models that integrate the Navier-Stokes equations (along with thermodynamic terms and sometimes athmospheric chemistry) on the Earth surface with a relevant spatial grid and temporal scale, in order to simulate the atmosphere and oceans. Taking gas concentration as an input they are used to forecast climate change. 68

Global Mean Surface Temperature It is the annual average temperature of the surface of Earth (which includes both the land surface and the ocean surface). It is computed thanks to several observations with a methodology detailed in [J. Hansen, R. Ruedy, M. Sato and Lo1, 2010] For information about the Global Mean Surface Temperature anomaly see anomaly in the glossary. 3–5, 10, 15, 19–23, 41, 45, 47–49, 59, 64, 66, 68

global warming hiatus It is is a period of relatively little change in globally averaged surface temperatures. Due to a very warm El Nino between 1997 and 1998, the increase of GMST appears very slight. This global warming hiatus raised and now explain many controversial debates about the reality of anthropogenic global warming. 24

heterotrophic respiration Heterotrophic respiration refers to the carbon lost by organisms in ecosystems other than the plants, the primary producers,themselves. It constitutes the respiration by animals that live above-ground. 13, 18

Impulse Response Function see Annex B page 50. 3, 8, 15, 50, 68

Intergovernmental Panel on Climate Change It is an intergovernmental body of the United Nations. Its goal is to provide the world an objective, scientific view of climate change, its natural, political and economic impacts and risks, and possible mitigation and adaptation response options. 68

Interior Point OPTimizer It is an open source software package for large-scale nonlinear optimization. Its main properties are presented in [Wächter and Lorenz, 2006]. 68

land-use change Land use change is a process by which human activities transform the natural landscape, referring to how land has been used, usually emphasizing the functional role of land for economic activities. Land use, land-use change, and forestry (LULUCF), also referred to as Forestry and other land use (FOLU), is defined by the United Nations Climate Change Secretariat as a "greenhouse gas inventory sector that covers emissions and removals of greenhouse gases resulting from direct human-induced land use such as settlements and commercial uses, land-use change, and forestry activities". 9, 10, 12, 19, 23, 37, 39, 47

Monte Carlo Monte Carlo methods, or Monte Carlo experiments, are a broad class of computational algorithms that rely on repeated random sampling to obtain numerical results. The underlying concept is to use randomness to solve problems that might be deterministic in principle. 1, 2, 31, 35

Net Primary Productivity It is the rate of production of biomass with the photosynthesis (Gross Primary Production) minus the respiration of the photosynthesizers. It is a flux expressed in units of mass per unit time. 13, 68

ocean heat content It refers to the heat absorbed by the ocean which is then stored as enthalpy. The ocean heat content at time t is often represented as its value at time t minus the average value over the period 1955-2006 [Levitus et al., 2012]. We follow the same convention in this study.. 9, 10, 21–23

permafrost In geoscience, it is ground (including rock or soil) whose mean annual temperature temperature is below -2°C. Most of this area is located in high latitudes in Siberia, northern Canada, Alaska and Greenland. The thawing of permafrost is a key issue regarding climate change, as it would release a rather uncertain but potentially huge amount of greenhouse gas such as CO_2 or CH_4 in the atmosphere.. 10, 15, 16, 18, 19

Preindustrial equilibrium It is an hypothesis often made in the field of climate science that the climate system is at an equilibrium (in the physical sense of the term) before the industrial revolutions (i.e. that the sum of all carbon flux is zero). This implies that the CO_2 concentration is constant and the CO_2-radiative forcing is zero as well. It is compared to this period that the Global Mean Surface Temperature anomaly is defined. 8, 14, 17, 64

Radiative Forcing Radiative forcing is the net change in the energy balance of the Earth system due to some imposed perturbation. It is usually expressed in watts per square meter averaged over a particular period of time and quantifies the energy imbalance that occurs when the imposed change takes place [IPCC, 2014a]. 9, 10, 19, 20, 64

Representative Concentration Pathway It is a greenhouse gas concentration (not emissions) trajectory. There are four pathways selected for climate modeling, which describe different climate futures. They are all considered possible depending on how much greenhouse gases are emitted in the years to come. The four RCPs, namely RCP2.6, RCP4.5, RCP6, and RCP8.5, are labelled after the reached in the year 2100 (2.6, 4.5, 6.0, and 8.5 $W.m^2$, respectively). 37, 69

Total Factor of Productivity In classical economic growth model, the Total Factor of Productivity is a multiplicative factor obtained by dividing an aggregate output such as the GDP by its weighted factors of production (that are usually capital and labor). Often considered as the primary contributor of the economic growth, it is interpreted as the the efficiency of the workers as well as the level of technology. The GDP is often represented with a Cobb-Douglas equation, A representing the TFP, K, the capital, L the labor and $0 < \gamma < 1$ is the elasticity of GDP with respect to capital:

$$Y_t = A_t K_t^{\gamma} L_t^{1-\gamma}$$

. 7, 37, 38, 47, 69

Total Fertility Rate In a given population, it is the average number of children that would be born from a woman, provided that she survive until the end of her reproductive life and she was to experience the exact current age-specific fertility rates (ASFRs) through her lifetime. 38, 69

Acronyms

AR1 Autoregressive model of order 1. 33

CMIP Coupled Model Intercomparison Project. 9, 26, 64

COIN-OR Computational Infrastructure for Operations Research. 65

DICE Dynamic Coupled Climate Economy. 1, 2, 4–9, 20–26, 28–30, 32, 34–42, 45–49, 52, 55–61

ECS Equilibrium Climate Sensivity. 9, 20, 21, 64

ERF Effective Radiative Forcing. 3, 20, 21, 23, 25, 26, 32, 34, 37, 39–41, 44–47, 49, 58, 59

ERM Earth Risk Management. 2, 8–10, 12, 15–17, 20, 21, 23, 26, 28, 29, 31, 32, 34, 35, 37, 39–42, 52, 55, 57–61, 64

FUND The Climate Framework for Uncertainty, Negotiation and Distribution. 5, 6

GAMS General Algebraic Modeling System. 23, 46

GCM General Circulation Model or Global Climate Model. 9, 20, 64, 65

GDP Gross Domestic Product. 3, 24, 27, 37–39, 42, 43, 46, 53, 60, 61, 66

GMST Global Mean Surface Temperature. 3–5, 7, 9–11, 13, 15–27, 32, 34, 35, 41, 42, 45, 47–49, 53, 55, 59, 60, 64, 65

IAM Integrated Assessment Model. 1, 2, 4–8, 46, 64

IIASA International Institute for Applied Systems Analysis. 37

IPCC Intergovernmental Panel on Climate Change. 8

IPOPT Interior Point OPTimizer. 23, 64

IRF Impulse Response Function. 3, 8, 9, 15, 50

MCMC Markov Chain Monte Carlo. 31

NPP Net Primary Productivity. 12, 13

OECD Organisation for Economic Cooperation and Development. 37

OLG Ordinary Least Square. 34, 39

OSCAR Occupation des Sols et cycle du CARbone. 11, 14

PAGE Policy Analysis of the Greenhouse Effect. 5, 6

PEM Policy Evaluation Model. 5, 6, 45

PIK Potsdam-Institut für Klimafolgenforschung. 37

POM Policy Optimization Model. 5–7, 45

ppm part per million. 13–15

RCP Representative Concentration Pathway. 37, 39–41, 43, 44

SCC Social Cost of Carbon. 1–7, 29, 30, 34–37, 43–46, 49, 53, 55, 61, 62, 64

SPA Shared climate Policy Assumptions. 36

SSP Shared Socioeconomic Pathway. 1–3, 32, 36–45, 56–63

TFP Total Factor of Productivity. 7, 23, 28, 37–39, 43, 46, 47

TFR Total Fertility Rate. 38

References

[Ackerman et al., 2009] Ackerman, F., DeCanio, S. J., Howarth, R. B., and Sheeran, K. (2009). Limitations of integrated assessment models of climate change. *Climatic Change*, 95(3-4):297–315.

[Basten et al., 2013] Basten, S., Sobokta, T., and Zeman, K. (2013). Future Fertility in Low Fertility Countries.

[Bauer et al., 2017] Bauer, N., Calvin, K., Emmerling, J., Fricko, O., Fujimori, S., Hilaire, J., Eom, J., Krey, V., Kriegler, E., Mouratiadou, I., Sytze de Boer, H., van den Berg, M., Carrara, S., Daioglou, V., Drouet, L., Edmonds, J. E., Gernaat, D., Havlik, P., Johnson, N., Klein, D., Kyle, P., Marangoni, G., Masui, T., Pietzcker, R. C., Strubegger, M., Wise, M., Riahi, K., and van Vuuren, D. P. (2017). Shared Socio-Economic Pathways of the Energy Sector – Quantifying the Narratives. *Global Environmental Change*, 42:316–330.

[Beal and Hedengren, 2018] Beal, L. and Hedengren, J. (2018). GEKKO Documentation.

[Beal and Hedengren, 2019] Beal, L. and Hedengren, J. (2019). GEKKO Documentation Release 0.0.3b1.

[Beal et al., 2018] Beal, L., Hill, D., Martin, R., and Hedengren, J. (2018). GEKKO Optimization Suite. *Processes*, 6(8):106.

[Bernie et al., 2010] Bernie, D., Lowe, J., Tyrrell, T., and Legge, O. (2010). Influence of mitigation policy on ocean acidification. *Geophysical Research Letters*, 37(15):1–5.

[Burke et al., 2015] Burke, M., Hsiang, S. M., and Miguel, E. (2015). Global non-linear effect of temperature on economic production. *Nature*, 527(7577):235–239.

[Calel and Stainforth, 2017] Calel, R. and Stainforth, D. A. (2017). On the physics of three integrated assessment models. *Bulletin of the American Meteorological Society*, 98(6):1199–1216.

[Calvin et al., 2017] Calvin, K., Bond-Lamberty, B., Clarke, L., Edmonds, J., Eom, J., Hartin, C., Kim, S., Kyle, P., Link, R., Moss, R., McJeon, H., Patel, P., Smith, S., Waldhoff, S., and Wise, M. (2017). The SSP4: A world of deepening inequality. *Global Environmental Change*, 42:284–296.

[Carpenter et al., 2017] Carpenter, B., Gelman, A., Hoffman, M. D., Lee, D., Goodrich, B., Betancourt, M., Brubaker, M., Guo, J., Li, P., and Riddell, A. (2017). Stan : A Probabilistic Programming Language. *Journal of Statistical Software*, 76(1).

[Cass, 1965] Cass, D. (1965). Optimum Growth of Capital in an Aggregative Model Accumulation. *The Review of Economic Studies*, 32(3):233–240.

[Crespo Cuaresma, 2017] Crespo Cuaresma, J. (2017). Income projections for climate change research: A framework based on human capital dynamics. *Global Environmental Change*, 42:226–236.

[Dellink et al., 2017] Dellink, R., Chateau, J., Lanzi, E., and Magné, B. (2017). Long-term economic growth projections in the Shared Socioeconomic Pathways. *Global Environmental Change*, 42:200–214.

[Enting, 2007] Enting, I. G. (2007). Laplace transform analysis of the carbon cycle. *Environmental Modelling and Software*, 22(10):1488–1497.

[Etheridge et al., 1996] Etheridge, D. M., Steele, L. P., Langenfelds, R. L., Francey, R. J., Barnola, J. M., and Morgan, V. I. (1996). in atmospheric the last 1000 years from air in Antarctic ice and firn. *Journal Of Geophysical Research-Atmospheres*, 101(D2):4115–4128.

[Farmer et al., 2015] Farmer, J. D., Hepburn, C., Mealy, P., and Teytelboym, A. (2015). A Third Wave in the Economics of Climate Change. *Environmental and Resource Economics*, 62(2):329–357.

[Fricko et al., 2017] Fricko, O., Havlik, P., Rogelj, J., Klimont, Z., Gusti, M., Johnson, N., Kolp, P., Strubegger, M., Valin, H., Amann, M., Ermolieva, T., Forsell, N., Herrero, M., Heyes, C., Kindermann, G., Krey, V., McCollum, D. L., Obersteiner, M., Pachauri, S., Rao, S., Schmid, E., Schoepp, W., and Riahi, K. (2017). The marker quantification of the Shared Socioeconomic Pathway 2: A middle-of-the-road scenario for the 21st century. *Global Environmental Change*, 42:251–267.

[Frisch, 2013] Frisch, M. (2013). Modeling climate policies: A critical look at integrated assessment models. *Philosophy and Technology*, 26(2):117–137.

[Fujimori et al., 2017] Fujimori, S., Hasegawa, T., Masui, T., Takahashi, K., Herran, D. S., Dai, H., Hijioka, Y., and Kainuma, M. (2017). SSP3: AIM implementation of Shared Socioeconomic Pathways. *Global Environmental Change*, 42:268–283.

[Gasser et al., 2017] Gasser, T., Ciais, P., Boucher, O., Quilcaille, Y., Tortora, M., Bopp, L., and Hauglustaine, D. (2017). The compact Earth system model OSCAR v2.2: Description and first results. *Geoscientific Model Development*, 10(1):271–319.

[Gasser et al., 2018] Gasser, T., Kechiar, M., Ciais, P., Burke, E. J., Kleinen, T., Zhu, D., Huang, Y., Ekici, A., and Obersteiner, M. (2018). Path-dependent reductions in CO 2 emission budgets caused by permafrost carbon release. *Nature Geoscience*, 11(11):830–835.

[Geoffroy et al., 2013a] Geoffroy, O., Saint-Martin, D., Bellon, G., Voldoire, A., Olivié, D. J., and Tytéca, S. (2013a). Transient climate response in a two-layer energy-balance model. Part II: Representation of the efficacy of deep-ocean heat uptake and validation for CMIP5 AOGCMs. *Journal of Climate*, 26(6):1859–1876.

[Geoffroy et al., 2013b] Geoffroy, O., Saint-Martin, D., Olivié, D. J. L., Voldoire, A., Bellon, G., and Tytéca, S. (2013b). Transient Climate Response in a Two-Layer Energy-Balance Model. Part I: Analytical Solution and Parameter Calibration Using CMIP5 AOGCM Experiments. *Journal of Climate*, 26(6):1841–1857.

[Goodwin et al., 2017] Goodwin, P., Haigh, I. D., Rohling, E. J., and Slangen, A. (2017). A new approach to projecting 21st century sea-level changes and extremes. *Earth's Future*, 5(2):240–253.

[Goujon and Fuchs, 2013] Goujon, A. and Fuchs, R. (2013). The Future Fertility of High Fertility Countries : A Model Incorporating Expert Arguments. (October).

[Hoyer and Hamman, 2017] Hoyer, S. and Hamman, J. J. (2017). xarray: N-D labeled Arrays and Datasets in Python. *Journal of Open Research Software*, 5:1–6.

[IPCC, 2013] IPCC (2013). AR5-Working Group 1, Chapter 6: Carbon and Other Biogeochemical Cycles 6 - Contribution of Working Group I. *Cambridge University Press*.

[IPCC, 2014a] IPCC (2014a). AR5 - Working Group 1, Chapter 8 : Anthropogenic and Natural Radiative Forcing - Contribution of Working Group I. *Cambridge University Press*, 23:56.

[IPCC, 2014b] IPCC (2014b). AR5 - Working Group 1, Chapter 8 : Anthropogenic and Natural Radiative Forcing - Contribution of Working Group I Supplementary Material. *Cambridge University Press*, pages 1–44.

[IPCC, 2014c] IPCC (2014c). *AR5 - Working Group 1, The Physical Science Basis, Contribution of Working Group I.*

[IPCC, 2014d] IPCC (2014d). *AR5 - Working Group 2, Impacts, Adaptation, and Vulnerability - Part A : Global and Sectoral Aspects - Contribution of Working Group II.*

[IPCC, 2018] IPCC (2018). IPCC Special Report 2018 - Annexes.

[J. Hansen, R. Ruedy, M. Sato and Lo1, 2010] J. Hansen, R. Ruedy, M. Sato and Lo1, K. (2010). Global Surface Temperature Change. *Review of Geophysics*, 5(2):1–29.

[Joos et al., 1996] Joos, F., Bruno, M., Fink, R., Siegenthaler, U., Stocker, T. F., Le Quéré, C., and Sarmiento, J. L. (1996). An Efficient and accurate representation of complex oceanic and biospheric models of anthropogenic carbon uptake.

[KC and Lutz, 2017] KC, S. and Lutz, W. (2017). The human core of the shared socioeconomic pathways: Population scenarios by age, sex and level of education for all countries to 2100. *Global Environmental Change*, 42:181–192.

[Koopmans, 1963] Koopmans, T. C. (1963). On the Concept of Optimal Economic Growth.

[Kriegler et al., 2017] Kriegler, E., Bauer, N., Popp, A., Humpenöder, F., Leimbach, M., Strefler, J., Baumstark, L., Bodirsky, B. L., Hilaire, J., Klein, D., Mouratiadou, I., Weindl, I., Bertram, C., Dietrich, J. P., Luderer, G., Pehl, M., Pietzcker, R., Piontek, F., Lotze-Campen, H., Biewald, A., Bonsch, M., Giannousakis, A., Kreidenweis, U., Müller, C., Rolinski, S., Schultes, A., Schwanitz, J., Stevanovic, M., Calvin, K., Emmerling, J., Fujimori, S., and Edenhofer, O. (2017). Fossil-fueled development (SSP5): An energy and resource intensive scenario for the 21st century. *Global Environmental Change*, 42:297–315.

[Kucukelbir et al., 2015] Kucukelbir, A., Ranganath, R., Gelman, A., and Blei, D. M. (2015). Automatic Variational Inference in Stan.

[Le Quéré et al., 2018] Le Quéré, C., Andrew, R. M., Friedlingstein, P., Sitch, S., Hauck, J., Pongratz, J., Pickers, P. A., Korsbakken, J. I., Peters, G. P., Canadell, J. G., Arneth, A., Arora, V. K., Barbero, L., Bastos, A., Bopp, L., and Zheng, B. (2018). Global Carbon Budget 2018. *Earth System Science Data*, pages 2141–2194.

[Leimbach et al., 2017] Leimbach, M., Kriegler, E., Roming, N., and Schwanitz, J. (2017). Future growth patterns of world regions – A GDP scenario approach. *Global Environmental Change*, 42:215–225.

[Levitus et al., 2012] Levitus, S., Antonov, J. I., Boyer, T. P., Baranova, O. K., Garcia, H. E., Locarnini, R. A., Mishonov, A. V., Reagan, J. R., Seidov, D., Yarosh, E. S., and Zweng, M. M. (2012). World ocean heat content and thermosteric sea level change (0-2000m), 1955-2010. *Geophysical Research Letters*, 39(10).

[Moore and Diaz, 2015] Moore, F. C. and Diaz, D. B. (2015). Temperature impacts on economic growth warrant stringent mitigation policy. *Nature Climate Change*, 5(2):127–131.

[Nordhaus, 2013] Nordhaus, W. D. (2013). DICE 2013R: Introduction and User's Manual. *Yale University Press*, (October):102.

[Nordhaus, 2017] Nordhaus, W. D. (2017). Revisiting the social cost of carbon. *Proceedings of the National Academy of Sciences*, 114(7):1518–1523.

[O'Neill et al., 2014] O'Neill, B. C., Kriegler, E., Riahi, K., Ebi, K. L., Hallegatte, S., Carter, T. R., Mathur, R., and van Vuuren, D. P. (2014). A new scenario framework for climate change research: The concept of shared socioeconomic pathways. *Climatic Change*, 122(3):387–400.

[Pinduyk, 2015] Pinduyk (2015). Economists agree: economic models underestimate climate change. *Vox*.

[Ramsey, 1928] Ramsey, F. P. (1928). A Mathematical Theory of Saving. *The Economic Journal*, 38(152):954–559.

[Riahi et al., 2017] Riahi, K., van Vuuren, D. P., Kriegler, E., Edmonds, J., O'Neill, B. C., Fujimori, S., Bauer, N., Calvin, K., Dellink, R., Fricko, O., Lutz, W., Popp, A., Cuaresma, J. C., KC, S., Leimbach, M., Jiang, L., Kram, T., Rao, S., Emmerling, J., Ebi, K., Hasegawa, T., Havlik, P., Humpenöder, F., Da Silva, L. A., Smith, S., Stehfest, E., Bosetti, V., Eom, J., Gernaat, D., Masui, T., Rogelj, J., Strefler, J., Drouet, L., Krey, V., Luderer, G., Harmsen, M., Takahashi, K., Baumstark, L., Doelman, J. C., Kainuma, M., Klimont, Z., Marangoni, G., Lotze-Campen, H., Obersteiner, M., Tabeau, A., and Tavoni, M. (2017). The Shared Socioeconomic Pathways and their energy, land use, and greenhouse gas emissions implications: An overview. *Global Environmental Change*, 42:153–168.

[Ricke et al., 2018] Ricke, K., Drouet, L., Caldeira, K., and Tavoni, M. (2018). Country-level social cost of carbon. *Nature Climate Change*, 8(10):895–900.

[Riddell, 2015] Riddell, A. B. (2015). PyStan Documentation.

[Stan Development Team, 2019] Stan Development Team (2019). Stan User's Guide. Version 2.19.

[Strassmann and Joos, 2018] Strassmann, K. M. and Joos, F. (2018). The Bern Simple Climate Model (BernSCM) v1.0: An extensible and fully documented open-source re-implementation of the Bern reduced-form model for global carbon cycle-climate simulations. *Geoscientific Model Development*, 11(5):1887–1908.

[Takahashi et al., 1993] Takahashi, T., Olafsson, J., Goddard, J. G., Chipman, D. W., and Sutherland, S. C. (1993). and nutrients in the high-latitude surface oceans: A comparative study. *Global Biogeochemical Cycles*, 7(4):843.

[United States Government, 2016] United States Government (2016). Technical Update of the Social Cost of Carbon for Regulatory Impact Analysis Under Executive Order 12866. *Interagency Working Group on Social Cost of Greenhouse Gases*, (August):1–21.

[van Vuuren et al., 2017] van Vuuren, D. P., Stehfest, E., Gernaat, D. E., Doelman, J. C., van den Berg, M., Harmsen, M., de Boer, H. S., Bouwman, L. F., Daioglou, V., Edelenbosch, O. Y., Girod, B., Kram, T., Lassaletta, L., Lucas, P. L., van Meijl, H., Müller, C., van Ruijven, B. J., van der Sluis, S., and Tabeau, A. (2017). Energy, land-use and greenhouse gas emissions trajectories under a green growth paradigm. *Global Environmental Change*, 42:237–250.

[Wächter and Lorenz, 2006] Wächter, A. and Lorenz, B. T. (2006). Digital Object Identifier (On the implementation of an interior-point filter line-search algorithm for large-scale nonlinear programming. *Math. Program., Ser. A*, 106:25–57.

[Weitzman, 2013] Weitzman, M. L. (2013). Tail-Hedge Discounting and the Social Cost of Carbon. *Journal of Economic Literature*, 51(3):873–882.